Biochemical and Molecular Identification of Pheophytinase, an Important Esterase of Chlorophyll Breakdown during Leaf Senescence and Fruit Ripening

Dissertation

zur Erlangung der naturwissenschaftlichen Doktorwürde

(Dr. sc. nat.)

vorgelegt

der

Mathematisch-naturwissenschaftlichen Fakultät

der Universität Zürich

von

Silvia Schelbert Hofstetter

von

Muotathal SZ

Promotionskomitee

Prof. Dr. Enrico Martinoia (Vorsitz)

Prof. Dr. Stefan Hörtensteiner (Leitung der Dissertation)

Prof. Dr. Beat Keller

Prof. Dr. Felix Kessler

Zürich, 2011

Abbreviations

ABC	ATP binding cassette
Acd	Accelerated cell death
ATP	Adenosine 5-trisphosphate
BCRP	Breast cancer resistance protein
BSA	Bovine serum albumin
CAB	Chl *a/b* binding protein
CAO	Chlorophyllide *a* oxygenase
Chl	Chlorophyll
Chlide	Chlorophyllide
Cl	Chlorophyll retainer
CLH/Chlase	Chlorophyllase
DMSO	Dimethylsulfoxide
EDTA	Ethylenediaminetetraacetic acid
EMS	Ethyl methane sulfonate
EST	Expressed sequence tag
ETR	Ethylene-resistant
FCC	Fluorescent chlorophyll catabolite
Fd	Ferredoxin
Gf	Green flesh
GFP	Green fluorescence protein
HEPES	2-(4-(2-Hydroxyethyl)-1-piperazinyl)-ethansulfonsäure
HMChl	Hydroxymethyl chlorophyll
HPLC	High pressure liquid chromatography
HR	Hypersensitive response
IBA	Indole-3-butyric acid
IPTG	Isopropyl-β-D-thiogalactopyranosid
IVT	In-vitro translation
JA	Jasmonic acid
Kb	Kilo base
kD	Kilo Dalton
LHC	Light harvesting complex
Lls	Lethal leaf spot
LSU	Large subunit of Rubisco
MBP	Maltose binding protein
MCS	Metal chelating substance
MDR	Multi-drug resistance
MES	2-(N-Morpholino)ethansulfonsäure
MeJA	Methyl jasmonate
Mg	Magnesium
MOPS	3-(N-morpholino)propanesulfonic acid

MRP	Multidrug resistance associated protein
MS	Mass spectrometry
MS	Murashige and Skoog medium or (MSO)
NAA	1-Naphthaleneacetic acid
NAN	navel negra
NCC	Non-fluorescent chl catabolite
NOL	Non yellowing colour-like
NYC	Non yellowing colour
ORE	from oresara `long-living` in korean
PAGE	Polyacrylamide gel electrophoresis
PCD	Programmed cell death
PAO	Pheophorbide *a* oxygenase
PCR	Polymerase chain reaction
PEG	Polyethylene glycol
Pheide	Pheophorbide
Phein	Pheopyhtin
PPD	Pheophorbide *a* demethylase
PPH	Pheophytin pheophorbide hydrolase
PS	Photosystem
RCC	Red chlorophyll catabolite
RCCR	Red chlorophyll catabolite reductase
ROS	Reactive oxygen species
RubisCO	Ribuloes-1,5-biphosphate carboxylase-oxygenase
SA	Salicylic acid
SAG	Senescence associated gene
SDS	Sodium dodecyl sulphate
SGR/NYE	Stay-green
TF	Transcription factor
TL	Thermolysin
Tris	Tris(hydroxymethyl)aminomethane
VTE	Vitamin E mutant
WBC	White brown complex
WT	Wilde typ
YFP	Yellow fluorescence protein

Table of contents

I Abstract

Chlorophyll (chl) breakdown occurs during leaf senescence and fruit ripening processes. Thereby, green chl is converted in a multistep pathway to linear colourless and nonfluorescent tetrapyrroles, NCCs that accumulate in the vacuole. Green pigment catabolism enables the remobilization of fixed nitrogen from photosystem proteins. Dephytylation, an early and important step in this pathway, increases water solubility of further chl catabolites. The first objective of this work was a re-examination of chlorophyllase (CLH) identity since these enzymes were believed to catalyze phytol hydrolysis during leaf senescence. We concluded that CLHs are not essential for dephytylation in *Arabidopsis thaliana*. This conclusion led to the major goal of my work, the identification of pheophytinase (PPH), which catalyzes phytol hydrolysis *in vivo*. Interestingly, PPH displayed high specificity towards Mg-free chl pigment (pheophytin) and deficiency of PPH in an *Arabidopsis* mutant caused indefinite retention of greenness. In summary, these investigations proof that pheophytinase and not chlorophyllase plays an important role in chl breakdown during leaf senescence and thus, we propose a new order of early chl catabolic reactions.

In addition, I studied the role of PPH in other instances of chl metabolism such as during fruit ripening of tomato. With this project I tried to elucidate whether chl catabolism in leaves and fruits follows the same route. Although little is known about the fate of chl during fruit ripening, work done on citrus, tomato and pepper fruit degreening indicate the same pathway to be active. Thus, NCCs, identified in ripe apples and pears were shown to be identical to those in senescent leaves of the fruit trees. Primary results of my work indicate that PPH is involved in the loss of chl during fruit ripening of tomato.

In addition, I attempted to elucidate whether the individual protein components of early chl breakdown function together in a multi-protein complex and how this complex is assembled and located *in vivo*. It is known that complexes facilitate substrate trafficking between different enzymes, thereby reducing the possibility that potentially dangerous intermediates will accumulate. In summary, I identified a multi-protein complex which is formed exclusively during senescence and acts at sites of dismantled thylakoid structures.

During my PhD thesis, I worked on several aspects of chl breakdown, *i.e.* phytol hydrolysis in leaves and fruits, and protein complex formation for breakdown intermediate channelling at early chl breakdown. The results of this work considerably improved our understanding of the chl degradation process. However, elucidation of the identity of the Mg-removing activity and of the role of SGR, a protein of the multi-enzyme complex with unknown function, represents other areas where additional research is required for a further dissection of this pathway.

1.1 Zusammenfassung

Chlorophyll wird hauptsächlich während der Blattseneszenz und der Fruchtreife abgebaut. Dabei wird das grüne Chlorophyll in mehreren Schritten zu farblosem, nicht fluoreszierendem Tetrapyrrol abgebaut, welches in der Vakuole akkumuliert. Der Abbau des grünen Pigments ermöglicht die Rückgewinnung von gebundenem Stickstoff aus dem Photosystem. Die Hydrolyse von Phytol ist ein früher und wichtiger Schritt im Chlorophyll Abbau, welcher die Wasserlöslichkeit von Folgekataboliten erhöht. Die erste Zielsetzung dieser Arbeit war die Überprüfung der Phytol Hydrolyse Aktivität der Chlorophyllasen während der Blattseneszenz. Unsere Resultate zeigen, dass Chlorophyllasen im Chlorophyll Abbau während der Blattseneszenz nicht beteiligt sind und dieser Abbauschritt im lebenden Organismus von einer anderen, noch unbekannten Esterase vollzogen wird. Diese Erkenntnis führte zum Hauptziel meiner Arbeit, der Identifizierung der Pheophytinase, welche die Phytol Hydrolyse in der Blattseneszenz katalysiert. Interessanterweise zeigt die Pheophytinase eine hohe Spezifität gegenüber dem Magnesium-freien Chlorophyll Pigment, Pheophytin. Diese Erforschung beweist, dass die Pheophytinase und nicht die Chlorophyllase eine wichtige Rolle im Chlorophyll Abbau während der Blattseneszenz darstellt.

In einem weiteren Schritt untersuchte ich die Rolle der Pheophytinase während der Fruchtreife von Tomaten, um aufzuklären ob Chlorophyll im Blatt wie auch in der Frucht mit dem gleichen Mechanismus abgebaut wird. Obwohl wenig über den Chlorophyll Abbau während der Fruchtreife bekannt ist, wurden an Zitrone, Tomate und Paprika einige Arbeiten durchgeführt, sowie die finalen Abbauprodukte des Chlorophylls in reifen Äpfeln und Birnen identifiziert. Diese Endprodukte waren identisch mit jenen in den alternden Blättern dieser Bäume. Erste Resultate meiner Arbeit bestätigen, dass die Pheophytinase im Chlorophyll Abbau während der Fruchtreife involviert ist.

In einem weiteren Projekt versuchte ich zu eruieren ob individuelle Enzyme des Chlorophyll Abbaus, zusammen in einem Multi-Protein Komplex agieren, welche Enzyme beteiligt sind und in welchem Kompartiment der Zelle dieser mögliche Komplex im lebenden Organismus vorkommt. Ich konnte ein Multi-Protein Komplex identifizieren, welcher ausschliesslich während der Blattseneszenz gebildet wird.

Während meiner Dissertation interessierten mich verschiedene Aspekte des Chlorophyll Abbaus; vor allem die Phytol Hydrolyse in Blatt und Frucht, sowie die Bildung eines Chlorophyll Abbau-Komplexes. Dennoch stellen die Identifizierung der Mg-lösenden Aktivität und die Aufklärung der Funktion des `Stay-Green` Proteins weitere Gebiete dar, in denen Forschung nötig ist um diesen Abbau Weg weiter zu analysieren.

II Introduction

Chlorophyll (chl) is one of the most abundant and complex pigments on earth demonstrating a key element of photosynthesis in living organisms. It is required for the absorption of sunlight in photosynthetic antenna systems, and for charge separation and electron transport within reaction centres. After a productive photosynthetic period, leaf cells enter the last stage of their development: senescence. Loss of green colour is the visual manifestation of leaf senescence and is probably one of the most remarkable developmental phenomena observed in nature. Bright autumn colours occurring during autumnal senescence of deciduous trees are due to excessive chl degradation, unmasking preexisting carotenoids and de novo synthesized anthocyanins (Ougham et al. 2005). A total annual turnover of chl is estimated to involve more than one billion tons (Hendry et al. 1987). Along senescence, an early and significant change in cell structure is the breakdown of chloroplasts. They are converted to gerontoplasts, loose volume and density, accumulate plastoglobules and slowly decrease photosynthetic capacity. Consequently breakdown and remobilization processes are initiated.
But, chl is a dangerous molecule and a potential cell phototoxin. As long as chl is associated with photosystem protein complexes, it is powerful and harmless. In contrast, free chl and its derivatives keep the capacity to absorb light energy resulting in the excessive production of reactive oxygen species (ROS). ROS in turn provokes cell death. Therefore, chl degradation can be seen as a highly coordinated detoxification process enabling the remobilization of fixed nitrogen from the photosystem protein complexes. Considering that a remarkable amount of 20% of cellular nitrogen is fixed to photosystem protein complexes whereas only 2% is contributed by chl (Hörtensteiner, 2006).
Until the beginning of the nineties, chl catabolism was designated as a biological enigma. A biochemical pathway for the degradation of chl was hardly documented. The stepwise elucidation of the chl breakdown pathway has its origin in 1991 when the structure of a final product of chl breakdown, a nonfluorescent chl catabolite (NCC) was first identified (Kräutler et al., 1991). Subsequent characterization of mutants being impaired in different steps of the pathway significantly contributed to the description of the degradation process. These mutant studies enabled the cloning of four enzymes involved such as pheophorbide *a* oxygenase (PAO), red chl catabolite reductase (RCCR), chl *b* reductase (NYC1/NOL) and just recently pheophytin pheophorbide hydrolase (PPH) (Wüthrich et al., 2000; Pružinská et al., 2003; Kusaba et al., 2007; Schelbert et al., 2009). The pathway became more and more detailed since reactions could be predicted and characterized and intermediates of breakdown identified. Figure 1 displays the actual knowledge of the chl breakdown pathway. Green chl is converted in a multistep pathway to linear colourless and nonfluorescent tetrapyrroles, NCCs. Early reactions take place within the chloroplast whereas the final breakdown products, NCCs, are indefinitely stored in the vacuole. The initial step of removing chl from the antenna and core complexes of

the photosystems remains unclear. In algae and higher plants the involvement of chl binding proteins and proteases in photosystem degradation are discussed. More recently, stay-green proteins (SGR) are believed to function in dismantling of photosynthetic chl- apoprotein complexes (Hörtensteiner, 2009) although the mechanism of SGR function remains unknown.

However, Chl *b* to *a* conversion is considered as an early; probably the first step of chl degradation (Hörtensteiner, 2006) followed by two consecutive steps removing phytol and Mg by chlorophyllase and a metal chelating substance (MCS). The role of chlorophyllase has recently been questioned and my own investigations proposed PPH catalyzing phytol hydrolysis during leaf sensescence (Schelbert et al., 2009; Schenk et al., 2007). Obtained pheophorbide (pheide) *a* is further converted to a colourless, blue-fluorescing intermediate, pFCC, in a two-step reaction by PAO and RCCR. pFCCs are directly or after further modifications exported from the plastid (Matile et al., 1992). Further steps are reminiscent of detoxification processes widely occurring in plants (Kreuz et al., 1996). Hence, pFCCs are activated by hydroxylation and after several modifications (R_1-R_3 in Figure 2) imported into the vacuole by a primary active transport system (Hinder et al., 1996; Frelet-Barrand et al., 2008). Due to the acidic vacuolar pH, modified FCCs are tought to be tautomerized non-enzymatically to their respective NCC isomers (Oberhuber et al., 2003; Hörtensteiner, 2006).

My work attempted to advance the knowledge on several aspects of the chl breakdown pathway. Namely, (i) Clarifying the long-proposed and established *in vivo* function of chlorophyllase (CLH) which led to identifying the esterase responsible for porphyrin-phytol hydrolysis, PPH; (ii) Studying the role of PPH in other instances of chl metabolism such as during fruit ripening of tomato; (iii) Investigating a possible degradation complex consisting of several chl catabolic enzymes, exclusively formed during senescence.

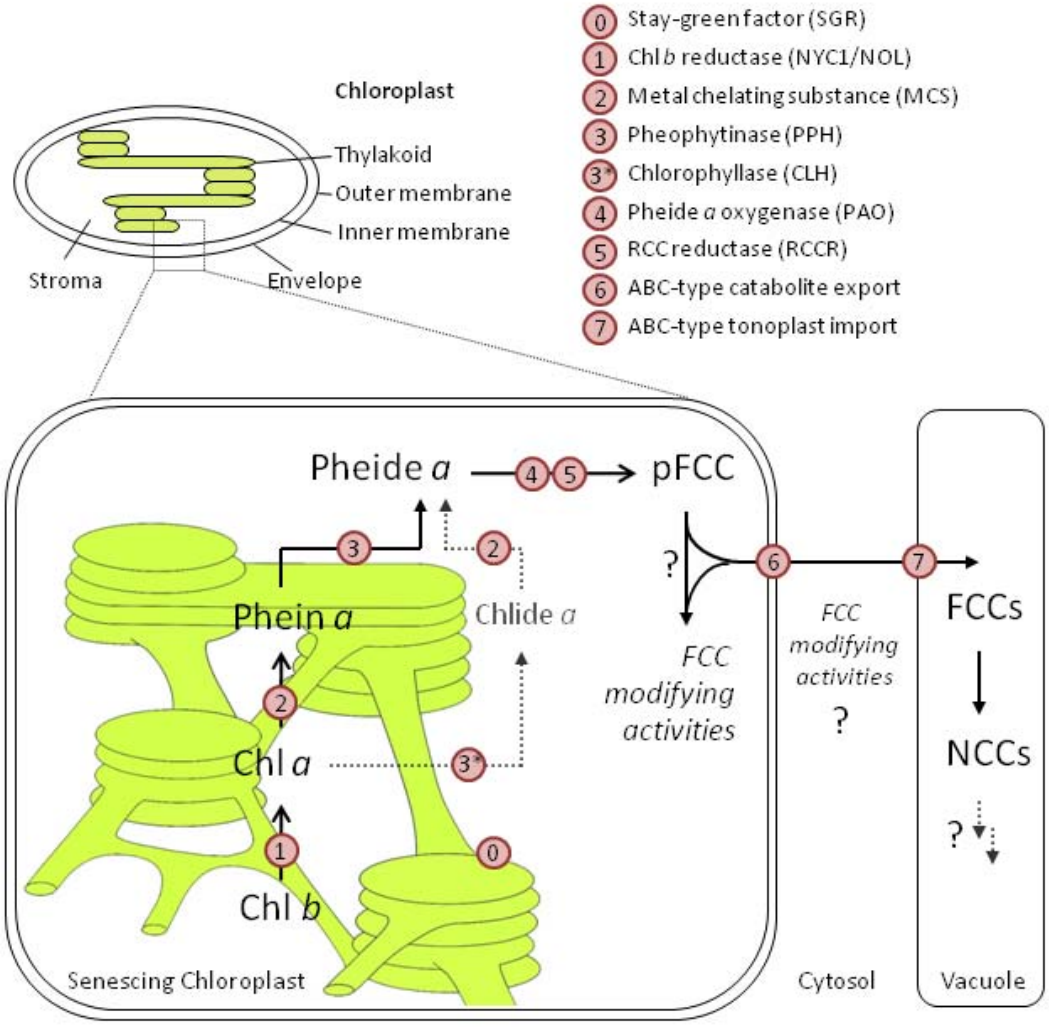

Figure 1 Schematic model of the chlorophyll degradation pathway in higher plants. The model integrates findings of this thesis. Involved steps are labeled by numbers and putative reactions are indicated with question marks. Thickness of arrows within the pathway reflects relative activities of respective enzymes. Therefore, CLHs only marginally contribute to chl breakdown, while the bulk of chl seems to be catabolized via pheophytin *a* by PPH (Schelbert et al. 2009).

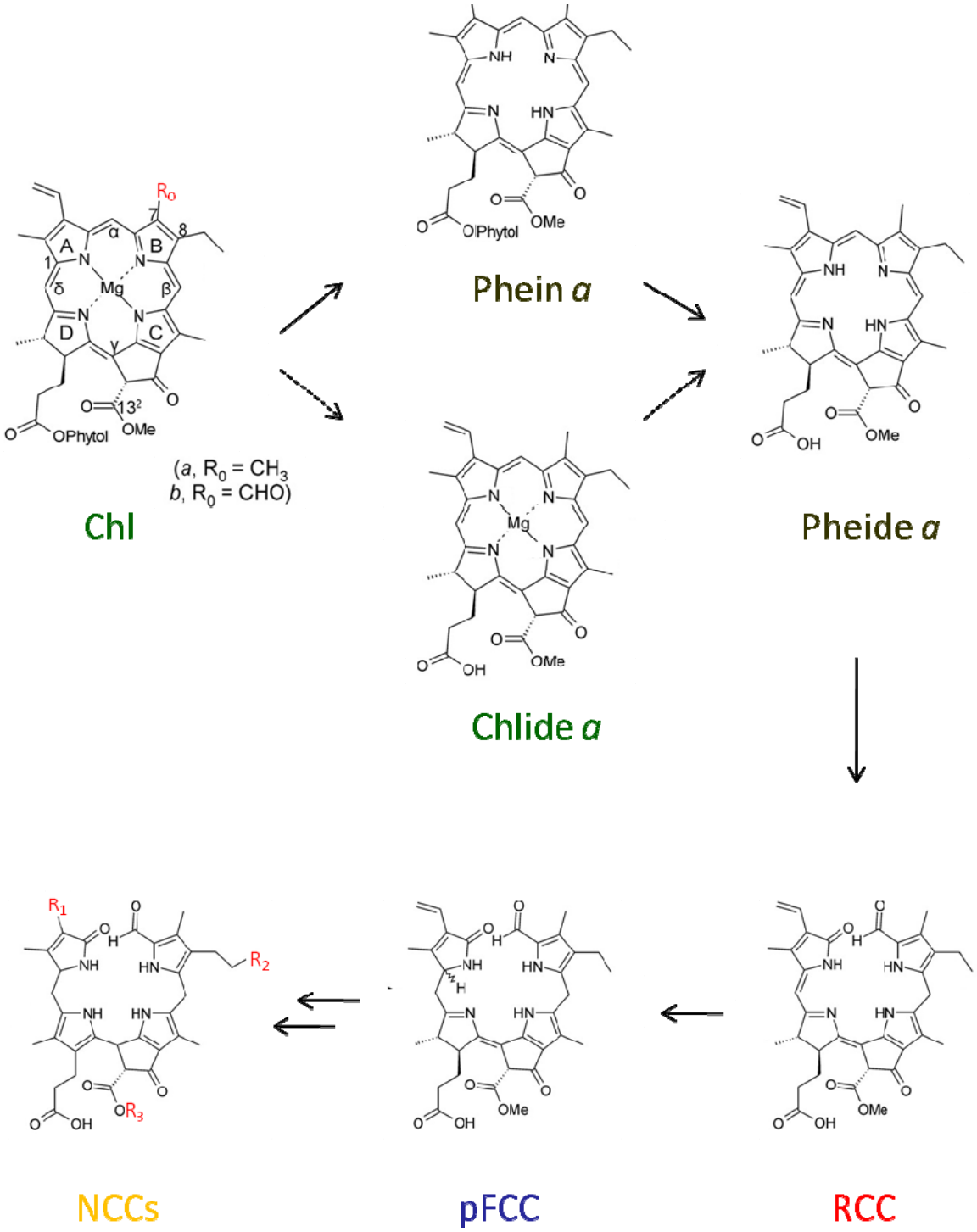

Figure 2 Chemical structures of chl and chl catabolites. Pyrrole rings (A-D), methine bridges (*α*-*δ*), and relevant carbon atoms are labeled in chl (*top left*). R_0= CH_3, chl *a*; R_0= CHO, chl *b*. R_1-R_3 in NCCs indicate modification sites.

2.1 Chlorophyll breakdown pathway

2.1.1 Removal of chlorophyll embedded in the photosystem

Whether chl-binding proteins are destabilized by proteases first and thereby allow chl release from the complexes or whether chl *b* reduction initiates complex destabilization is not clear. Light harvesting complex (LHC) II apoproteins are synthesized in chl *b*-less mutants, but undergo fast turnover (Harrison et al., 1993). Further, proteolytic cleavage does not initiate LHCII degradation in the stay-green (Bf993) genotype of *Festuca* (Thomas and Howarth, 2000). Early chl breakdown mutants deficient in chl *b* reductase (*nyc1/nol*) or pheophytinase (*pph-1*) as well as stay-green mutants (*sgr*) from different plant species display a clear retention of subunits of photosystem protein complexes (Park et al., 2007, Sato et al., 2009, Schelbert et al., 2009). The lack of chl-photosystem complex dismantling in these mutants indicates an interplay between proteolytic and chl catabolic activities during senescence. Thereby, the chl *b* to *a* conversion is suggested to be a prerequisite for the degradation of chl-associated proteins (Kusaba et al., 2007).

2.1.2 Chl *b* reductase

All but one of the NCCs isolated so far was shown to derive from chl *a* (Hörtensteiner, 2006; Müller et al., 2006). Therefore, it can be argued that chl is degraded only after the conversion of chl *b* to *a*. This is reasonable since PAO is highly specific to pheide *a*, with pheide *b* being a competitive inhibitor (Hörtensteiner et al., 1995). Chl *b* is a component of the antenna complexes (LHCs) manly of photosystem II. Removal of chl *b* from the LHCs leads to a destabilisation of the chl-protein complexes and a decline in PSII-associated light-harvesting complex II proteins (LCHbs) (Tanaka et al., 2001; Tanaka and Tanaka, 2005; Hörtensteiner, 2006). Therefore, *b* to *a* conversion is proposed to be the initial step of chl breakdown (Hörtensteiner, 2006).

The chlorophyll cycle describes the interconversion between chl(ide) *a* and *b* suggested being important in adjustment of the chl *a*/*b* ratio in various physiological conditions (Ito et al., 1996; Rüdiger, 2002). The oxidative part of the cycle acts mainly on chlide and is catalyzed by chlorophyllide *a* oxygenase (CAO) (Tanaka et al., 1998). Thereby, the C_7 methyl group of chlide *a* is oxidized to a formyl group via a C_7-hydroxy chlide *a* intermediate (Rüdiger, 2002). The reductive parts occur at the level of chl and are catalyzed by two consecutive reductions by different enzymes, a NADPH- dependent chl *b* reductase (NYC1/NOL) and a ferredoxin-dependent C_7-hydroxy chlide *a* reductase. Non yellowing coloring 1 (NYC1) and NYC1-like (NOL) proteins are thought to encode the chl *b* reductase (Kusaba et al., 2007). They co-localize in thylakoid membranes facing the stromal side where they act in the form of a complex (Sato et al., 2009).

2.1.3 Mg-dechelation

Two types of activities which are responsible for the release of the central Mg^{2+} ion of the porphyrin ring molecule were described in the past. One of them is a heat-stable, low-molecular weight compound demonstrating a metal-releasing activity in *Chenopodium album* extracts (Shioi et al., 1996), designated as metal-chelating substance (MCS) (formerly Mg-dechelating substance). The other is a constitutive Mg-dechelatase enzyme associated with chloroplast membranes (Vicentini et al., 1995). These divergent findings are explained by the possibility that MCS might act as a cofactor of Mg-dechelatase, working on its own. Further attempts on Mg-releasing activities were done by members of the Shioi lab (Suzuki and Shioi, 2002; Suzuki et al., 2005) where they show that the Mg-dechelatase enzyme displayed Mg-releasing activity in the presence of a common artificial substrate, chlorophyllin, but not on the native substrate chlide, whereas MCS was active on both. Molecular mass and especially biochemical properties of MCS differ between species (Costa et al., 2002; Suzuki and Shioi, 2002; Suzuki et al., 2005). Hence, it can be concluded that Mg-removal in the chl breakdown pathway is likely performed by low-molecular weight compounds whose structures are not known.

2.1.4 Phytol hydrolysis and its recycling

Dephytylation is an early step of the chl breakdown pathway in which chl is converted to chlorophyllide (chlide) and phytol. The hydrolysis of the lipophilic ester bond increases water solubility of further breakdown products. It is widely accepted that this hydrolysis is conducted by chlorophyllase (Chlase, CLH) which was first discovered by (Willstätter and Stoll, 1913). In the past, Chlase has been purified from a variety of plants and phytol-hydrolyzing activities were demonstrated in barley leaves, Citrus fruits and leaves as well as in Gingko leaves (Garcia and Galindo, 1991; Trebitsh et al., 1993; Matile et al., 1997; Okazawa et al., 2006). The *Arabidopsis* Chlase1 (named *COR1* or *CLH1*) was first identified as a gene induced by coronatine (Benedetti et al., 1998), a chlorosis-inducing phytotoxin produced by various plant pathogenic bacteria. *AtCLH1* was shown to be up regulated in leaves by methyl jasmonate (MeJA) treatment and wounding. In 1999, chloropyhllase genes were cloned from different organisms such as from *Citrus sinensis* fruits (*CsCLH1)*, and from *Chenopodium album* (*CaCLH*) and *Arabidopsis* leaves (*AtCLH1* and *AtCLH2*) (Jakob-Wilk et al., 1999; Tsuchiya et al., 1999).
Intracellular localization is often a key element elucidating enzyme function and regulation *in vivo*. This has been a controversial issue regarding the enzyme Chlase. Different proposed subcellular localization in the plastid inner envelope (Matile et al., 1997; Harpaz-Saad et al., 2007) or thylakoid membrane (Okazawa et al., 2006) has added to the confusion. Moreover, cloned *Citrus* and *Chenopodium* Chlase were suggested to be N-terminally processed and do not exhibit typical N-terminal

plastid transit peptides (Jakob-Wilk et al., 1999; Tsuchiya et al., 1999) leading to speculation that some chlorophyllases might be targeted elsewhere in the cell (Takamiya et al., 2000). These controversial findings questioned the involvement of Chlase in chl breakdown (Hörtensteiner, 2006). Indeed, we could provide reliable evidence that the *Arabidopsis* CLH1 and CLH2 are not essential during dark induced leaf senescence *in vivo* (Schenk et al., 2007). *At*CLHs displayed cytosolic localization when fused to GFP. Moreover, a study of insertion mutants of either CLH1 or CLH2 and a double mutant did not show any obvious phenotype during dark induced senescence.

Recently, we proposed an alternative hydrolase, pheopyhtinase (PPH) (Schelbert et al., 2009). PPH is a chloroplast-located and senescence-induced hydrolase widely distributed in higher plants. It is catalyzing the hydrolysis of the ester bond of the Mg-free chl pigment, pheopyhtin (phein), producing pheide and phytol. An *Arabidopsis* mutant (*pph-1*) was unable to degrade chl and thus, displayed a stay-green phenotype. Moreover, a similar phenotype is described for the rice homolog (*nyc3*) (Morita et al., 2009). In addition, PPH was identified in a proteome analysis on tomato chromoplasts (Barsan et al., 2010) indicating that chromoplasts comprise chl breakdown processes similar to those occurring in leaves (Thomas et al., 2009). These data lead to the conclusion that PPH and not CLH plays an important role in chl breakdown during senescence (Schelbert et al., 2009). By contrast, there is a study on Citrus fruit colour-break demonstrating that Chlase was located in the plastid of ethylene-treated fruit peel (flavedo) tissue in *Citrus limon* (Azoulay Shemer et al., 2008). Chlase accumulation was negatively correlated with chl quantity at the cellular level.

Whether PPH and Chlase have distinct roles and whether various tissues evolve different types of chl degradation, needs to be demonstrated. Further investigations are needed to fully understand the involvement of PPH and/or Chlase at early steps of chl breakdown during leaf senescence and fruit ripening.

Recycling of phytol Free phytol is generated by the hydrolysis of phein and chl by PPH and CLH, respectively. Little is known about the metabolic fate of phytol. Phytol derived from chl breakdown was shown to be either re-esterified to fatty acids (Peisker et al., 1989; Patterson et al., 1993) or irreversibly destroyed by photo degradation (Rontani et al., 1996). It has been suggested that chl-derived phytol could serve as a precursor of tocopherol biosynthesis since tocopherol increased concomitantly with the breakdown of chl in several plant species (Rise et al., 1989). Several lines of evidence support this conclusion. Incubation of labeled phytol with *Arabidopsis* seedlings led to the accumulation of labeled tocopherol (Ischebeck et al., 2006). This accumulation was abolished in *vte1* and *vte2* mutant seedlings, being defective in tocopherol biosynthesis. Moreover, heterologously expressed *At*VTE5 efficiently phosphorylated phytol to phytyldiphosphate in two steps (Valentin et al., 2006).

Based on data from the *vte5-1* mutant it has been estimated that 65% of the tocopherol phytyl side chain in leaves originates from VTE5-dependent recycling of free phytol from chl breakdown. Additionally, it has repeatedly been shown that fatty acid phytyl esters derived from phytol accumulated in plastoglobules (Bortlik, 1990; Gaude et al., 2007) which are present in increasing number and size during senescence progression. However, although it is well established that tocopherol serves as a potent antioxidant, a physiological advantage for phytol recycling serving for tocopherol synthesis in senescing tissue remains unknown.

2.1.5 Porphyrin ring opening by PAO

The first linear tetrapyrrole detectable in the chl breakdown pathway is the primary fluorescent chl catabolite (pFCC). pFCC is generated by the oxidative cleavage and reduction of pheide *a* by the activity of two enzymes; PAO and RCCR (Figure 3). The double reaction is performed via an unstable intermediate, RCC. Opening of the ring cycle is considered as a key step in chl catabolism, as it is irreversible and formed breakdown intermediates lose colour and toxicity by linearization and deconjugation of the remaining methine-bridges between the pyrrole units.

The establishment of an *in vitro* assay converting the intermediate pheide *a* to pFCC (Hörtensteiner et al., 1995) gave rise to the biochemical characterization followed by the molecular identification of PAO and RCCR (Wüthrich et al., 2000; Pružinská et al., 2003). *At*PAO is a Fe-dependent Rieske-type monooxygenase and as for other Rieske-type oxygenases the electron source driving the redox reaction is derived from reduced ferredoxin (Fd) (Hörtensteiner et al., 1995). PAO is introducing one atom of dioxygen at the α-methine bridge on ring B of pheide *a* to form RCC (Figure 3). The second oxygen atom of ring A is in all probability derived from water (Hörtensteiner, 1998; Hörtensteiner et al., 1998). Further, PAO activity is highly specific to pheide *a* as substrate, with pheide *b* being a competitive inhibitor (Hörtensteiner et al., 1995). The findings of *At*NCC-3 being hydroxylated at C_7 (Pružinská et al., 2005) that might derive from chl *b* without being fully reduced to chl *a* while entering the catabolic pathway questions the unique specificity of PAO to pheide *a* as substrate (Müller et al., 2006). A PAO-like monooxygenase identified in *Chlorella prototheco*ides (Curty et al., 1995) is less specific, causing the occurrence of chl *a* and *b*-derived degradation products (Iturraspe et al., 1995; Engel et al., 1996).

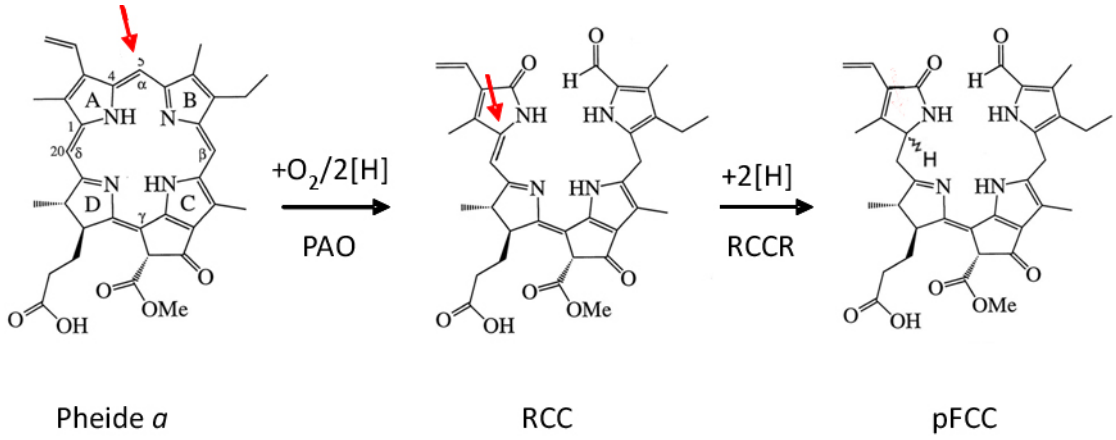

Figure 3 Opening of the porphyrin ring. Two-step cleavage of pheide *a* to pFCC with RCC as an intermediate**.** PAO is opening the ring cycle on the α-methine bridge and adds one oxygen on ring B. A second oxygen is added on ring A from water. Electron equivalents necessary for the reaction are derived from Fd. The subsequent reduction step of the C_{20}/C_1 double bond is performed by RCCR, creating a stereocenter in C_1, thereby forming either pFCC-1 or pFCC-2. Arrows indicate site of reactions. Adapted from Hörtensteiner, 1998.

PAO displays high activity during senescence even though basic activity levels are detected before the onset of senescence (Pružinská et al., 2003; Roca et al., 2004; Yang et al., 2004; Pružinská et al., 2005). Further, PAO was suggested to be associated with the envelope of gerontoplasts (Matile and Schellenberg, 1996). In contrast, PAO was recently localized at the thylakoid membrane not the envelope using PAO-GFP fusion analysis and immunoblot analysis of chloroplast membrane fractions (Hörtensteier lab, unpublished). Thylakoid localization is reasonable since early breakdown reactions take place at the origin of chl localization.

2.1.6 RCC reduction by RCCR

RCCR (alternatively named ACD2) catalyzes the reduction of the C_{20}/C_1 double bond of RCC to produce pFCC in a stereospecific manner (Rodoni et al., 1997) (Figure 3). RCCR is a soluble stromal protein requiring reduced Fd for RCC reduction but unlike PAO lacks a metal or flavin cofactor (Kräutler, 2003). Further, RCCR is related to a family of Fd-dependent bilin reductases, widely distributed among higher plants and related proteins are found in cyanobacteria (Frankenberg et al., 2001; Sugishima et al., 2009). It has been shown that in the coupled reaction of PAO and RCCR, one of two possible C_1 epimers of pFCC, either pFCC-1 (Mühlecker et al., 1997) or pFCC-2 (=1-*epi*-pFCC) (Mühlecker et al., 2000) is produced, depending on the plant species employed as a source of RCCR. The suggestion that the stereospecific action of RCCR is uniform within a plant family (Rodoni et al., 1997) could be confirmed by screening of 60 plant species (Hörtensteiner et al., 2000). This study displayed that indeed genera and species of the same family produce the same isomer. For example, RCCR in *Arabidopsis* forms pFCC-1 whereas in tomato, pFCC-2 is formed solely. Stereospecificity of

Arabidopsis RCCR is defined by a small protein domain, and a single amino acid exchange (F_{218} to V) alters the C_1 stereospecificity from pFCC-1 to pFCC-2 (Pružinská et al., 2007). RCCR mutants (*acd2-2*) functionally complemented with *At*RCCRs exhibiting alternative specificities displayed that downstream products, FCCs and NCCs followed the specificity of the complementing RCCRs. A recent study on the crystal structure of RCCR displayed that F_{218} is located on the inner side of the putative substrate-binding pocket, implying that substitution of this residue changes the shape of the pocket (Sugishima et al., 2009). Indeed, determination of the crystal structures of RCC-bound *At*RCCR and RCC-bound F_{218}V *At*RCCR, respectively revealed that the RCC in F_{218}V *At*RCCR rotated slightly compared with that in wild type (Sugishima et al., 2010). Thus, the geometrical arrangement of RCC and the two conserved acidic residues, Glu_{154} and Asp_{291}, appeared to be essential for the stereospecificity of the RCCR reaction.

In contrast, when chemically synthesized RCC (Kräutler et al., 1997) is incubated with RCCR *in vitro* stereospecificity is lost and both stereoisomers are formed, suggesting an influence of PAO or another factor (Rodoni et al., 1997). Indeed, RCC in not accumulating *in vivo* and only traces are detectable *in vitro* in respective assays (Rodoni et al., 1997). Moreover, biochemical interaction between PAO and RCCR was demonstrated in a bacterial two-hybrid screen (Pružinská et al., 2007). Therefore, it is highly likely that RCC is reduced by RCCR without release from PAO (Hörtensteiner, 1999).

RCCR is a single-copy gene in *Arabidopsis* constitutively expressed at all stages of leaf development (Pružinská et al., 2005). RCCR protein can be imported into chloroplasts *in vitro* (Wüthrich et al., 2000) and localizes to chloroplasts in mature leaves (Mach et al., 2001). In young seedlings and in response to stress, it is localized partially to both chloroplasts and mitochondria (Mach et al., 2001; Yao et al., 2004; Yao and Greenberg, 2006). However, localization in non-photosynthetic tissue and in mitochondria implies other function of RCCR (Yao and Greenberg, 2006). Thereby, a role of RCCR/ACD2 in cell death control triggered by *Pseudomonas syringae* and protoporphyrin IX treatments was discussed (Yao et al., 2004).

2.1.7 Membrane transport, modifications and final storage

Due to the identification of NCCs in the vacuole, a transport of chl catabolites from the senescing chloroplast (gerontoplast) into the vacuole has been concluded (Matile et al., 1988; Hinder et al., 1996). This process requires that catabolites cross the envelope of the chloroplast and the tonoplast.

Chloroplast export An ATP-dependent export of FCCs has been shown in senescing chloroplasts of barley (Matile et al., 1992). But the nature of the exporter is not known. Rather good substrate specificity can be expected for the respective chloroplast exporter, considering that pheide *a* accumulating in *pao* mutant lines is restricted to the chloroplast with no detection outside the organelle

(S. Aubry, personal communication). By contrast, RCCs were located outside the chloroplast in RCCR-deficient lines (Pružinská et al., 2007). This might be explained by the similar conformation of RCC and FCC, both being linear tetrapyrroles, hence acting as substrates. The mammalian ABCG2 transporter, also termed breast cancer resistance protein 1 (BCRP1), was shown to be involved in extrusion of diverse structurally unrelated chemicals out of the cell, among them porphyrins (Abbott, 2003; Hardwick et al., 2007). Knockout mice deficient in BCRP1 showed a porphyria-like phenotype, due to the accumulation of pheide *a* and protoporphyrin IX in their blood (Jonker et al., 2002). Thus plant homologs of ABCGs, so called White Brown Complex (WBC) proteins are likely candidates for FCC export from the plastid. The WBC subfamily is fairly high presented in the *Arabidopsis* genome with 28 members (Rea, 2007). Two members, WBC23 and 28 display increased gene expression levels during senescence (Zimmermann et al., 2004) and are predicted to be localized to the chloroplast (http://aramemnon.botanik.uni-koeln.de/). Moreover, WBC23-deficient plants (*wbc23-1*) exhibited a temporary stay-green phenotype in dark-induced senescence (Aubry, 2008). However, whether these WBC members are involved in FCC or other porphyrin or tetrapyrrole metabolite export during senescence remains to be shown.

FCC modifications Modifications found in NCCs occur after the formation of pFCC on its way to the vacuole. Modifications increase polarity and enable deposition of NCCs in the vacuole. Due to the diversity of NCCs found in different plant species, modifications can be classified into i) common reactions, found in NCCs of all investigated species or ii) species-specific modifications restricted to three positions at peripheral side chains (R_1-R_3 in Figure 2, for review see Hörtensteiner, 2006). Hydroxylation at C_8^2 and final isomerization of FCCs to NCCs in the acidic vacuole sap are present in all species whereas the dihydroxylation of the vinyl group of pyrrole A (R_1), a glucosylation and/or malonylation at position R_2 and C_{13}^2 demethylation (R_3) occur in a species- specific manner. Additionally, NCCs occur in two stereospecificities (see 2.1.6) either derived from pFCC-1 or pFCC-2. All but one (*At*NCC-3) (Pružinská et al., 2005; Müller et al., 2006) NCCs structurally analyzed so far originate from chl *a* subsequently, NCCs share tetrapyrrolic structures (Figure 2).

Demethylation at the C_{13}^2 carboxymethyl group has been described to be catalysed by the enzyme pheophorbidase (PPD) at the level of pheide (Shioi et al., 1996). PPD is, however, distributed in limited plant species (Suzuki et al., 2002). A possible connection of PPD presence and respective NCC formation has been suggested (Hörtensteiner, 2006) but cytosolic localization (Shioi et al. 1996) pointed this modification reaction to occur on the level of FCCs. Indeed, *At*PPD was located in the cytosol when fused to GFP and both, pFCCs and pheide served as substrates when incubated with *At*PPD after functional expression in *E. coli*. An *Arabidopsis* mutant line (*mes-16*) deficient in PPD showed high accumulation of FCCs (B. Christ, personal communication) indicating that in *Arabidopsis*

a failure of demethylation on the level of FCC results in an inhibited vacuolar import, or slower isomerization to NCCs.

Vacuole import A primary energized transport across the tonoplast of barley vacuoles has been demonstrated for *Bn*-NCC-1 (Hinder et al., 1996). Rather unexpectedly, the transport of *Bn*-NCC-1 was strongly inhibited by the barley-specific catabolite, *Hv*-FCC-2. These findings raised the possibility that FCCs rather than NCCs are transported across the tonoplast *in vivo* and conversion to NCCs occurs within the vacuole. This suggestion was supported by the findings of a nonenzymatic reaction accounting for the formation of NCCs (Oberhuber et al., 2003).

Two members of the multidrug resistance-associated protein (MRP) subfamily of ATP binding cassette (ABC) transporters, *At*MRP2 and *At*MRP3, were capable to transport NCCs (*Bn*-NCC-1) when expressed in yeast (Lu et al., 1998; Tommasini et al., 1998). In addition, a recent study proposed *At*MRP2 being involved in chl degradation since *AtMRP2* expression level is induced during senescence and ethylene-treated rosettes of *atmrp2* mutants showed reduced senescence (Frelet-Barrand et al., 2008)**.** Moreover, vacuolar uptake studies demonstrated that *AtMRP2* contributes significantly to overall organic anion pump activity *in vivo*. Taken together it can be hypothesized that *At*MRP2 acts as a vacuolar transporter for chl catabolites. However, since a high number of ABC transporters are encoded in the *Arabidopsis* genome (Sanchez-Fernandez et al., 2001) and their multi substrate acceptance causes difficulties identifying respective transporters, it is likely that several transporters are involved in FCC translocation over the tonoplast.

Final storage A nonenzymatic reaction accounting for the formation of NCCs implies that FCCs delivered to the acidic vacuole sap undergo a rapid, stereoselective isomerization which results in complete deconjugation of the four pyrrole units (Oberhuber et al., 2003). Some species keep final catabolites (NCCs) proportional to chl amount degraded such as demonstrated in *Arabidopsis* or oilseed rape (*Brassica napus*) (Mühlecker and Kräutler, 1996; Pružinská et al., 2005) whereas in other species such as tobacco and spinach, NCC levels are decreasing towards late stages of senescence (Hörtensteiner, 2006). Three different oxidation products of chl, probably degraded monopyrrole derivatives were found in senescing cotyledons of barley and radish (Suzuki and Shioi, 1999; Suzuki et al., 1999) which decreased towards late stages of senescence concomitant with an accumulation of unknown compound(s). This findings stress the assumption of NCCs being the final catabolites of chl breakdown (Matile, 1999; Hörtensteiner, 1999) and gives potential for further degradation of NCCs into low-molecular-weight compounds. Whether a further degradation of NCCs is coordinated or represents unspecific oxidation reactions which happen after loss of tissue integrity, remains unclear. Recently, accumulation of persistent FCCs which are modified at C_{17^3} were discovered in banana peels (*Musa acuminate*) and in senescent banana leaves as well as in de-greened leaves of *Spathi-*

phyllum wallisii (Moser et al., 2008; Banala et al., 2010; Kräutler et al., 2010). These `hypermodified` FCCs were stable against their typical and rapid, spontaneous isomerisation to NCCs.

2.2 Chlorophyll retention causes stay-greenness

Stay-green is the general term given to a variant plant in which senescence is delayed compared to a reference plant. Stay-green mutants have been found in many different plant species in dicotyledons such as *Arabidopsis*, tomato, *Nicotiana* and *Populus* and in monocotyledons including major crop plants (for review see (Hortensteiner, 2009). Stay-greenness can, in respect of retention or loss of photosynthetic activity, be classified into two categories: functional and non functional (cosmetic) stay-greens (Thomas and Howarth, 2000). Functional stay-greens display a delayed initiation (type A) or a slower progression (type B) of senescence (Figure 4). This can result in a higher yield and is therefore of great agronomical interest. For example, stay-greenness in a rice variety SNU-SG1 displayed increased grain yield (You et al., 2007). Non functional stay-greens (type C), being solely impaired in chl breakdown while other senescence parameters are not affected, are suitable to study and elucidate the chl degradation pathway.

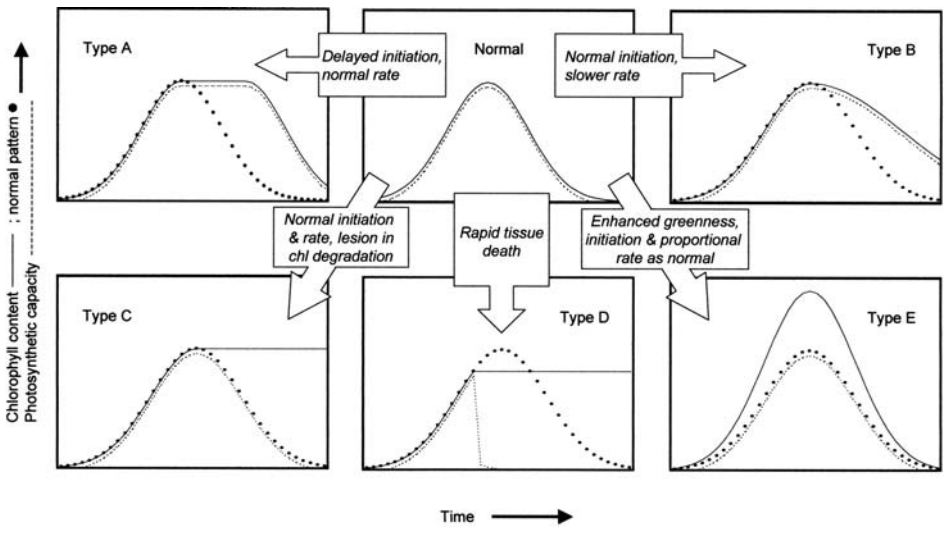

Figure 4. Five ways to stay green; Classification of different types of known stay-green mutants. Curves show chl content (solid line) and photosynthetic capacity (dashed line) for a representative leaf or plant. Type **A** stay-greens display a delay in the start of senescence, in type **B** senescence is progressed more slowly, type **C** stay-greens undergo normal functional senescence while chl breakdown is abolished, type **D** are staying green because of rapid tissue death and type **E** display a intensely green phenotype following the normal ontogenetic pattern. From Thomas and Howarth, 2000.

2.2.1 Stay-green factor (SGR)

Stay-green genes have only been identified recently but became a major focus in plant senescence research. It all started with a mutant study in *Festuca pratensis* (Thomas, 1987), where photosynthetic proteins remained stable although photosynthetic activity was reduced (Thomas et al., 1992). The gene was termed *SID (senescence-induced degradation)*. Introgression of the *sid* locus of *Festuca* into *Lolium* species allowed the molecular tagging of the gene (Thomas et al., 1997; Moore et al., 2005). The stay-green conferring *sid* locus was within a syntenic region in rice (Armstead et al., 2002; Sim et al., 2005) that contained a quantitative trait locus for stay-green, *sgr(t)* (Cha et al., 2002). Of several genes associated with this region, one rice gene, Os09g36200 displayed high similarity with the *Arabidopsis* gene At4g22920 having a senescence specific expression pattern (Zimmermann et al., 2004) and its loss of function conferred stay-greenness (Armstead et al., 2007). Independent analysis of two rice *sgr* mutants (Jiang et al., 2007; Park et al., 2007) and the *Arabidopsis nye1-1* mutant (Ren et al., 2007) further identified orthologous genes being responsible for the stay-green character. These findings paved the way for identifying genetic lesions of further mutants with defects in stay-green genes. These include Mendel`s green cotyledon mutant of pea (Armstead et al., 2007; Sato et al., 2007), tomato green flesh *gf* (Barry et al., 2008), bell pepper *cl* (Barry et al., 2008; Borovsky and Paran, 2008) and further rice alleles (Sato et al., 2007).

The identification of SGR proteins did not indicate a possible function since they do not contain any known domain. Neither photosynthesis- nor senescence-associated processes were significantly affected in *nye1-1* mutants (Ren et al., 2007). It was shown that SGR is not directly acting in chl breakdown by a catalytic activity (Park et al. 2007) or Mg-dechelating substance (Hortensteiner, 2009). PAO expression and protein abundance was not altered in several stay-green mutants (pea, rice, *Arabidopsis* and *Festuca*) when compared to respective wild types (Ougham et al., 2007; Ren et al., 2007; Sato et al., 2007; Aubry et al., 2008) concluding that SGR acts independently and upstream of PAO.

A common feature of SGR mutants is the retention of chl-binding proteins of the photosynthetic apparatus during senescence. Especially, LHCII subunits are highly stable in all SGR-deficient mutants analyzed so far (Jiang et al., 2007; Park et al., 2007; Sato et al., 2007; Aubry et al., 2008). Following the suggestion that chl binds to a carrier protein for proper chl extraction from the chl-protein complexes (Matile et al., 1999), a chl binding capacity of SGR *in vitro* could not be confirmed (Park et al., 2007). Interestingly, a co-immunoprecipitation experiment displayed that *Os*SGR specifically interacts with LHCII subunits *in vivo* (Park et al., 2007). This binding was not affected by the V99M mutation of one of the *Os*SGR mutants, suggesting that the mutation interrupts unknown enzymatic activity or binding of further regulatory factors.

In conclusion, stay-green genes encode members of a new family of chloroplast-located proteins which are likely to function in dismantling of photosynthetic chl- apoprotein complexes (Hörtensteiner, 2009). The mechanism of SGR function remains unknown.

2.2.2 Other stay-green mutants

Chl *b* reductase (NYC1/NOL) Cloning of non-yellow coloring1 (NYC1) and NYC1-like (NOL) from rice and analysis of respective mutants revealed that both *nyc1* and *nol* displayed a stay-green phenotype due to the retention of chl *b* with no prominent further enhancement of inhibition in the double mutant (Kusaba et al., 2007; Sato et al., 2009). Leaf functionality was lost although LHCII family members were selectively retained during senescence. Therefore, mutants displayed a cosmetic, non-functional type C stay-green phenotype with no lesions formed. Immunoprecipitation experiments demonstrated NYC1 and NOL interaction *in vitro* (Sato et al., 2009). Since chl *b* plays an important role in LHCII stability (Horn and Paulsen, 2004) mutant phenotypes revealed that the NYC1/NOL complex acts as a chl *b* reductase. A recent study confirmed chl *b* reductase activity for NOL in *Arabidopsis* and respective *in vitro* experiments demonstrated that chl *b* reductase converts not only free chl *b* but also chl *b* in LHCII into 7-hydroxymethyl chl *a* (Horie et al., 2009) suggesting that chl *b* reductase participates in the initial step of LHCII degradation.

Pheophytinase (PPH) The *Arabidopsis pph-1* mutant being impaired in dephytylation of Mg-free chl pigment (phein) during leaf senescence displayed a stay-green phenotype, in which senescence parameters were uncoupled from chl breakdown. Therefore, *pph-1* represents another example of a cosmetic, non-functional type C stay-green mutant. Although *pph-1* accumulated phein *a*, a lesion-mimic phenotype could not be detected (Schelbert et al., 2009). This is in contrast with *pao1/acd1* and *acd2* mutants accumulating potential phototoxic chl catabolites such as pheide *a* and RCC (Pružinská et al., 2005 and 2007). This might be explained by the fact that either phein *a* accumulation is moderate and does therefore not provoke cell death or phein *a* phototoxicity is prevented by its binding to LHCs. A similar phenotype was described for a rice mutant (*nyc3*) defective in the orthologous gene (Morita et al., 2009).

Pheophorbide *a* oxygenase (PAO) Another type C stay-green mutant also being directly impaired in an enzymatic step of chl degradation is *pao/acd1* having a non functional pheophorbide *a* oxygenase (PAO). PAO is identical to accelerated cell death 1 (ACD1) in *Arabidopsis* and its homolog in maize is characterized as lethal leaf spot 1 (LLS1) (Pružinská et al., 2003; Yang et al., 2004). A stay-green phenotype in *pao* is only visible during dark induced senescence. In natural senescence, where a plant is exposed to light, *pao* exhibits a lesion-mimic phenotype due to the accumulation of phototoxic pheide *a* at high quantities. Premature cell death was observed in *pao1* leaves and flowers.

Whether a feedback mechanism exists, which limits chl breakdown in mutants that are unable to degrade chl beyond pheide *a* (Pružinská et al., 2005), needs to be shown.

2.3 Significance of detoxifying porphyrins

2.3.1 Leaf senescence

Leaf senescence is a developmental process comprising structural changes such as the transition from chloroplasts to gerontoplasts, and biochemical processes such as the catabolism of macromolecules including chl. Senescence as the name implies, usually occurs at the end of the life of a leaf and could be classified as a type of programmed cell death (Ougham et al., 2005). But, senescence in plants has properties that distinguish it from other cell death processes. In fact, plant senescence is reversible and can rather be seen as a differentiation event (Thomas et al., 2003). Senescence appears to occur as a consequence of reproduction, as a result of competition for resources (older leaves versus younger foliage), and autumnal senescence of deciduous trees may be a consequence of decreasing daylight and temperature. It is an active and highly coordinated process with the aim to recycle nutrients from green tissues. In *Arabidopsis*, senescing leaves loose 85% of the nitrogen content, 37% of the carbon content and significant amounts of phosphate, potassium, sulphur and micronutrients (Himelblau and Amasino, 2001). As little CO_2 assimilation occurs during senescence, respiration can result in a net loss of C. Whether mobilization or respiration or both causes a decrease in observed C levels is unclear. Chl degradation is part of this complex process and becomes activated on the onset of senescence.

An early and significant change in cell structure is the breakdown of (mesophyll) chloroplasts, containing 70% of the overall leaf protein (Hörtensteiner and Feller, 2002; Lim et al., 2003). Chloroplasts are converted to gerontoplasts which in contrast to all other forms of plastids are, solely catabolic. Gerontoplasts loose volume and density due to the loss of stromal components and thylakoid structures, and the number and size of lipophilic plastoglobules increase (Matile et al., 1999). As a consequence breakdown and remobilization processes are initiated. Nucleus and mitochondria remain intact until the final stages of leaf senescence enabling senescence-associated gene (SAG) expression and respiration.

Whereas chromoplasts are typical forms of chl-free plastids in flowers and fruits, transition of chloroplasts into chromoplasts or gerontoplasts is comparable in respect of chl breakdown and the disassembly of thylakoids. But chromoplast differentiation is distinguished by the incorporation of a set of new proteins for *de novo* synthesis of carotenoids (Camara et al., 1995).

More than 800 genes show increased transcript levels during developmental leaf senescence in *Arabidopsis*, including several genes collectively termed senescence-associated genes (SAGs) (Bu-

chanan-Wollaston et al. 2005). A screening for SAGs illustrated the complexity of this network since most individual SAGs did not exhibit significant effects on the initiation and/or progression of leaf senescence when inactivated or overexpressed alone (He et al., 2001). Recently, increasing efforts have been made identifying senescence-regulating genes in *Arabidopsis* by analyzing the expression patterns of various transcription factors (TF). The NAC and WRKY transcription factors, such as *At*-NAP, *At*WRKY6 and *At*WRKY53 genes appeared to be involved in the regulation of senescence (Hinderhofer and Zentgraf, 2001; Robatzek and Somssich, 2001; Guo and Gan, 2006). More recently, out of 1500 TF annotated in *Arabidopsis*, microarray data show that around 100 genes encoding putative TF showed increased expression in developmental leaf senescence (Buchanan-Wollaston et al., 2005). In contrast, 81 TF were down-regulated during dark-induced senescence (Lin and Wu, 2004). However, the senescence TF network seems to be highly complex assumably with significant functional redundancy.

Plant hormones have been implicated in the regulation of various cellular processes, including senescence. Cytokinins are the most effective senescence-retarding growth regulators. Exogenous application of cytokinins delays leaf senescence in *Arabidopsis* and other plants. Transgenic tobacco and lettuce plants harbouring a cytokinin-producing system under the control of a senescence-specific promotor showed delayed post-harvest leaf senescence (Ori et al., 1999). In contrast, ethylene, methyl jasmonate, brassinosteroids and salicylic acid are known to promote signs of senescence (Gan and Amasino, 1997). Ethylen has long been known to be an endogenous regulator of senescence being involved in fruit ripening, flower and leaf senescence. For example, ethylene-insensitive mutants in *Arabidopsis*, *etr1* and *ore3*, exhibited a measurable delay in the initiation of leaf senescence (Oh et al., 1997). In *Citrus*, CLH1 expression is highly upregulated by ethylene (Jakob-Wilk et al., 1999; Azoulay Shemer et al., 2008) and *At*CLH1 levels increase under MeJA treatment (Tsuchiya et al., 1999). Additionally, transgenic tomato that have reduced ethylene synthesis trough expression of a bacterial ACC deaminase, exhibited significant delay in fruit ripening and deterioration (Klee et al., 1991). In conclusion, leaf senescence is controlled by a complex regulatory network with cross-linking of different hormonal pathways and TF, and including external factors.

2.3.2 Photosensitivity and cell death

Accumulation of free porphyrin in plants or animals causes cell death, due to light-dependent oxidative stress. The conjugated electron system of the pyrrole ring has the ability to absorb light energy even though it is uncoupled from the photosystem machinery. As a consequence, singlet oxygen is produced in large amounts, provoking cell death directly or inducing cell death signalling cascades (Wagner et al., 2004). Free porphyrin in a cell might accumulate when a step in synthesis or breakdown of any porphyrin is impaired.

In plants, lesion mimic mutants that accumulate large quantities of chl intermediates are showing dramatic consequences of the phototoxic ability of these intermediates. This is contrary to stay-green mutants such as *nye1, pph-1* or *nyc1/nol* which are defective at early steps of the pathway where chl is almost completely embedded in chl-photosystem complexes. The lesion mimic phenotype largely resembles the localized necrosis occurring during a hypersensitive response (HR) (Lorrain et al., 2003). In some lesion mimic mutants like *les22* in maize (Hu et al., 1998) or mutants displaying defects in steps of chl biosynthesis (Grimm, 1998) free porphyrin is accumulating in the cells. Related phenotypes occur in humans suffering of diverse types of porphyria, a photosensitive dermatosis (Ajioka et al., 2006), most of which are due to a specific defect in heme biosynthesis.
pao1/acd1 and *acd2* were isolated from a mutagenesis screen for plants showing a lesion mimic phenotype earlier then wild-type upon pathogen infection (Greenberg and Ausubel, 1993; Greenberg et al., 1994) both mutants accumulate large amounts of reactive oxygen species (ROS), being suggested to largely contribute to the lesion formation (Gray et al., 2002). In the case of *pao1*, pheide *a* accumulation was clearly shown to induce cell death (Pružinská et al., 2003; Tanaka et al., 2003; Pružinská et al., 2005). In *acd2-2*, RCC accumulation was shown to be positively correlated with the cell death progression as well (Pružinská et al., 2007). The mechanism by which cell death is conducted has not been elucidated to date.

2.3.3 Nitrogen economy

Nitrogen displays an essential nutrient for plants, representing a major constituent of numerous cellular compounds, including proteins, nucleic acids and lipids. A remarkable amount of 20% of the cellular nitrogen is bound in photosystem protein complexes; whereas only 2% is contributed by chl (Hörtensteiner, 2006). During leaf senescence nutrients are mobilized to seeds, storage organs or new vegetative growth (Himelblau and Amasino, 2001). Therefore, chl degradation can be seen as a detoxification process enabling the remobilization of nutrients which are energetically costly to aquire, such as fixed nitrogen from the photosystem protein complexes. Interestingly, nitrogen present in the chl pigment is not exported from senescing leaves, but remains within the cells in the form of linear tetrapyrrolic catabolites that accumulate in the vacuole.

III Aim of the thesis

During my PhD, I attempted to advance the knowledge on several aspects of the chl degradation pathway in leaf senescence and fruit ripening of higher plants by the following topics:

- Identifying the enzyme responsible for dephytylating activity in chl breakdown of senescing leaves in *Arabidopsis*, namely pheopyhtinase (PPH).
- Purifying heterologously expressed *At*PPH and determining its biochemical properties.
- Studying the role of PPH in other instances of chl metabolism, such as during fruit ripening of tomato.
- Identifying a possible degradation complex consisting of several chl catabolic enzymes, formed exclusively during senescence.
- Clarifying the long-proposed *in vivo* function of chlorophyllase (CLH).

My analyses provide substantial improvement in understanding the early reactions of chl breakdown in leaf senescence. Further, my findings underline the crucial role of PPH not only in leaf senescence but also in fruit ripening. Nevertheless, it also raises new issues for further work to be done.

IV Results

4.1 Own publications

4.1.1 The chlorophyllases AtCLH1 and AtCLH2 are not essential for senescence-related chlorophyll breakdown in *Arabidopsis thaliana*

Nicole Schenk*, Silvia Schelbert*, Marion Kanwischer, Eliezer E. Goldschmidt, Peter Dörmann, Stefan Hörtensteiner

* Joint first co-authors

Reprinted from: *FEBS Letters* 581 (2007): 5517- 5525

Phytol hydrolysis displays an early and important step in chl breakdown because it increases water solubility of further chl catabolites. *At*CLH1 and *At*CLH2 were considered to catalyze phytol hydrolysis during leaf senescence. This study provides evidence that these two chlorophyllases are not essential for senescence-related chl breakdown *in vivo*. A GFP fusion study revealed that *At*CLH1 and *At*CLH2 are located outside the chloroplast. Moreover, *clh1* and *clh2* single and double knockout lines degraded chl similar to wild type. These findings propose that an alternative, at the time of publication unknown esterase could act as chlorophyllase *in vivo*.

FEBS Letters 581 (2007) 5517 5525

The chlorophyllases AtCLH1 and AtCLH2 are not essential for senescence-related chlorophyll breakdown in *Arabidopsis thaliana*

Nicole Schenk[a,1], Silvia Schelbert[b,1], Marion Kanwischer[c], Eliezer E. Goldschmidt[d], Peter Dörmann[c], Stefan Hörtensteiner[a,b,*]

[a] *Institute of Plant Sciences, University of Bern, Altenbergrain 21, CH-3013 Bern, Switzerland*
[b] *Institute of Plant Biology, University of Zurich, Zollikerstrasse 107, CH-8008 Zurich, Switzerland*
[c] *Max-Planck-Institute of Molecular Plant Physiology, Am Mühlenberg 1, D-14476 Golm, Germany*
[d] *The Robert H. Smith Institute of Plant Sciences and Genetics in Agriculture, The Hebrew University of Jerusalem, Rehovot 76100, Israel*

Received 4 September 2007; revised 30 October 2007; accepted 31 October 2007

Available online 8 November 2007

Edited by Miguel De la Rosa

Abstract **One important reaction of chlorophyll (chl) breakdown during plant senescence is the removal of the lipophilic phytol moiety by chlorophyllase. AtCLH1 and AtCLH2 were considered to be required for this reaction in *Arabidopsis thaliana*. Here we present evidence against this assumption. Using green fluorescent protein fusions, neither AtCLH isoform localizes to chloroplasts, the predicted site of chlorophyll breakdown. Furthermore, *clh1* and *clh2* single and double knockout lines are still able to degrade chlorophyll during senescence. From our data we conclude that AtCLHs are not required for senescence-related chlorophyll breakdown in vivo and propose that genuine chlorophyllase has not yet been molecularly identified.**

Keywords: Chlorophyllase; Chlorophyll catabolites; Chlorophyll breakdown; Phytol; Senescence

1. Introduction

Chlorophyllase catalyzes the hydrolysis of chlorophyll (chl) to chlorophyllide (Chlide) and phytol. It is considered as the first enzyme of chl breakdown during leaf senescence and fruit ripening [1,2]. The enzyme is found in higher plants and algae, and chlorophyllases have been purified from different sources, including *Citrus sinensis*, *Chenopodium album* and *Pheaodactylum tricurnutum* [3–5]. In 1999, two research groups independently succeeded in cloning chlorophyllase genes (tentatively termed *CLH*) from *C. sinensis* (*CsCLH1*), *C. album* (*CaCLH*) and *Arabidopsis thaliana* (*AtCLH1* and *AtCLH2*) [6,7] and further genes have been described since then [2]. Surprisingly, not all molecularly identified CLHs contained a predicted chloroplast transit peptide. Thus, e.g. CaCLH was suggested to be imported into the vacuole *via* the ER [1,7]. Consequently, in addition to the pheophorbide *a* oxygenase (PAO)- and red chlorophyll catabolite reductase (RCCR)-dependent pathway that operates in senescing chloroplasts [2], extraplastidial CLHs together with so far unknown oxidases were considered to degrade chl inside the vacuole [1].

Several lines of evidence question the existence of and need for such an extraplastidial chl degradation machinery and raise doubts on the participation of CLHs in senescence-related chl breakdown in vivo. (i) Alteration of AtCLH1 levels by RNA interference did not cause a senescence-related phenotype [8]. (ii) Heterologously expressed CLH from wheat exhibited an equally high specificity for chl and unrelated hydrophobic *p*-nitrophenyl esters [9]. (iii) Except for PAO, chl oxidizing activities have so far not been molecularly identified nor have breakdown products of respective activities been identified [2].

In this work we aimed at elucidating whether AtCLH1 and AtCLH2 participate in senescence-related chl breakdown in *A. thaliana* in vivo. By using green fluorescent protein (GFP) fusions, we show that neither AtCLH isoform is located in chloroplasts. Furthermore, single and double knockout mutants of *AtCLHs* are only marginally affected in chl breakdown during senescence. Collectively, our data strongly support the hypothesis that in *A. thaliana* CLHs are not essential for senescence-related chl breakdown.

2. Materials and methods

2.1. Plant material

A. thaliana T-DNA insertion lines SALK_124978 (designated *clh1-1*; ecotype Columbia) and SAIL_646_E09 (*clh2-2*; Columbia) were obtained from the European Arabidopsis Stock Center, Nottingham, UK. FLAG_076H05 (designated *clh2-1*; ecotype Wassilewskija) was from INRA, Versailles, France. Homozygous plants were identified by PCR using T-DNA and gene-specific primers as listed in Supplementary Table 1 (see Fig. 2A). The T-DNA positions were confirmed by sequencing. Double mutants were obtained by crossing *clh1-1* with either *clh2-1* or *clh2-2*. Double homozygous F_2-plants were identified by PCR as above. Plants were grown on soil in long day (16 h light) growth rooms under fluorescent light of 60 120 μmol photons m^{-2} s^{-1} at 22 °C. Because chl degradation and chl degradation-related parameters had been shown to be identical in Wassilewskija and Columbia (Col-0) [10], the latter was used as representative wild type only. Senescence was induced by placing 3- to 4-week-old detached leaves on wet filter paper and incubating in permanent darkness for up to 7 d.

*Corresponding author. Address: Institute of Plant Biology, University of Zurich, Zollikerstrasse 107, CH-8008 Zurich, Switzerland.
E-mail address: shorten@botinst.uzh.ch (S. Hörtensteiner).

[1]These authors contributed equally to this work.

Abbreviations: chl, chlorophyll; Chlide, chlorophyllide; FCC, fluorescent chlorophyll catabolite; GFP, green fluorescent protein; NCC, non-fluorescent chlorophyll catabolite; PAO, pheophorbide *a* oxygenase; RCCR, red chlorophyll catabolite reductase

0014-5793/$32.00
doi:10.1016/j.febslet.2007.10.060

2.2. Generation and confocal microscopic analysis of GFP constructs

cDNAs for AtCLH1 (pda09091) and AtCLH2 (pdz786270) were obtained from the RIKEN resource. The insert of pdz786270 was confirmed by sequencing. For C-terminal fusions (AtCLH-GFP), cDNAs were PCR-amplified using Pfu polymerase (Promega) with primers as listed in Supplementary Table 1. After restriction digest, fragments were cloned into XmaI/SpeI-digested pUC18-GFP5T-sp [11]. Likewise, for N-terminal fusions (GFP-AtCLH), PCR fragments were cloned into pUC18-spGFP6 [11]. For a fusion between the N-terminal region of AtCLH2 and GFP, the AtCLH2-GFP construct was used as template to amplify by inverse PCR the relevant plasmid part. After DpnI digest to remove the template, amplification products were restricted with SpeI and religated. Constructs were confirmed by sequencing. Free GFP expressed from pUC18-spGFP6 and TIC110-GFP expressed from pCL60-FLTIC110-GFP (F. Kessler, personal communication) were used as controls. *A. thaliana* mesophyll protoplast isolation and confocal microscopic analyses were performed essentially as described [10,11].

2.3. Gene expression analysis

For RT-PCR analysis, total RNA was isolated from green leaves and reverse transcribed as described [12]. Semiquantitative PCR was performed using primers as listed in Supplementary Table 1. For Northern blot analysis of *CLH1*, RNA was isolated from 3-week-old plants grown on plates, which were incubated for 7 h in 20 mM MES, 10 μM Na_2HPO_4, pH 6.5 containing 1 mM methyl jasmonate or DMSO. For Northern blot analysis of *CLH2*, leaf material from plants grown for 6 weeks in long day conditions was used for RNA extraction. RNA electrophoresis (20 μg) and hybridization was according to standard procedures. A cDNA fragment derived from *CLH1* and a PCR product amplified with PD415 and PD414 (Supplementary Table 1) served as a probe for *CLH1* and *CLH2*, respectively.

2.4. Extraction and analysis of pigments

Fluorescent chlorophyll catabolites (FCCs) and non-fluorescent chlorophyll catabolites (NCCs) were extracted, quantified, and analyzed photometrically (chl) or by HPLC (NCCs, FCCs) according to published procedures [10,12]. For the determination of in vivo contents of Chlide, a fast isolation method was used in order to minimize artificial production of Chlide by chlorophyllases that become rapidly activated upon leaf tissue rupture during extraction. Leaves were ground in liquid nitrogen and suspended in 10% (v/v) 0.2 M Tris HCl pH 8 in acetone, cooled to −20 °C (5 ml g^{-1} fresh weight). After centrifugation (18000 × *g*, 2 min, 4 °C) the supernatant was analyzed by HPLC as described [12]. Chlide/chl ratios were calculated from peak areas recorded at 665 nm.

2.5. Protein extraction and immunoblot analysis

After grinding of leaf disks (1 cm diameter), total proteins were extracted into 20 mM sodium phosphate pH 7.5, 1% (w/v) polyvinylpyrrolidone, 0.1% (v/v) β-mercaptoethanol (25 μl $disk^{-1}$). Extracts were filtered through two layers of miracloth. Immunoblot analysis was performed as described [10] using anti-LHCII antibodies (1:2000) [13].

2.6. Chlorophyllase activity

Two different assays were employed to assess chlorophyllase activity. For an acetone-based assay, material from green leaves was extracted into 0.2 M Tris HCl pH 8:acetone, 1:1 (v/v) (5 ml g^{-1} fresh weight) and incubated at 25 °C in the dark. Reactions were stopped by the addition of 1 volume of acetone. For separation of Chlide from chl, 0.5 volume of hexane were added. Chlide in the lower aqueous/acetone phase was quantified photometrically. The Triton-X100-based assay was performed essentially as described [14]. Chloroplasts were isolated from green or senescent leaves as described [15].

3. Results

3.1. AtCLH1 and AtCLH2 are located outside the chloroplast

Only for AtCLH2 (At5g43860), a majority of available servers that predict subcellular localization of plant proteins [16], indicate a plastidial localization (Table 1). Yet, the scores found with e.g. TargetP, PProwler or Predotar were rather low, compared to PAO and RCCR, which have been experimentally shown to localize to plastids [2]. In the case of AtCLH1 (At1g19670) none of the used prediction servers favored localization within the chloroplast. In order to investigate the subcellular localization of AtCLHs in *A. thaliana* protoplasts, C-terminal (AtCLH-GFP) and N-terminal (GFP-AtCLH) GFP fusions were analyzed. Neither of the two AtCLHs targeted GFP to the plastid. Instead, green fluorescence was detected in the cytosol, like free GFP (Fig. 1A). Identical results were obtained with N-terminal fusions (data not shown). Cytosolic localization was also obtained when fusing GFP directly to the N-terminal 47 amino acids of AtCLH2, weakly predicted by ChloroP (Table 1) to contain a chloroplast transit peptide (data not shown). To investigate, whether targeting of AtCLHs to the chloroplast could be senescence-specifically regulated, C-terminal GFP fusions were expressed in protoplasts isolated from senescent leaves (Fig. 1B). Again, AtCLHs were not targeted to the plastids, but sometimes AtCLH2 was enriched in granular structures within the cytosol. The nature of these structures remains unknown.

3.2. Isolation of AtCLH T-DNA insertion lines

A T-DNA insertion line for AtCLH1 (*clh1-1*) and two lines for AtCLH2 (*clh2-1* and *clh2-2*) were obtained as shown in Fig. 2A. Double mutants were produced by crossing *clh1-1* with either *clh2-1* (*clh1-1 2-1*) or *clh2-2* (*clh1-1 2-2*). In each case, homozygous progeny was identified by PCR (data not shown). Expression of *AtCLH1* and/or *AtCLH2* transcripts was analyzed by Northern blots and/or by semiquantitative RT-PCR (Fig. 2B–D). Absence of *CLH1* transcripts could be confirmed in all lines containing the homozygous *clh1-1* allele. In *clh2-2* and *clh1-1 2-2*, *CLH2* transcripts were absent as well, but using RT-PCR, the *clh2-1* allele gave strong signals at the correct size (Fig. 2B). Northern blot analysis using a *CLH2* probe showed a strong 3.3 kb band, compared to the wild type *CLH2* signal at 1.6 kb (Fig. 2D). This indicated that transcription from a strong promoter within the FLAG T-DNA had occurred. The search for translational start sites in the putative T-DNA–CLH2 transcript revealed that translation could not be initiated from this chimeric mRNA (data not shown), hence the occurrence of active CLH2 protein in *clh2-1* and *clh1-1 2-1* can be ruled out. Collectively, the homozygous genotype and the expression analysis of the different mutants strongly suggested that the respective mutants represent null alleles. None of the *clh* mutants exhibited any obvious phenotype during entire plant development, including natural senescence (data not shown).

3.3. Absence of AtCLHs has a minor effect on dark-induced leaf senescence

Under detached leaf senescence, all *clh* mutants showed leaf yellowing after 5–7 d and were hardly distinguishable from wild type (Fig. 3A). Chl content decreased linearly during the senescence period in all lines. After 7 d some retention of chl was observed in the double knockout lines and in *clh2-1*, but yet more than 70% of the chl amount originally present had then been degraded (Fig. 3B). Increase of chl *a*/*b* ratios, a typical feature of senescence-related chl breakdown in *A. thaliana* [12], occurred in all investigated lines (results not shown). Loss of chl was accompanied by the loss of chl-binding pro-

Table 1
Prediction of subcellular localization of enzymes involved in chl degradation

Program[a]	Prediction range[b]	AtCLH1 At1g19670	Score	AtCLH2 At5g43860	Score	AtPAO At3g44880	Score	AtRCCR At4g37000	Score
ChloroP	0 1 (>0.5)	Not Chlpl	0.44	Chlpl	0.51	Chlpl	0.58	Chlpl	0.56
TargetP	0 1 (>0.5)	mTP	0.02 (3)[c]	mTP	0.08 (4)[c]	mTP	0.04 (1)[c]	mTP	0.21 (3)[c]
		cTP	0.16	cTP	0.71	cTP	0.97	cTP	0.73
		SP	0.26	SP	0.02	SP	0.01	SP	0.03
		Other	0.73	Other	0.31	Other	0.1	Other	0.07
iPSort	0 1[d] (<0.083)	Not Mito or Chlpl	0.13	Not Mito or Chlpl	0.1	Mito or Chlpl	0	Mito or Chlpl	0
						Chlpl	Yes	Chlpl	Yes
PCLR	0 1 (>0.42)	NonC	0.15	Chlpl	0.85	Chlpl	0.99	Chlpl	0.6
PProwler	0 1	mTP	0.09	mTP	0.14	mTP	0	mTP	0.01
		cTP	0.01	cTP	0.61	cTP	0.99	cTP	0.98
		SP	0.03	SP	0.17	SP	0	SP	0
		Other	0.86	Other	0.07	Other	0	Other	0
Predotar	0 1	mTP	0.01	mTP	0.01	mTP	0.07	mTP	0.07
		cTP	0.01	cTP	0	cTP	0.86	cTP	0.96
		SP	0.01	SP	0	SP	0.01	SP	0
		Other	0.97	Other	0.99	Other	0.13	Other	0.03
WoLF-PSORT	0 1[e]	Cyto	0.93	Chlpl	0.32	Chlpl	0.29	Chlpl	0.61
				Mito or Chlpl	0.29	Mito	0.21	Mito or Chlpl	0.42
				Cyto	0.21	Plas	0.21	Nucl	0.21
				Mito	0.18	Golg	0.14	Mito	0.14

Chlpl, chloroplast; cTP, chloroplast transit peptide; Golg, golgi; Mito, mitochondrium; mTP, mitochondrial transit peptide; Nucl, Nucleus; Plas, plasma membrane; SP, secretory pathway.
[a]For references, see [16] and http://aramemmon.botanik.uni-koeln.de.
[b]Threshold values are given in parentheses.
[c]Reliability classes 1 (highest) to 5 (lowest) are given in parantheses.
[d]Scoring according to average negative charge.
[e]Comparison done with 14 best neighbour proteins.

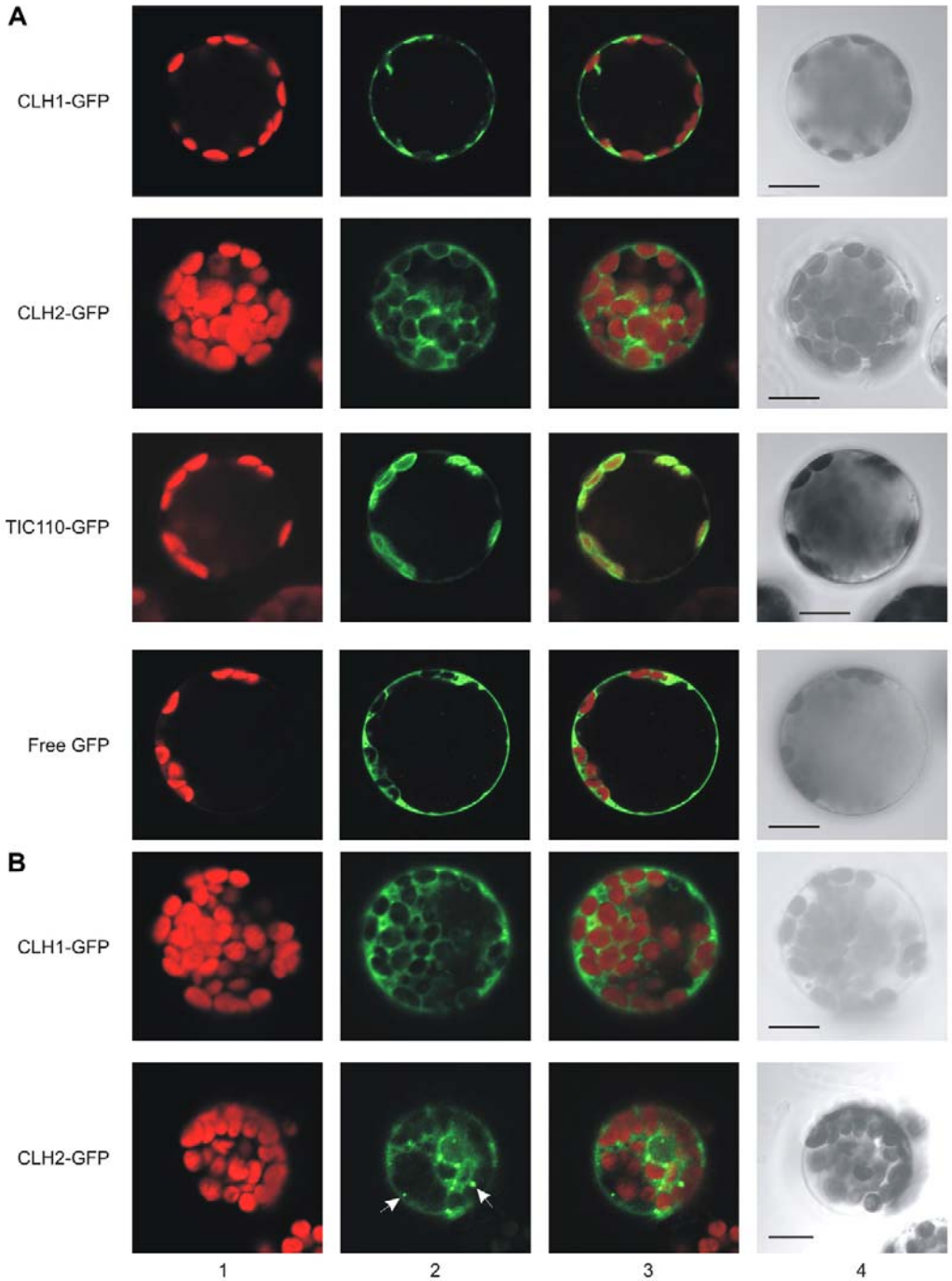

Fig. 1. In vivo targeting of GFP constructs to *A. thaliana* mesophyll protoplasts. After transfer of CLH1-GFP, CLH2-GFP, TIC110-GFP and free GFP in protoplasts isolated from green (A) or 3 d-dark incubated leaves (B), GFP fusions were monitored by confocal laser scanning microscopy. Lane 1, autofluorescence; lane 2, GFP fluorescence; lane 3, merge of GFP and autofluorescence; lane 4, bright field images. In panel B, arrows point to GFP-stained vesicles. Bar length, 10 μm.

teins in all *clh* mutants and wild type as judged from immunoblots using anti-LHCII antibodies (Fig. 3C). Thereby loss of LHCII abundance was slightly delayed in CLH2-deficient lines.

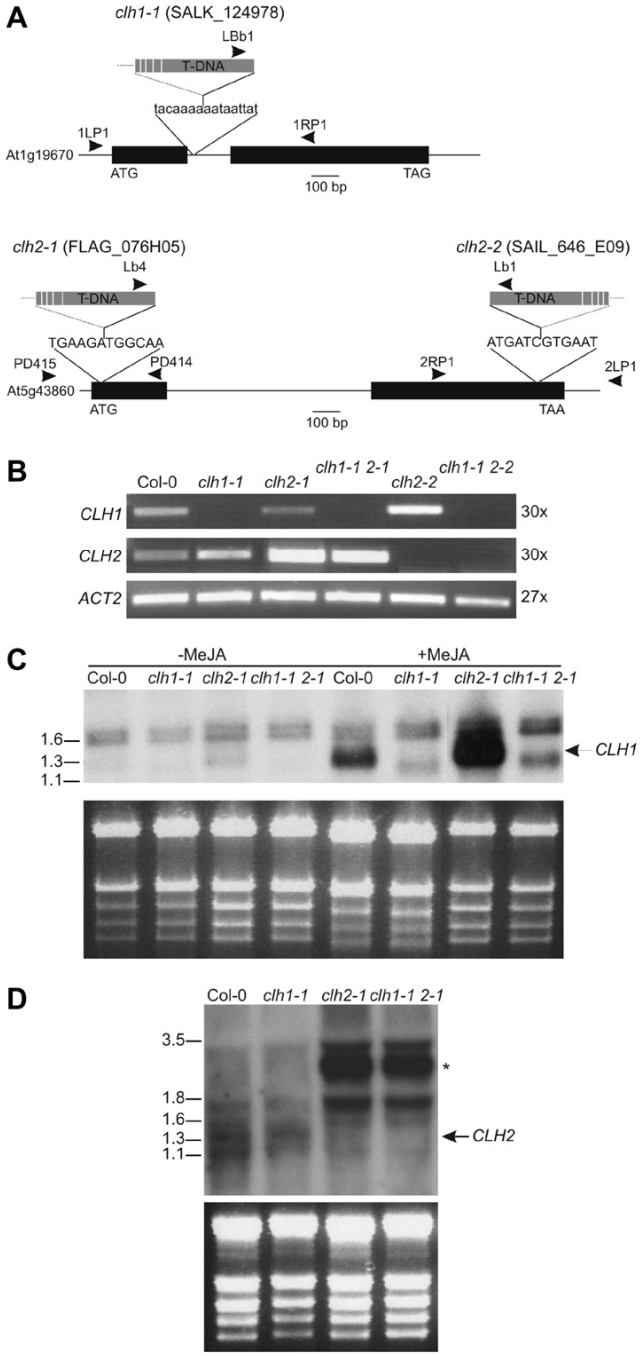

Fig. 2. Identification of *A. thaliana clh* mutants. (A) Gene structures of *CLH1* (At1g19670) and *CLH2* (At5g43860) showing the sites of T-DNA insertion in *clh1-1*, *clh2-1* and *clh2-2*. Arrowheads indicate the location of primers used for PCR analyses. (B) RT-PCR analysis of *CLH1* and *CLH2* gene expression in *clh* single and double mutants. *Actin2* (*ACT2*) was used as control. Numbers of PCR cycles performed are indicated on the right. (C) Northern blot analysis of *CLH1* expression in the absence (−MeJA) or after exposure to 1 mM methyljasmonate (+MeJA) for 7 h. (D) Northern blot analysis of *CLH2* expression. An additional 3.3 kb band cross-reacting with the *CLH2* probe in lines containing the *clh2-1* allele is labeled with an asterisk. See Section 3.2. for further details. The bottom parts of panels C and D show the RNA gel as loading control. Sizes of RNA marker bands are in kb.

To determine the contribution of the two CLHs to overall chlorophyllase activity, in vitro activities were assessed in two different well-established assays, using either acetone or Triton X100 for solubilization (Fig. 4A). Absence of CLH2 did only marginally affect chlorophyllase activity, but activities were drastically reduced in the absence of CLH1. The two ana-

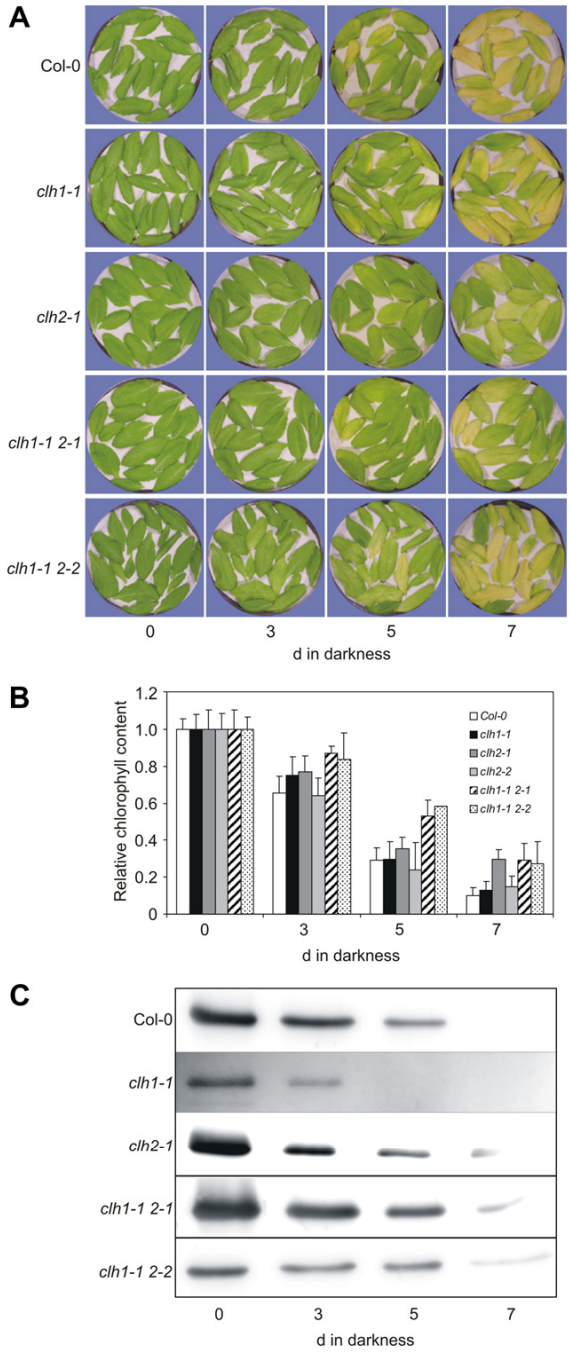

Fig. 3. Characterization of *clh1* and *clh2* single and double knockout lines during dark-induced senescence. (A) Phenotype of leaves. (B) Determination of total chl content. Values are means ± S.D. of at least two independent experiments with each three replicates. (C) Immunodetection of LHCII.

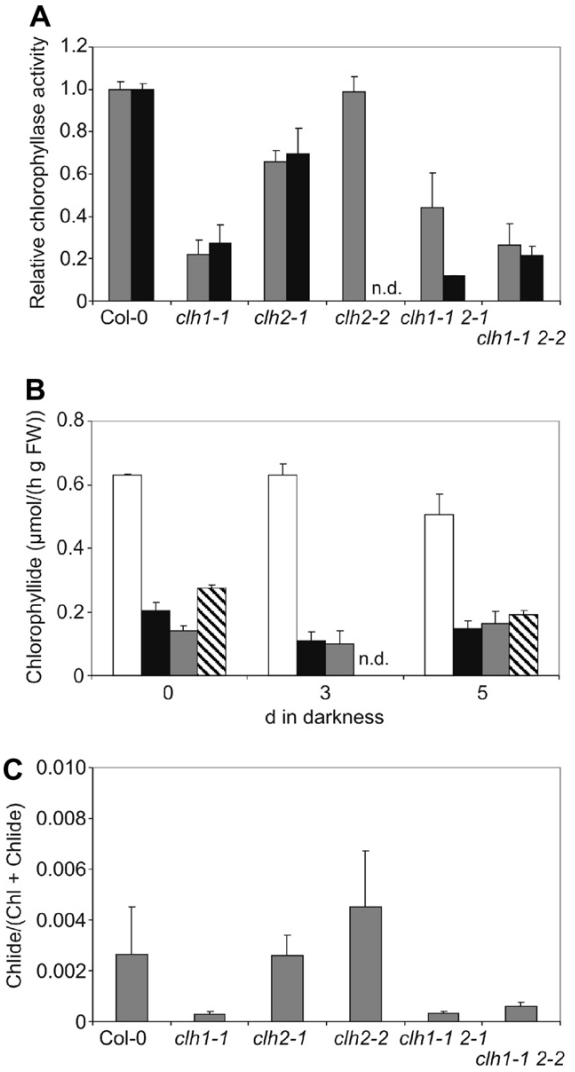

Fig. 4. Determination of chlorophyllase activity in *clh1* and *clh2* single and double knockout lines. (A) Relative in vitro chlorophyllase activity was assessed after solubilization with either Triton X100 (gray) or acetone (black). See Section 2.6. for further details. Values are means ± S.D. of at least four independent experiments with each three replicates. (B) Chlorophyllase activity during dark-induced senescence. Assays were performed after Triton X100-solubilization of total leaf extracts of Col-0 (white), *clh1-1 2-1* (black) and *clh1-1 2-2* (gray), or of isolated Col-0 plastids (hatched). Values are means ± S.D. of two independent experiments with each three replicates. (C) Quantification of the chlorophyllide fraction (Chlide) of total green pigments in non-senescent leaves. Chlide and chl were separated by HPLC as described in Section 2.4. Values are means ± S.D. of two independent experiments with each three replicates. n.d., not determined.

lyzed double mutants retained significant activity (about 25–45% in the Triton X100-based assay), which was similar to the activity residing within isolated chloroplasts of the wild type (Fig. 4B). During dark-induced senescence, in vitro chlorophyllase activity slightly decreased in wild type and no significant increase in overall activity was evident in the two double knockout lines or in isolated wild type chloroplasts (Fig. 4B). Thus, neither the absence of cytosolic AtCLH1 and AtCLH2 in isolated wild type chloroplasts, nor *clh1 clh2* double knockouts uncovered alternative senescence-regulated chlorophyllases. Possibly, genuine chlorophyllases are not senescence-regulated, or, more probably, their activity cannot be assessed under the applied assay conditions.

To analyze in vivo chlorophyllase activities, Chlide contents in the different mutants were measured. In all lines, the Chlide fraction of total chl was below 0.5%. Chlide amounts largely correlated to the in vitro measured chlorophyllase activities (Fig. 4A) and, hence, Chlide accumulation in Col-0 and *clh2* single knockout lines mainly resulted from some residual activity of AtCLH1 during extraction (Fig. 4C).

3.4. *AtCLH mutants degrade chl via PAO/RCCR-catalyzed formation of FCCs and NCCs*

The fact that *clh* mutants degraded chl at similar rates like wild type raised the question whether in the mutants breakdown of chl followed the PAO/RCCR pathway, which leads to the accumulation of FCCs and NCCs [2,12]. Alternatively, oxidative or peroxidative pathways have been postulated [17], which could be active in the mutants, but this would not lead to the formation of FCCs and NCCs. To distinguish between these possibilities, FCC and NCC formation was analyzed (Fig. 5). In wild type, three known NCCs (*At*-NCC-1, 2 and 5) and three FCCs (*At*-FCC-1, 2 and 3 (pFCC-1)) were identified in respective HPLC chromatograms. The same catabolites were formed in single and double *clh* mutants (data shown for *clh1-1*, *clh2-1* and *clh1-1 2-1*).

4. Discussion

Structure elucidation of NCCs from different plant species revealed the existence of dephytylated linear tetrapyrroles derived from chl *a* [2,18]. Likewise, mutations in genes of different chl catabolic enzymes, such as *A. thaliana pao1* and *acd2-2*, cause the accumulation of dephytylated intermediates [10,12,13] indicating that removal of the phytol moiety by chlorophyllase is an early step in senescence-related chl breakdown. Two independent groups reported the molecular nature of chlorophyllases (termed CLHs) in 1999 [6,7], but the in vivo involvement of CLHs in chl breakdown during senescence has so far not been verified.

4.1. *AtCLHs are located outside the plastid*

Except for *Citrus* CLHs [9,19] and (partially) for AtCLH2 (Table 1) [1,7], all other CLHs were predicted to localize out-

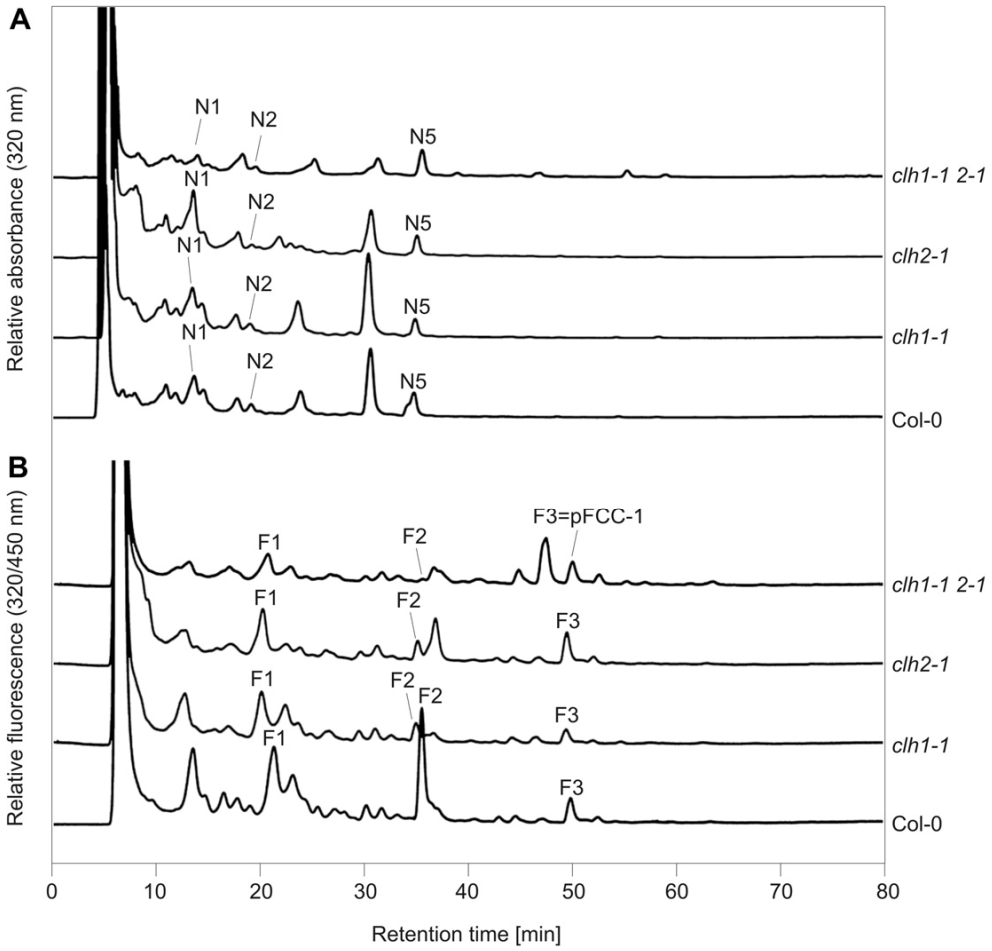

Fig. 5. HPLC analysis of colorless chl breakdown products in *clh* mutants. Chl catabolites after 5 d of dark-induced senescence were separated by HPLC, and absorbance (A) and fluorescence (B) were recorded for the identification of *A. thaliana* NCCs and FCCs, respectively [12]. N1, *At*-NCC-1; N2, *At*-NCC-2; N5, *At*-NCC-5; F1, *At*-FCC-1; F2, *At*-FCC-2, F3, *At*-FCC-3 (= pFCC-1).

side the chloroplast [1,9]. Experimental confirmation of such prediction has so far only been obtained in two cases, i.e. CsCLH1 and *Ginkgo biloba* [19,20]. Our finding of cytosolic localization of AtCLHs is in line with the fact that AtCLHs have so far not been identified in chloroplast proteome approaches [21,22]. When senescent mesophyll protoplasts were used for transient expression, green fluorescence was sometimes found in cytoplasmic vesicles (Fig. 1B). The alternative extraplastidial chl breakdown pathway proposed by Takamiya et al. [1] was supposed to involve transfer of chl via chloroplast-derived lipophilic globules. These globules occur in a senescence-specific manner, and as demonstrated by confocal imaging contain chl [23]. It cannot be ruled out that in senescent cells, some AtCLH2 locates to such globules, where it might act as chlorophyllase in vivo. Indeed, *clh2* mutants showed a slight delay in chl degradation, which was accompanied with some retention of LHCII protein, a feature known from different types of true stay green mutants [24]. Despite, the overall contribution of such a mechanism appears to be marginal.

4.2. Does a chl degradation pathway exist outside plastids?

PAO and RCCR have been shown to locate to chloroplasts [22,25], suggesting that their respective substrates, pheophorbide *a* and red chl catabolite, are formed inside the plastid. Following this concept, it is highly likely to assume that also the preceding dephytylation and dechelation steps take place within the chloroplast. If an alternative (extraplastidial) pathway exists (see above), its contribution to overall chl breakdown during senescence can be estimated from mutants that are blocked in the PAO/RCCR pathway. Yet, chl is largely retained in *pao1* and *lls1* [12,13] indicating that no significant chl degradation occurred through a bypass *via* such alternative degradation machinery. Furthermore, in several plant species including *A. thaliana*, the amounts of NCCs accumulating in senescent leaves correlate to the amount of chl present in green leaves [12], implying that the PAO/RCCR pathway is (almost) exclusively responsible to account for senescence-related chl degradation. Finally, neither *AtCLH1* nor *AtCLH2* expression is positively regulated with leaf senescence [26,27], nor does overall activity increase during senescence (Fig. 4B). Our data indicate slight retention of chl degradation in the absence of AtCLH2, but not AtCLH1. Collectively, we like to conclude that AtCLH2 might marginally contribute to overall chl breakdown in *A. thaliana* leaf senescence, but rule out the requirement of AtCLH1. Nevertheless, overall in vitro wild type activity seems to be mainly dominated by CLH1, raising the question what function CLH1 might have? *CLH1* expression is highly up-regulated by necrotrophic pathogens [8] and, thus, it might function in chl degradation in pathogen-infected tissue, i.e. after cell disintegration, thereby minimizing oxidative effects to the surrounding non-infected tissue.

4.3. Are other enzymes acting as chlorophyllases in vivo?

Expressed sequence tags of CLHs are available for different higher and lower plants, and algae. In contrast, within the genome of the diatom *Pheaodactylum tricornutum*, which contains a highly active chlorophyllase [5], sequences with significant homology to higher plant CLHs are not readily identifiable (S. Hörtensteiner, unpublished). This indicates, that chlorophyllase activity is not unequivocally linked to proteins with structural similarity to CLH, but implies that alternative enzymes could act as chlorophyllases in vivo. Our data support this assumption and provokes the notion that the genuine chlorophyllases might have escaped molecular identification so far. What is the molecular nature of alternative chlorophyllases? It is reasonable to assume that, like CLHs [28], alternative chlorophyllases would also contain motifs common to lipases or lipolytic enzymes. The *A. thaliana* genome encodes more than 70 potential lipase-like proteins, several of which are predicted to locate to the chloroplast. Future work analyzing respective candidate proteins might shed light on new chlorophyllases that possibly are required for senescence-related chl breakdown in vivo.

Acknowledgements: We thank F. Kessler for pCL60-FLTIC110-GFP and D. Rentsch for pUC18-spGFP6 and pUC18-GFP5T-sp. We thank S. Meier and C. Brinkmann for their help with confocal microscopy and I. Anders for technical support. This project was funded by the Swiss National Science Foundation (3100A0-105389) and the National Center of Competence in Research Plant Survival, research program of the Swiss National Science Foundation.

Appendix A. Supplementary data

Supplementary data associated with this article can be found, in the online version, at doi:10.1016/j.febslet.2007.10.060.

References

[1] Takamiya, K., Tsuchiya, T. and Ohta, H. (2000) Degradation pathway(s) of chlorophyll: what has gene cloning revealed? Trends Plant Sci. 5, 426–431.
[2] Hörtensteiner, S. (2006) Chlorophyll degradation during senescence. Annu. Rev. Plant Biol. 57, 55–77.
[3] Trebitsh, T., Goldschmidt, E.E. and Riov, J. (1993) Ethylene induces *de novo* synthesis of chlorophyllase, a chlorophyll degrading enzyme, in *Citrus* fruit peel. Proc. Natl. Acad. Sci. USA 90, 9441–9445.
[4] Tsuchiya, T., Ohta, H., Masuda, T., Mikami, B., Kita, N., Shioi, Y. and Takamiya, K. (1997) Purification and characterization of two isozymes of chlorophyllase from mature leaves of *Chenopodium album*. Plant Cell Physiol. 38, 1026–1031.
[5] Terpstra, W. (1981) Identification of chlorophyllase as a glycoprotein. FEBS Lett. 126, 231–235.
[6] Jakob-Wilk, D., Holland, D., Goldschmidt, E.E., Riov, J. and Eyal, Y. (1999) Chlorophyll breakdown by chlorophyllase: isolation and functional expression of the *Chlase1* gene from ethylene-treated *Citrus* fruit and its regulation during development. Plant J. 20, 653–661.
[7] Tsuchiya, T., Ohta, H., Okawa, K., Iwamatsu, A., Shimada, H., Masuda, T. and Takamiya, K. (1999) Cloning of chlorophyllase, the key enzyme in chlorophyll degradation: finding of a lipase motif and the induction by methyl jasmonate. Proc. Natl. Acad. Sci. USA 96, 15362–15367.
[8] Kariola, T., Brader, G., Li, J. and Palva, E.T. (2005) Chlorophyllase 1, a damage control enzyme, affects the balance between defense pathways in plants. Plant Cell 17, 282–294.
[9] Arkus, K.A.J., Cahoon, E.B. and Jez, J.M. (2005) Mechanistic analysis of wheat chlorophyllase. Arch. Biochem. Biophys. 438, 146–155.
[10] Pružinská, A., Anders, I., Aubry, S., Schenk, N., Tapernoux-Lüthi, E., Müller, T., Kräutler, B. and Hörtensteiner, S. (2007) In vivo participation of red chlorophyll catabolite reductase in chlorophyll breakdown. Plant Cell 19, 369–387.
[11] Meyer, A., Eskandari, S., Grallath, S. and Rentsch, D. (2006) AtGAT1, a high affinity transporter for γ-aminobutyric acid in *Arabidopsis thaliana*. J. Biol. Chem. 281, 7197–7204.

[12] Pružinská, A. et al. (2005) Chlorophyll breakdown in senescent Arabidopsis leaves: characterization of chlorophyll catabolites and of chlorophyll catabolic enzymes involved in the degreening reaction. Plant Physiol. 139, 52–63.
[13] Pružinská, A., Anders, I., Tanner, G., Roca, M. and Hörtensteiner, S. (2003) Chlorophyll breakdown: pheophorbide *a* oxygenase is a Rieske-type iron-sulfur protein, encoded by the *accelerated cell death 1* gene. Proc. Natl. Acad. Sci. USA 100, 15259–15264.
[14] Ben-Yaakov, E., Harpaz-Saad, S., Galili, D., Eyal, Y. and Goldschmidt, E.E. (2006) The relationship between chlorophyllase activity and chlorophyll degradation during the course of leaf senescence in various plant species. Israel J. Plant Sci. 54, 129–135.
[15] Matile, P., Schellenberg, M. and Vicentini, F. (1997) Localization of chlorophyllase in the chloroplast envelope. Planta 201, 96–99.
[16] Schwacke, R., Flügge, U.I. and Kunze, R. (2004) Plant membrane proteome databases. Plant Physiol. Biochem. 42, 1023–1034.
[17] Janave, M.T. (1997) Enzymic degradation of chlorophyll in cavendish bananas: in vitro evidence for two independent degradative pathways. Plant Physiol. Biochem. 35, 837–846.
[18] Kräutler, B., Jaun, B., Bortlik, K.-H., Schellenberg, M. and Matile, P. (1991) On the enigma of chlorophyll degradation: the constitution of a secoporphinoid catabolite. Angew. Chem. Int. Ed. Engl. 30, 1315–1318.
[19] Harpaz-Saad, S. et al. (2007) Chlorophyllase is a rate-limiting enzyme in chlorophyll catabolism and is posttranslationally regulated. Plant Cell 19, 1007–1022.
[20] Okazawa, A., Tang, L., Itoh, Y., Fukusaki, E. and Kobayashi, A. (2006) Characterization and subcellular localization of chlorophyllase from *Ginkgo biloba*. Z. Naturforsch. C 61, 111–117.
[21] Ferro, M. et al. (2003) Proteomics of the chloroplast envelope membranes from *Arabidopsis thaliana*. Mol. Cell Prot. 2, 325–345.
[22] Kleffmann, T., Russenberger, D., von Zychlinski, A., Christopher, W., Sjolander, K., Gruissem, W. and Baginsky, S. (2004) The *Arabidopsis thaliana* chloroplast proteome reveals pathway abundance and novel protein functions. Curr. Biol. 14, 354–362.
[23] Guiamét, J.J., Pichersky, E. and Noodén, L.D. (1999) Mass exodus from senescing soybean chloroplasts. Plant Cell Physiol. 40, 986–992.
[24] Park, S.-Y. et al. (2007) The senescence-induced staygreen protein regulates chlorophyll degradation. Plant Cell 19, 1649–1664.
[25] Wüthrich, K.L., Bovet, L., Hunziker, P.E., Donnison, I.S. and Hörtensteiner, S. (2000) Molecular cloning, functional expression and characterisation of RCC reductase involved in chlorophyll catabolism. Plant J. 21, 189–198.
[26] Liao, Y., An, K., Zhou, X., Chen, W.-J. and Kuai, B.-K. (2007) *AtCLH2*, a typical but possibly distinctive chlorophyllase gene in *Arabidopsis*. J. Integr. Plant Biol. 49, 531–539.
[27] Zimmermann, P., Hirsch-Hoffmann, M., Hennig, L. and Gruissem, W. (2004) GENEVESTIGATOR. Arabidopsis microarray database and analysis toolbox. Plant Physiol. 136, 2621–2632.
[28] Tsuchiya, T., Suzuki, T., Yamada, T., Shimada, H., Masuda, T., Ohta, H. and Takamiya, K. (2003) Chlorophyllase as a serine hydrolase: identification of a putative catalytic triad. Plant Cell. Physiol. 44, 96–101.

4.1.2 Pheophytin pheophorbide hydrolase is involved in chlorophyll breakdown during leaf senescence in *Arabidopsis*

Silvia Schelbert, Sylvain Aubry, Bo Burla, Birgit Agne, Felix Kessler, Karin Krupinska, and Stefan Hörtensteiner

Reprinted from: *The Plant Cell* 21 (2009): 767-785

This study unequivocally demonstrates the identification of a new esterase, pheophytinase (PPH) being responsible for the phytol-hydrolyzing step in chl breakdown. PPH is shown to be a chloroplast-located and senescence-induced hydrolase being highly specific for the Mg-free chl pigment (pheophytin), producing pheophorbide and phytol. An *Arabidopsis* mutant (*pph-1*) was unable to degrade chl and, thus, displayed a stay-green phenotype. Hence, PPH is proposed as being the major dephytylating activity in chl breakdown during leaf senescence.

The Plant Cell, Vol. 21: 767–785, March 2009, www.plantcell.org © 2009 American Society of Plant Biologists

Pheophytin Pheophorbide Hydrolase (Pheophytinase) Is Involved in Chlorophyll Breakdown during Leaf Senescence in *Arabidopsis* [W][OA]

Silvia Schelbert,[a] Sylvain Aubry,[a,1] Bo Burla,[a,b] Birgit Agne,[c] Felix Kessler,[c] Karin Krupinska,[d] and Stefan Hörtensteiner[a,2]

[a] Institute of Plant Biology, University of Zürich, CH-8008 Zurich, Switzerland
[b] Postech-University of Zürich Global Research Laboratory Pohang, University of Science and Technology, Pohang, 790-784, Korea
[c] Laboratoire de Physiologie Végétale, Institut de Biologie, Université de Neuchâtel, CH-2009 Neuchâtel, Switzerland
[d] Institute of Botany and Central Microscopy, University of Kiel, D-24098 Kiel, Germany

During leaf senescence, chlorophyll is removed from thylakoid membranes and converted in a multistep pathway to colorless breakdown products that are stored in vacuoles. Dephytylation, an early step of this pathway, increases water solubility of the breakdown products. It is widely accepted that chlorophyll is converted into pheophorbide via chlorophyllide. However, chlorophyllase, which converts chlorophyll to chlorophyllide, was found not to be essential for dephytylation in *Arabidopsis thaliana*. Here, we identify pheophytinase (PPH), a chloroplast-located and senescence-induced hydrolase widely distributed in algae and land plants. In vitro, *Arabidopsis* PPH specifically dephytylates the Mg-free chlorophyll pigment, pheophytin (phein), yielding pheophorbide. An *Arabidopsis* mutant deficient in PPH (*pph-1*) is unable to degrade chlorophyll during senescence and therefore exhibits a stay-green phenotype. Furthermore, *pph-1* accumulates phein during senescence. Therefore, PPH is an important component of the chlorophyll breakdown machinery of senescent leaves, and we propose that the sequence of early chlorophyll catabolic reactions be revised. Removal of Mg most likely precedes dephytylation, resulting in the following order of early breakdown intermediates: chlorophyll → pheophytin → pheophorbide. Chlorophyllide, the last precursor of chlorophyll biosynthesis, is most likely not an intermediate of breakdown. Thus, chlorophyll anabolic and catabolic reactions are metabolically separated.

INTRODUCTION

Loss of green color is the most obvious sign of leaf senescence. A pathway of chlorophyll breakdown, comprising several enzymic reactions, has been elucidated in recent years (Hörtensteiner, 2006; Kräutler and Hörtensteiner, 2006). The early steps are localized in the chloroplast, but the final products of chlorophyll, linear tetrapyrrolic compounds termed nonfluorescent chlorophyll catabolites (NCCs) (Kräutler et al., 1991), are stored in the vacuole. The pathway starts with the removal of phytol and Mg by chlorophyllase (Willstätter and Stoll, 1913) and metal-chelating substance (Suzuki et al., 2005), respectively, before the porphyrin ring of the resulting intermediate, pheophorbide (pheide), is oxygenolytically opened by pheide *a* oxygenase (PAO) (Hörtensteiner et al., 1998). The product of this reaction is red chlorophyll catabolite, which, without release from PAO, is site-specifically reduced by red chlorophyll catabolite reductase to yield the primary fluorescent chlorophyll catabolite (FCC), pFCC (Mühlecker et al., 1997; Rodoni et al., 1997). After export from the chloroplast (Matile et al., 1992), pFCC is modified by reactions reminiscent of detoxification processes widely occurring in plants (Kreuz et al., 1996). Thus, pFCC is hydroxylated and after further (species-specific) modification (Kräutler, 2003; Hörtensteiner, 2006), the resulting FCCs are imported into the vacuole by a primary active transport process (Hinder et al., 1996). Finally, FCCs are converted to their respective NCCs by nonenzymatic tautomerization, catalyzed by the acidic vacuolar sap (Oberhuber et al., 2003). Structure analysis of NCCs from different plant species has revealed that, with one exception, they are all derived from chlorophyll *a* (Kräutler, 2003; Müller et al., 2006). A reason for this is the exclusive specificity of PAO for pheide *a* (Hörtensteiner et al., 1995), and it has been proposed that chlorophyll *b* to chlorophyll *a* conversion is a prerequisite for breakdown beyond the level of pheide (Hörtensteiner, 2006). It was suggested that decreasing the chlorophyll *b* portion in the chlorophyll-protein complexes of the photosystems causes their destabilization (Horn and Paulsen, 2004) and could trigger both apoprotein and chlorophyll degradation (Rüdiger, 2002; Hörtensteiner, 2006). This was corroborated recently by cloning of *NON-YELLOW COLORING1* (*NYC1*) and *NYC1-LIKE* (*NOL*) (Kusaba et al., 2007; Sato et al., 2009). *NYC1* and *NOL* encode two subunits of chlorophyll *b* reductase (Sato et al., 2009), which

[1] Current address: Department of Plant Sciences, University of Cambridge, Downing Street, Cambridge CB2 3EA, UK.
[2] Address correspondence to shorten@botinst.uzh.ch.
The author responsible for distribution of materials integral to the findings presented in this article in accordance with the policy described in the Instructions for Authors (www.plantcell.org) is: Stefan Hörtensteiner (shorten@botinst.uzh.ch).
[W]Online version contains Web-only data.
[OA]Open Access articles can be viewed online without a subscription.
www.plantcell.org/cgi/doi/10.1105/tpc.108.064089

catalyzes the first half of chlorophyll *b* to chlorophyll *a* reduction, i.e., conversion of chlorophyll *b* to 7-hydoxymethyl chlorophyll *a*. *nyc1* and *nol* mutants stay green during senescence and thereby selectively retain photosystem II (PSII) light-harvesting complex subunits (LHCII) and exhibit particularly high concentrations of chlorophyll *b*.

Mutants that retain greenness during senescence are collectively called stay-green mutants. Different types of stay-greens have been defined (Thomas and Howarth, 2000), and type C mutants were thought to be specifically impaired in chlorophyll catabolism, while other senescence-related processes proceed as normal. To date, three groups of type C stay-green mutants have been characterized, and their genetic lesion identified. Besides *nyc1*/*nol*, deficiency in the *PAO* gene was shown to cause a stay-green phenotype when senescence is induced in permanent darkness (Pružinská et al., 2005). In contrast with *nyc1*, *pao* mutants exhibit a lesion mimic phenotype under natural senescence, a consequence of the phototoxicity of the pheide *a* that accumulates in these mutants (Pružinská et al., 2003, 2005; Tanaka et al., 2003). Recently, a third group of type C stay-green mutants has become a major focus in plant senescence research. The best characterized of these mutants, Bf993 of *Festuca pratensis*, is defective in a gene now termed *stay-green* (*SGR*) (Thomas, 1987). *Festuca SGR* (Armstead et al., 2006, 2007) and orthologous genes have been molecularly identified from mutants of different species, such as *Arabidopsis thaliana* (*non yellowing1* [*nye1*]) (Ren et al., 2007), rice (*Oryza sativa*) (Jiang et al., 2007; Park et al., 2007; Sato et al., 2007), pea (*Pisum sativum*) (Sato et al., 2007; Aubry et al., 2008), bell pepper (*Capsicum annuum*) (Barry et al., 2008; Borovsky and Paran, 2008), and tomato (*Solanum lycopersicon*) (Barry et al., 2008). The *SGR* genes encode a family of novel chloroplast-located proteins, which most likely are required for chlorophyll-protein complex dismantling as a prerequisite for chlorophyll degrading enzymes to access their substrate (Park et al., 1998).

Chlorophyllase, which catalyzes the hydrolysis of chlorophyll to chlorophyllide (chlide) and phytol, was considered to be the rate-limiting step of the pathway (Takamiya et al., 2000; Harpaz-Saad et al., 2007). In 1999, chlorophyllase genes (termed *Chlase* or *CLH*) were cloned from orange fruit (*Citrus sinensis*) (Jakob-Wilk et al., 1999) as well as from Lamb's quarters (*Chenopodium album*) and *Arabidopsis* leaves (Tsuchiya et al., 1999), and further genes have been described since then (Hörtensteiner, 2006). Surprisingly, using well-established web-based programs, only some of these chlorophyllases were predicted to localize to the chloroplast, which led to the suggestion of alternative pathways of chlorophyll breakdown operating outside the plastid (Takamiya et al., 2000), or questioned the involvement of CLHs in chlorophyll breakdown (Hörtensteiner, 2006). Recently, it was shown that the two *Arabidopsis* chlorophyllases (CLH1 and CLH2) are not essential for in vivo chlorophyll breakdown during leaf senescence (Schenk et al., 2007).

Here, we report the identification of candidates for chlorophyll dephytylation based on a functional genomic approach that considers features expected for such a hydrolase, including senescence-related regulation and chloroplast localization. In the course of our investigations, we show that one of the candidate genes (At5g13800) encodes a pheophytin (phein = Mg-free chlorophyll) hydrolase. We therefore named At5g13800 pheophytinase (PPH). *PPH* mutants, termed *pph*, exhibit a type C stay-green phenotype during senescence. *pph-1* retains thylakoid ultrastructure and photosystem protein subcomplexes. Heterologously expressed PPH dephytylates phein to pheide but does not accept chlorophyll as substrate. Small but significant quantities of phein *a* are found in *pph-1*, indicating that also in vivo, PPH functions as a phein hydrolase. PPH orthologs are present in different higher plant genomes, indicating an important function. Collectively, we identified a likely candidate for porphyrin-phytol hydrolysis involved in senescence-related chlorophyll breakdown in vivo. The enzyme is active on phein but not chlorophyll. We therefore propose that the early reactions of chlorophyll breakdown in leaves proceed in the following order: chlorophyll *b* → chlorophyll *a* → phein *a* → pheide *a*.

RESULTS

Identification of Possible Phytol-Hydrolyzing Proteins in *Arabidopsis*

Biochemical and molecular analysis of chlorophyll breakdown together with structure elucidation of FCCs and NCCs had indicated that pigment dephytylation is an early reaction of the pathway most likely occurring inside the chloroplast (Hörtensteiner, 2006). Chemically, phytol cleavage is an ester hydrolysis reaction; thus, candidate proteins, like most esterases and lipases (Fojan et al., 2000), likely contain an α/β hydrolase fold. Using The Arabidopsis Information Resource (TAIR) *Arabidopsis* genome annotation (release 8), we screened for proteins whose descriptions contained the phrase "alpha/beta" (Figure 1A). Of the resulting 462 proteins, 42 were predicted by ChloroP (Emanuelsson et al., 1999) to localize to the chloroplast. No function had yet been assigned for 30 of these proteins belonging to 24 gene loci. Similar to other genes involved in chlorophyll catabolism (*SGR1*, *NYC1*, and *PAO*), expression of the candidates was expected to be rather high during senescence. According to microarray expression data of the 24 candidate genes (Zimmermann et al., 2004), three genes, namely, At1g54570, At3g26840, and At5g13800, showed a leaf senescence-related expression pattern (Figure 1B). We focused on these genes and analyzed respective T-DNA insertion mutants. These were obtained from the SALK resource (Alonso et al., 2003) (*at1g54570-1*, SALK_034549; *at3g26840-1*, SALK_071769; and *at5g13800-1* [*pph-1*], SALK_000095), and homozygous progeny were identified by PCR. Since At1g54570 and At3g26840 are homologous genes that could have redundant function, we also produced an *at1g54570-1 at3g26840-1* double knockout line. When detached leaves were incubated in darkness to induce senescence, all lines except *at5g13800-1* degraded chlorophyll like the wild type (Figure 1C). Thus, absence of At5g13800 caused a stay-green phenotype. In addition, *At5g13800* expression was highly correlated with *PAO* expression when analyzing coexpression with web-based analysis tools (http://www.Arabidopsis.leeds.ac.uk/act/coexpanalyser.php; http://csbdb.mpimp-golm.mpg.de/csbdb/dbcor/ath.html). We concluded that At5g13800 might be a genuine chlorophyllase, but in the course of our investigations

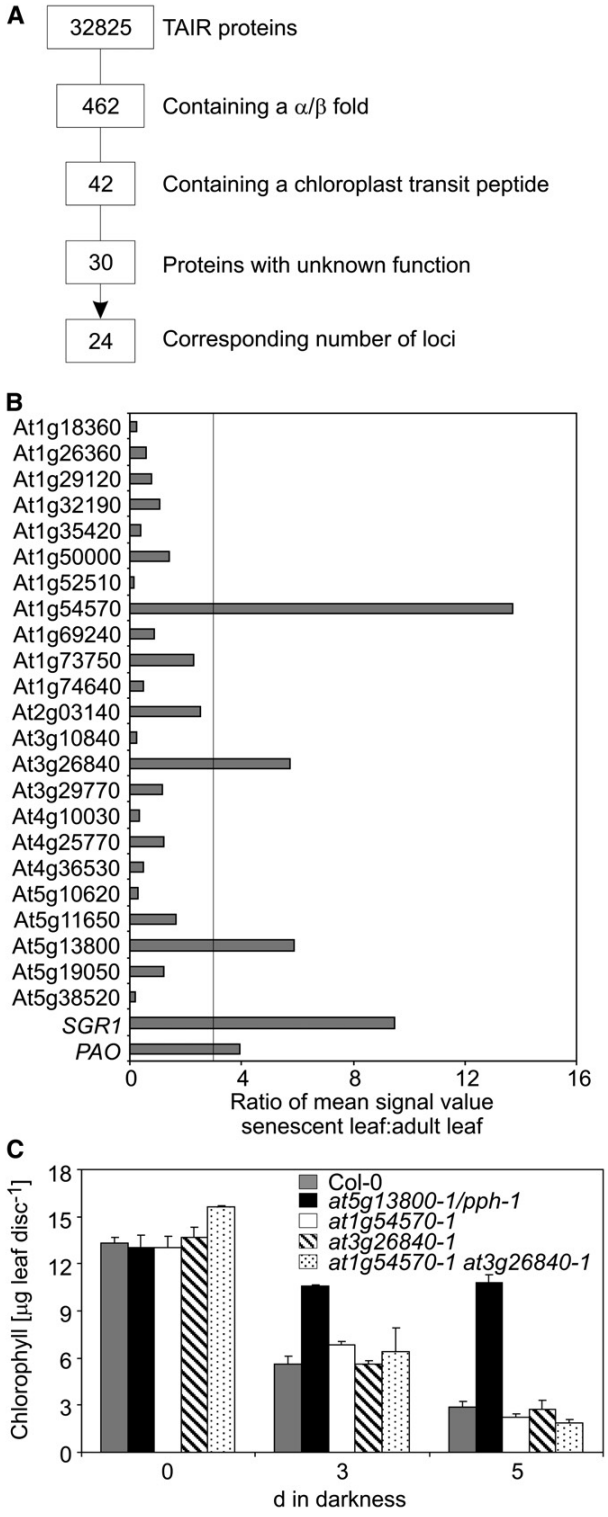

Figure 1. Identification and Analysis of Candidates for Phytol Hydrolysis in *Arabidopsis*.

(A) Screening of the TAIR protein database (version 8) for proteins with properties expected for a phytol-hydrolyzing enzyme.

(B) Analysis of senescence-related expression of candidate genes using the Genevestigator Meta-Analyzer tool (Zimmermann et al., 2004). The ratio of mean fluorescence values from senescent leaves (organ #44, number of chips: 3) and adult leaves (organ #42, number of chips: 274) is shown. Values for *SGR1* and *PAO* are shown as reference. A cutoff of 3 was chosen for significantly upregulated genes. Note that one of the 24 candidate genes (At5g47860) was not present on the 22K microarray chip.

(C) Degradation of chlorophyll during dark-induced senescence in mutants of candidate genes. Data are mean values of a representative experiment with three technical replicates. Error bars indicate SD.

identified that the enzyme specifically hydrolyzed the phytolester of phein but not chlorophyll (see below). We therefore named At5g13800 PPH and focused on analyzing respective *pph* mutants.

PPH Deficiency Results in a Stay-Green Phenotype

Microarray data analyzed by Genevestigator (Zimmermann et al., 2004) indicated enhanced *PPH* expression during leaf senescence (Figure 1B). We confirmed this by RT-PCR analysis of the wild type (Figure 2B). To confirm that absence of PPH was responsible for the stay-green phenotype observed in *at5g13800-1* (*pph-1*) (Figure 1C), two additional homozygous T-DNA insertion lines for At5g13800, namely, *pph-2* (GABI_453A08) and *pph-3* (SM_3_15198) (Figure 2A), were analyzed. In all cases, high levels of chlorophyll were retained during natural (see Supplemental Figure 1 online) and dark-induced senescence (Figures 2C and 2D), and *pph-1* was exclusively used in our subsequent studies. Furthermore, we introduced *PPH* cDNA into *pph-1* under the control of the 35S promoter. The stay-green phenotype was complemented in *pph-1/35S:PPH* plants (i.e., upon dark-induced senescence, chlorophyll was degraded like in the wild type) (Figure 2E). Complementation depended on the presence of the Ser-221 residue of *Arabidopsis* PPH, which possibly represents the active site residue (see below). Thus, *pph-1/35S:PPH*$_{S221A}$ lines retained indefinite greenness. Altogether the data indicated that *PPH* absence causes a stay-green phenotype during leaf senescence.

pph-1 Is a Type C Stay-Green Mutant

Stay-green mutants have been classified into functional stay-greens, in which both chlorophyll degradation and photosynthetic capacity are retained longer compared with the wild type, and cosmetic ones (e.g., type C), which specifically retain chlorophyll while other senescence parameters are not affected (Thomas and Howarth, 2000). To examine the correlation between greenness and leaf functionality in *pph-1*, we determined the maximal fluorescence yield of PSII (F_v/F_m) (Figure 3A) and CO_2 consumption in correlation to light intensities (see Supplemental Figure 2 online). For these experiments, senescence was induced by covering attached leaves with aluminum foil. F_v/F_m decreased more rapidly in *pph-1* than in the wild type. Likewise,

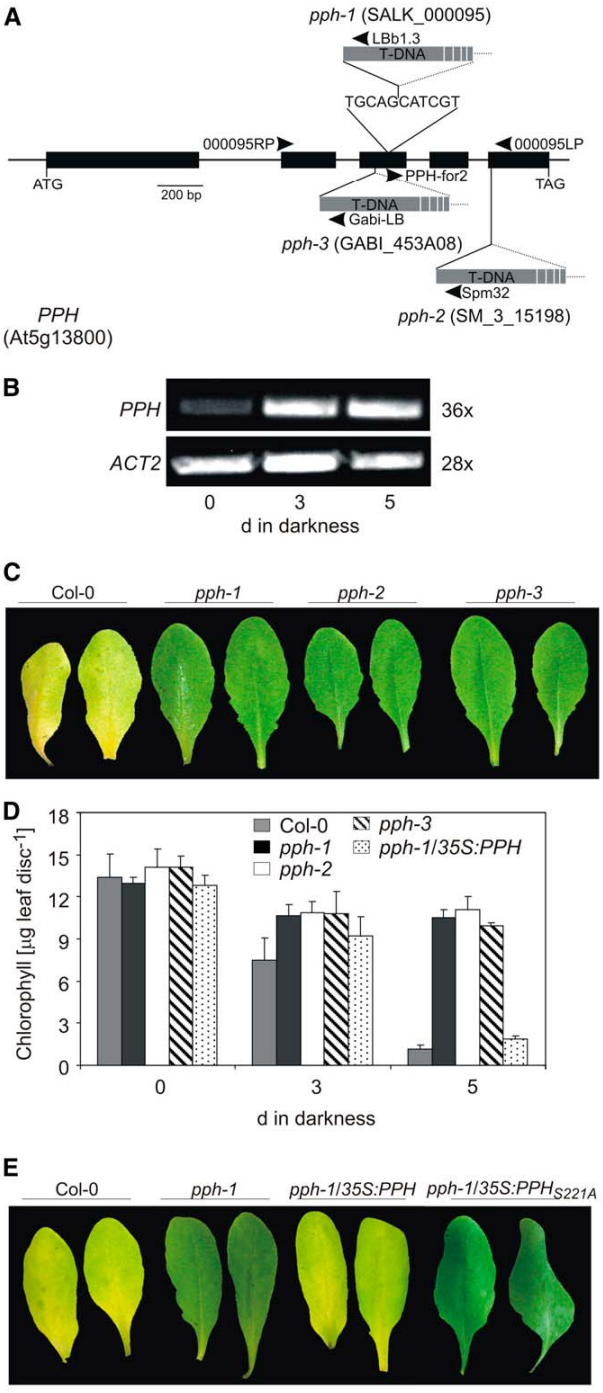

Figure 2. Deficiency of PPH Causes a Stay-Green Phenotype.

(A) Gene structure of *PPH* showing the T-DNA insertion sites of the different *pph* mutants studied here. For *pph-1*, the site of T-DNA insertion was verified by sequencing. Position of primers used for isolation of homozygous lines is shown.

(B) Analysis of *PPH* expression during dark-induced senescence. *ACT2* was used as control. Expression was analyzed with nonsaturating numbers of PCR cycles as shown at the right. The results from one of three independent experiments with similar results are shown. PCR products were separated on agarose gels and visualized with ethidium bromide.

(C) Phenotype of three *pph* mutants after 5 d of dark-induced senescence.

(D) Chlorophyll degradation of *pph* mutants and *pph-1* complemented with a *35S-PPH* cDNA construct (*pph-1/35S:PPH*) during dark-induced senescence. Data are mean values of a representative experiment with three replicates. Error bars indicate SD.

(E) Complementation of the stay-green phenotype of *pph-1* with a *35S-PPH* cDNA construct. A construct harboring a mutation of the proposed active-site Ser residue (*35S-PPH*$_{S221A}$) did not complement *pph-1*. Leaves after 5 d of dark-induced senescence are shown.

CO_2 fixation rates decreased faster in *pph-1* (see Supplemental Figure 2 online), demonstrating that functionality of photosynthesis was strongly affected in *pph-1* upon senescence induction. To further characterize the senescence behavior of *pph-1*, expression of *SAG12*, a commonly accepted marker of senescence, was analyzed by RT-PCR (Figure 3B). In both the wild type and *pph-1* mutant, *SAG12* expression increased to a similar extent upon senescence induction. In addition, senescence-regulated genes of chlorophyll degradation (i.e., *NYC1*, *SGR1*, and *PAO*) were induced in *pph-1* (Figure 3B), indicating that chlorophyll was retained in the mutant despite the induction of the chlorophyll degradation pathway. We analyzed metabolism of photosynthesis-related proteins as a further marker of senescence progression (Figure 3C). As had been shown in other instances of type C stay-green mutants (Thomas and Hilditch, 1987; Pružinská et al., 2003; Kusaba et al., 2007; Park et al., 2007), degradation of LHC subunits was delayed in *pph-1*, while ribulose-1,5-bisphosphate carboxylase/oxygenase (Rubisco) was degraded like in the wild type. In addition, PsbA (D1), a subunit of the core complex of PSII, was also partially retained in *pph-1*. By contrast, PsaA degradation in *pph-1* was indistinguishable from that of the wild type. Collectively, these data showed that *pph-1* is a type C stay-green mutant specifically impaired in chlorophyll catabolism.

PPH Is Required for Chloroplast and Photosystem Degradation

Type C stay-green mutants are characterized by an increased stability of chloroplast membranes and of chlorophyll-protein complexes (Kusaba et al., 2007; Park et al., 2007; Sato et al., 2007). Ultrastructural analysis showed that chloroplast structure of short day-grown *pph-1* plants was similar to that of the wild type before senescence (Figure 4A). After 6 d of dark-induced senescence, grana thylakoid stacking in *pph-1* was nearly unchanged. In some cases, stacks with significantly more lamellae per granum were present, probably due to fusion of several grana stacks as reported earlier (Kusaba et al., 2007). By contrast, in the wild type, grana were largely unstacked and overall thylakoid membrane density was reduced. This indicated that PPH absence prevented proper degradation of the thylakoid membrane

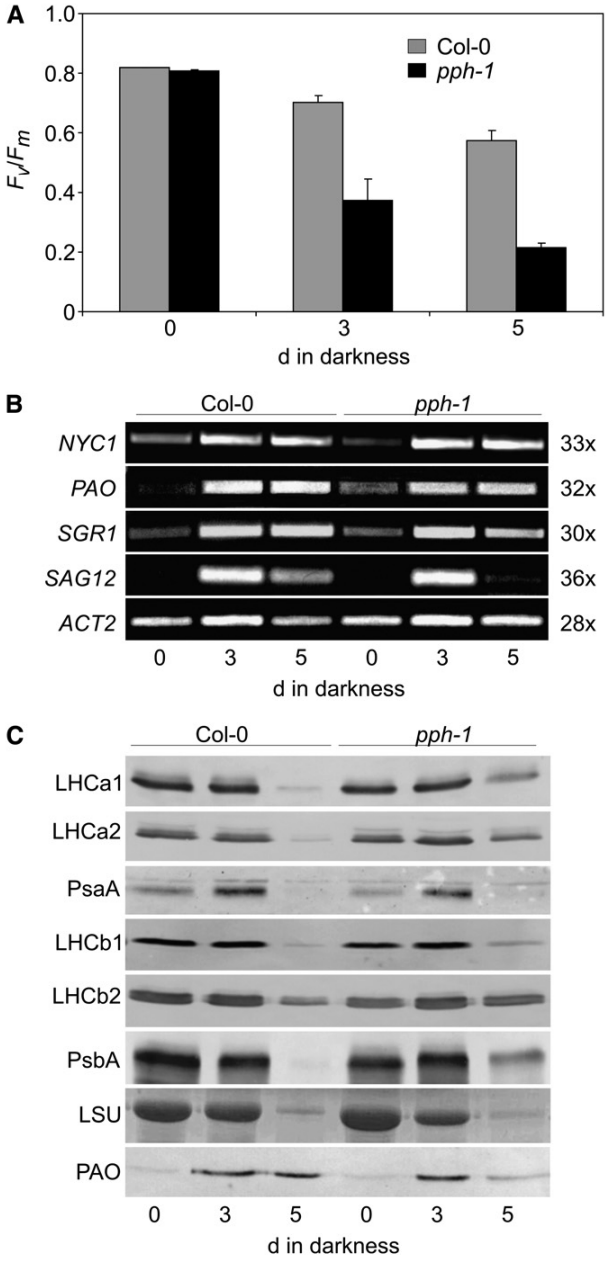

Figure 3. Characterization of Senescence Parameters in *pph-1*.

(A) Maximum quantum yield of PSII (F_v/F_m) during senescence in Col-0 (gray) and *pph-1* (black). For senescence induction, attached leaves were covered with aluminum foil. Data are mean values of a representative experiment with three to six replicates. Error bars indicate SE.

(B) Analysis of gene expression during dark-induced senescence in Col-0 and *pph-1*. *ACT2* was used as control. Expression was analyzed with nonsaturating numbers of PCR cycles as shown at the right. The results from one of two independent experiments with similar results are shown. PCR products were separated on agarose gels and visualized with ethidium bromide.

(C) Immunoblot analysis of degradation of photosynthesis-related proteins during dark-induced senescence in Col-0 and *pph-1*. PAO was used as a marker for senescence induction. Gel loadings are based on equal size of leaf area. LSU, Rubisco large subunit.

system. To further analyze composition and stability of photosystem subcomplexes, isolated and mildly solubilized chloroplast membranes were separated by sucrose density gradient centrifugation (Figure 4B; see Supplemental Figure 3 online). In *pph-1*, the photosynthetic complex structure remained largely unchanged upon senescence induction. By contrast, all complexes were degraded in the wild type. Immunoanalysis of sucrose density gradient fractions indicated that after 5 d of dark-induced senescence, the LHCII and PSII core complexes formed bands at lower densities in both the wild type and *pph-1* (see Supplemental Figure 3 online). This occurred reproducibly in several independent experiments, possibly due to changes in ultrastructural composition of respective complexes or altered detergent solubilization properties. Furthermore, as seen before (Figure 3C), PsaA was degraded in both lines, while the abundance of all other subunits analyzed by immunoblots remained largely unchanged in *pph-1* (see Supplemental Figure 3 online).

PPH Is Localized in the Chloroplast

The above-described chloroplast metabolism-related phenotype of *pph-1* indicated localization of PPH inside the chloroplast. Furthermore, ChloroP predicted the presence in PPH of a N-terminal chloroplast transit peptide of 46 amino acids. An N-terminal fusion with PPH (PPH-GFP) targeted green fluorescent protein (GFP) to the chloroplasts of *Arabidopsis* mesophyll protoplasts (Figure 5A). Thereby, GFP fluorescence largely colocalized with chlorophyll fluorescence. By contrast, GFP fusions with translocon of the inner chloroplast envelope110 (TIC110) resulted in distinct chlorophyll and GFP fluorescences as expected (Schenk et al., 2007), indicating envelope localization. In addition, we performed import experiments of [^{35}S]-labeled PPH into isolated *Arabidopsis* mesophyll chloroplasts, followed by chloroplast reisolation and subfractionation (Figure 5B). PPH was efficiently imported into the plastids and was found in the soluble fraction. From these experiments, we conclude that PPH is located inside the chloroplast, most likely as a soluble protein in the stroma.

pph-1 Has a Defect in Chlorophyll Degradation and Accumulates Pheophytin *a*

Different stay-green mutants have been shown to accumulate green intermediates of chlorophyll breakdown (i.e., chlide and/or pheide) (Roca et al., 2004; Park et al., 2007). To investigate the pigment composition in *pph-1* during senescence, green pigments were extracted and separated by reverse-phase HPLC (Figure 6A). Before senescence, the wild type and *pph-1* were indistinguishable, and after 5 d of dark-induced senescence, chlorophyll *a* and chlorophyll *b* levels diminished in the wild type (Figure 6A). By contrast, in *pph-1*, large quantities of chlorophyll *a*

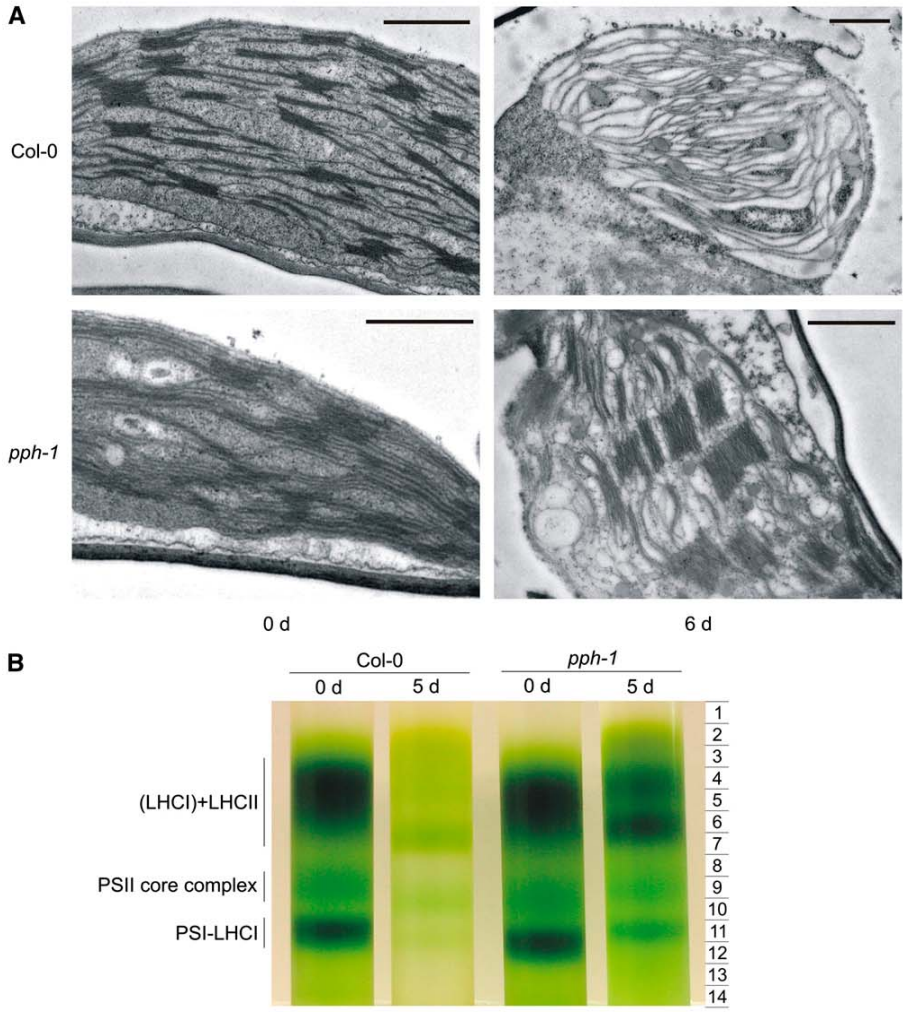

Figure 4. Analysis of Photosystem Organization During Senescence in *pph-1*.

(A) Transmission electron micrographs of plastids from short-day-grown Col-0 and *pph-1* before (0 d) and after 6 d of dark-induced senescence. Bars = 1 μm.

(B) Sucrose gradient fractionation of thylakoid membranes from Col-0 and *pph-1* before (0 d) and after 5 d of dark-induced senescence. Dodecylmaltoside-solubilized thylakoid membranes corresponding to equal amounts of fresh weight were loaded on each gradient. Gradient fractions (1 to 14) used for further analysis are shown at the right. The position of photosystem subcomplexes, as identified by immunoblot analysis of individual photosystem subunits (see Supplemental Figure 3 online), is indicated at the left. Note that during senescence, the LHCII band separated into two distinct bands in both Col-0 and *pph-1*.

and in particular chlorophyll *b* were retained (Figure 6B), with the result that the chlorophyll *a*/*b* ratio decreased during senescence (Figure 6C). This occurred in three different *pph* mutants. When plants had been grown under strong light, significant quantities of chlorophyll *a* were converted to C_{13}-hydroxy chlorophyll *a*, and two additional minor chlorophyll *a*-like peaks formed upon senescence induction in *pph-1*, but not in Columbia-0 (Col-0) (see Supplemental Figure 4 online). Production of these modified pigments could be induced in the wild type and the mutant by treatment with H_2O_2 (see Supplemental Figure 4 online), indicating that their formation was due to (unspecific) peroxidative activities.

pph-1 accumulated increasing amounts of phein *a* (Figure 6D) after 3 and 5 d of dark-induced senescence. This was not seen in the wild type, indicating that absence of PPH in the mutant was responsible for the observed phein accumulation. To investigate the possibility that phein accumulation in *pph-1* could be limited by some capacity on the part of PAO to cause conversion of phein *a* to an FCC-like pigment, we produced a *pph-1 pao1* double mutant. We found that phein *a* accumulation in *pph-1 pao1* was

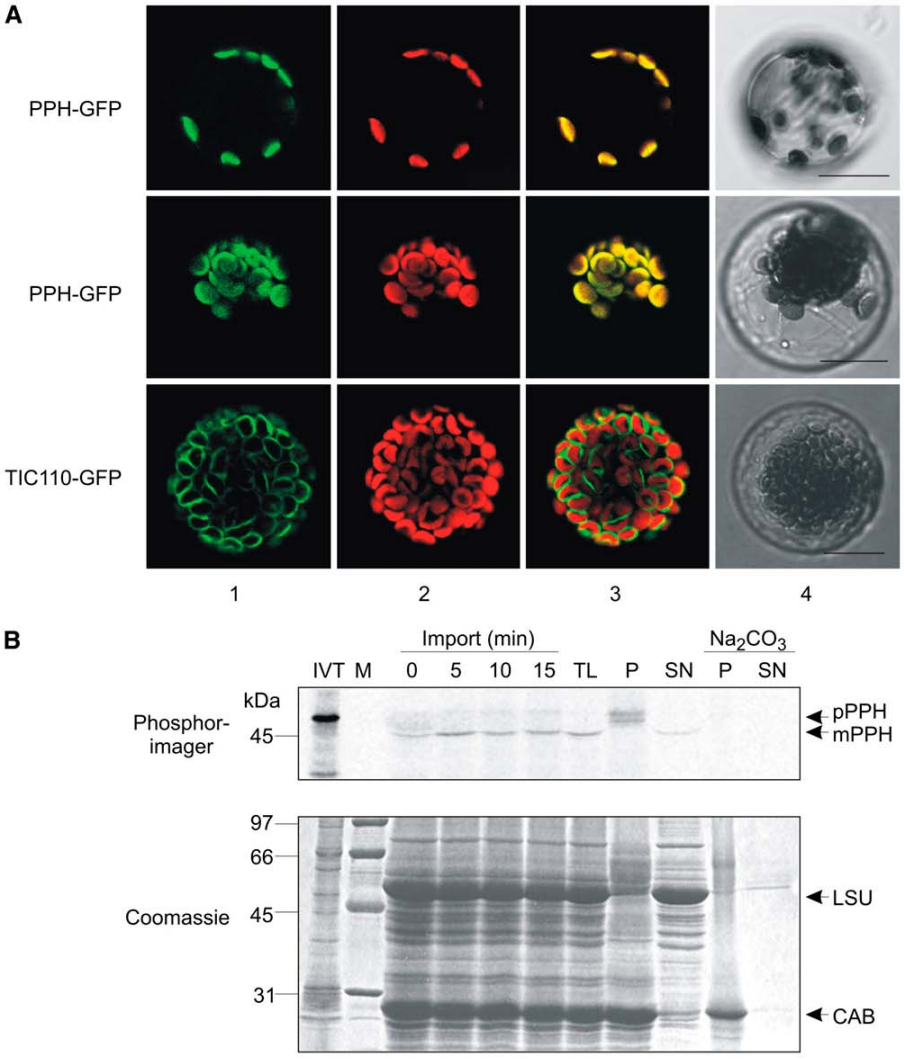

Figure 5. Analysis of Subcellular PPH Localization.

(A) Transient expression in *Arabidopsis* mesophyll protoplasts of GFP fused in frame to the C terminus of PPH (PPH-GFP). TIC110-GFP was used as control for chloroplast envelope localization. GFP fluorescence (column 1) and chlorophyll autofluorescence (column 2) were examined by confocal laser scanning microscopy. Column 3, merge of GFP and autofluorescence; column 4, bright field image. Bars = 10 μm.

(B) Import of [^{35}S]-Met–labeled precursor of PPH (pPPH) in *Arabidopsis* chloroplasts. Import was allowed to proceed for 5, 10, and 15 min and mature PPH (mPPH) accumulated. After 15 min of import, chloroplasts were treated with thermolysin (TL) to digest surface-bound and nonimported precursor. To determine the subchloroplast PPH localization, chloroplasts were lysed and separated into stromal (SN) and membrane (P) fractions. The membrane fraction was subjected to alkaline extraction (Na_2CO_3) and separated into Na_2CO_3-resistant proteins (P) or proteins extractable by this treatment (SN). M, molecular size markers (kD) are indicated at the left. IVT, in vitro translation product; LSU, large subunit of Rubisco; CAB, chlorophyll *a/b* binding protein.

similar to that in *pph-1* (Figure 6D). Only small amounts of polar NCCs (i.e., linear tetrapyrroles known as late products of chlorophyll breakdown in *Arabidopsis* [Pružinská et al., 2005]) were found in *pph-1* (Figure 6E), indicating that, in *pph-1*, chlorophyll breakdown was largely blocked at the level of porphyrinic, phytol-containing pigments.

PPH Is a Pheophytinase (PPH)

To investigate the enzymatic activity of PPH, a truncated version, devoid of the predicted chloroplast transit peptide (ΔPPH), was expressed in *Escherichia coli* as a maltose binding protein (MBP) fusion (MBP-ΔPPH). The recombinant protein was highly stable

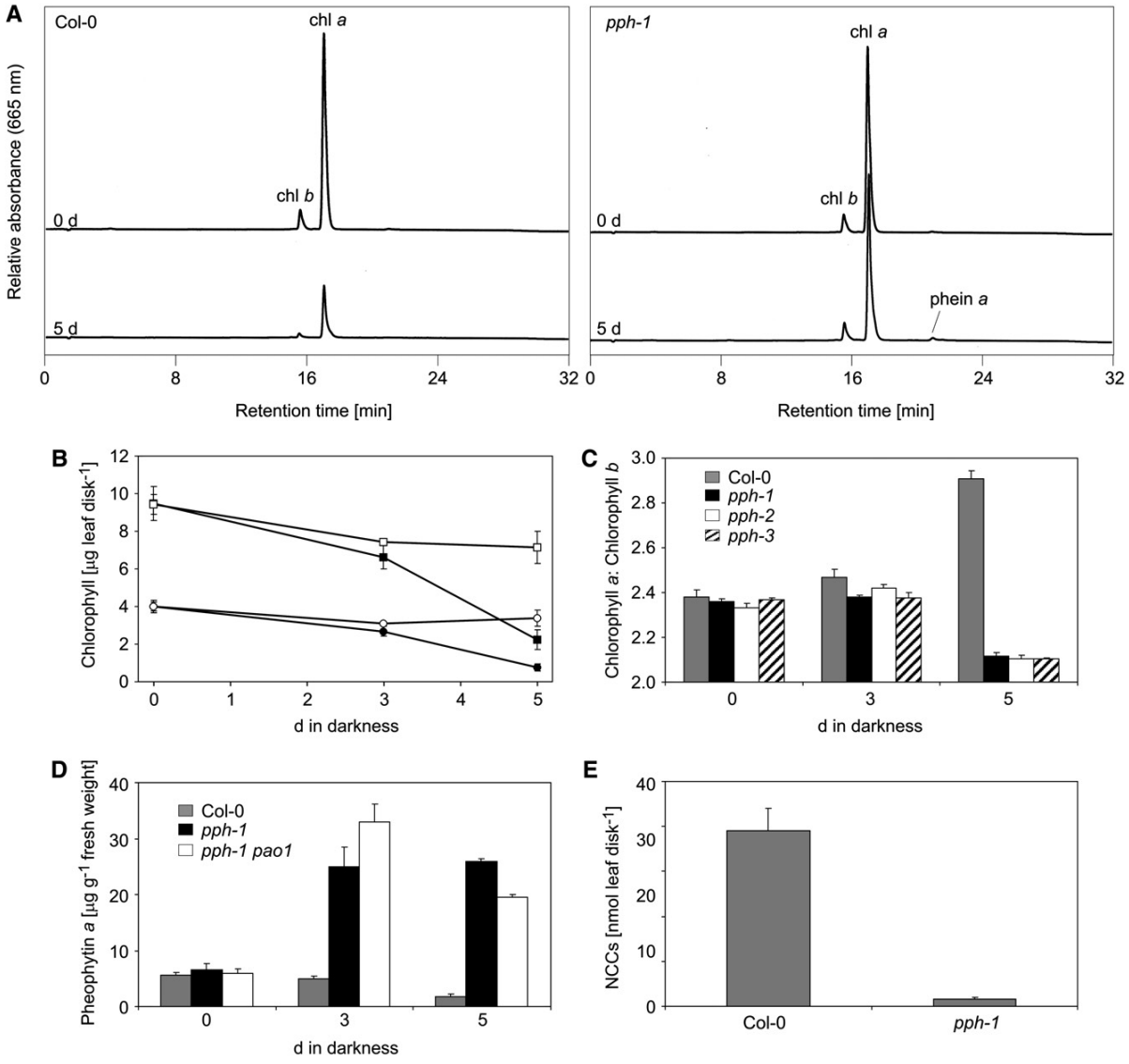

Figure 6. Analysis of Pigment Composition during Dark-Induced Senescence in *pph-1*.

(A) HPLC traces (A_{665}) of leaf extracts of Col-0 (left) and *pph-1* (right) before (0 d) and after 5 d of senescence. HPLC injections correspond to equal amounts of fresh weight. Chl, chlorophyll.

(B) Degradation of chlorophyll *a* (squares) and chlorophyll *b* (circles) during senescence of Col-0 (closed) and *pph-1* (open).

(C) Ratio of chlorophyll *a* to chlorophyll *b* during senescence of Col-0 and different *pph* mutants.

(D) Amounts of phein *a* (pheophytin *a*) accumulating during senescence in Col-0 (gray), *pph-1* (black), and *pph-1 pao1* (white).

(E) Amount of total NCCs found in Col-0 and *pph-1* after 5 d of dark-induced senescence.

Data in **(B)** to **(E)** are mean values ± SD of representative experiments each with three replicates.

and was largely located in the soluble cell fraction (Figure 7A). Crude soluble *E. coli* extracts were employed in assays containing chlorophyll *a*/*b* mixtures as likely substrates. MBP-ΔPPH did not convert chlorophyll to chlide (Figure 7B), in contrast with recombinant *Citrus* chlorophyllase (Chlase1), which was highly active (see Supplemental Figure 5A online). Since phein accumulated in *pph-1* (Figure 6D), we explored the possibility of the Mg-free pigment being a substrate of PPH. Indeed, MBP-ΔPPH (Figure 7C) converted phein to the respective dephytylated pigment, pheide, thereby reacting with both phein *a* and phein *b* (Figures 7C and 7D). Activity was identical before and after cleavage of the fusion protein with factor XA (see Supplemental

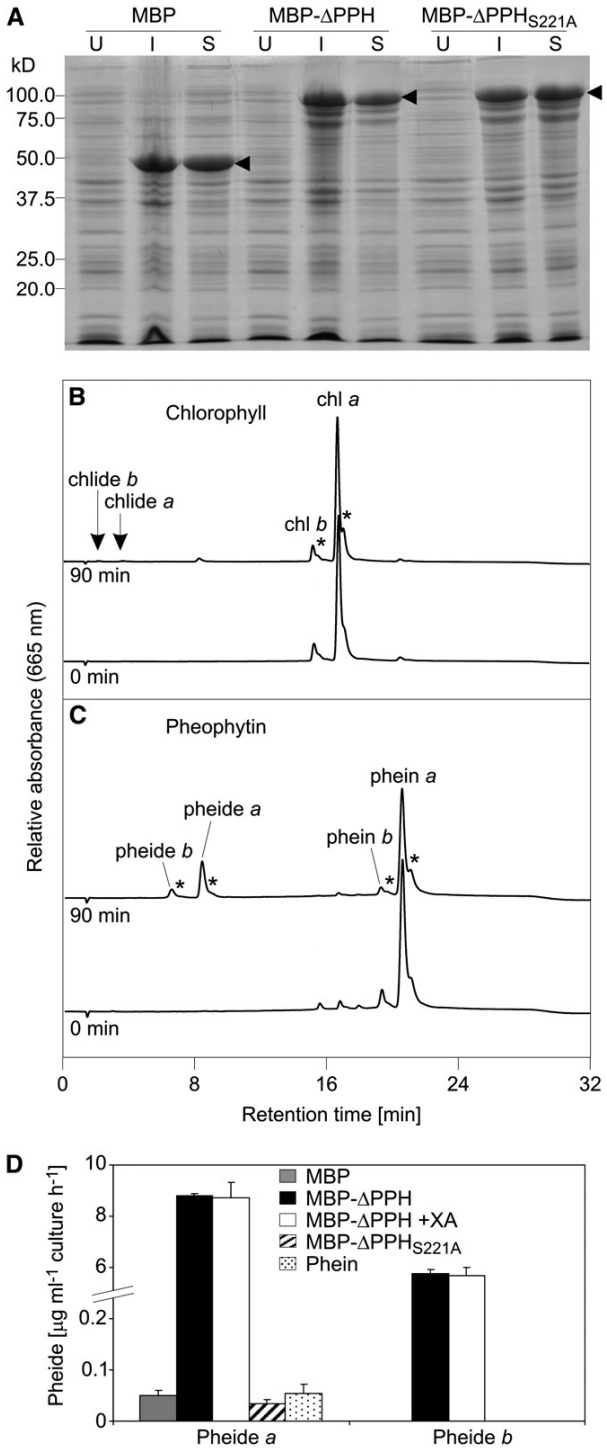

Figure 7. Analysis of Recombinant and Native PPH.

(A) Coomassie blue–stained SDS-PAGE gel of *E. coli* cells (BL21 DE3) expressing an N-terminal truncated version of PPH (ΔPPH) fused to MBP (MBP-ΔPPH). In addition, a missense mutation of PPH (MBP-ΔPPH$_{S221A}$) was analyzed. A strain expressing free MBP was used as control. After induction with isopropyl-β-D-thiogalactopyranosid for 3 h (I), cells were lysed, and soluble proteins (S) were isolated as described in Methods. U, cells before isopropyl-β-D-thiogalactopyranosid induction. Gel loadings are based on equal amounts of cell cultures at OD_{600} = 1.5. Arrowheads indicate position of recombinant proteins. Molecular size markers (kD) are indicated at the left.

(B) and **(C)** HPLC analysis of assays employing soluble *E. coli* lysates expressing recombinant MBP-ΔPPH with chlorophyll **(B)** or phein **(C)** as substrate. HPLC traces at A_{665} before (0 min) and after 90 min of incubation at 25°C are shown. Note that only in the case of phein were the respective dephytylated products (pheides) formed. Asterisks indicate the C_{13} epimers of adjacent peaks. In **(B)**, arrows indicate the expected position of chlide *b* and chlide *a*, respectively. Chl, chlorophyll.

(D) Pheide *a* (left) and pheide *b* (right) formation from phein in assays with recombinant MBP-ΔPPH before (black) and after (white) 24 h of digestion with factor XA. As controls, the substrate was incubated with the vector control (MBP, gray), recombinant MBP-ΔPPH$_{S221A}$ (hatched), or without *E. coli* extract (Phein; dotted). Data are mean ± SD of three independent assays.

Figure 6C online; Figure 7D), and *E. coli* extracts containing the uncut MBP-ΔPPH fusion were employed in subsequent assays. In competition experiments, a 10-fold excess of chlorophyll did not inhibit phein hydolysis. Thus, PPH exhibited a surprising specificity for the Mg-free form of chlorophyll, in contrast with *Citrus* Chlase1, which catalyzed dephytylation of both chlorophyll and phein (see Supplemental Figures 5A and 5B online). While chlorophyllase showed the known specificity (Fiedor et al., 1992) toward *a* and *b* forms of pigments and did not react with the respective C_{13} epimers (see Supplemental Figures 5A and 5B online), PPH accepted both C_{13} epimers of phein *a* and phein *b* (Figure 7C). The phein hydrolytic activity of recombinant MBP-ΔPPH was time dependent and exhibited a temperature optimum of 25 to 30°C (see Supplemental Figure 6 online). Neither the vector control nor the mutation of a Ser residue (Ser-221), possibly representing the active site residue of *Arabidopsis* PPH (MBP-ΔPPH$_{S221A}$), acted on phein (Figure 7D) or chlorophyll.

PPH Is a Ser-Type Hydrolase Widely Distributed in Eukaryotic Photosynthetic Organisms

BLASTP searches (Altschul et al., 1997) for homologous PPH proteins using databases at the National Center for Biotechnology Information and the Joint Genome Institute identified PPH-related proteins from higher and lower plant species and from cyanobacteria. To investigate the relationship between these proteins, we performed a phylogenetic analysis on selected proteins within the BLAST hits. We included all nonredundant eukaryotic proteins, but for better visibility, left out bacterial species, except for proteins from *Synechocystis* sp PCC6803 and *Synechococcus* sp PCC7002 (Figure 8A; see Supplemental Data Set 1 online). *Arabidopsis* PPH clustered into a clade (clade I) with one protein each from eukaryotic plant species included in the analysis, but not with bacterial sequences. Two further clades (clade II and III), clearly separated from clade I, were obtained. This indicated that PPH orthologs are commonly present in eukaryotic photosynthesizing organisms, but absent in cyanobacteria. The distribution within the tree further indicated

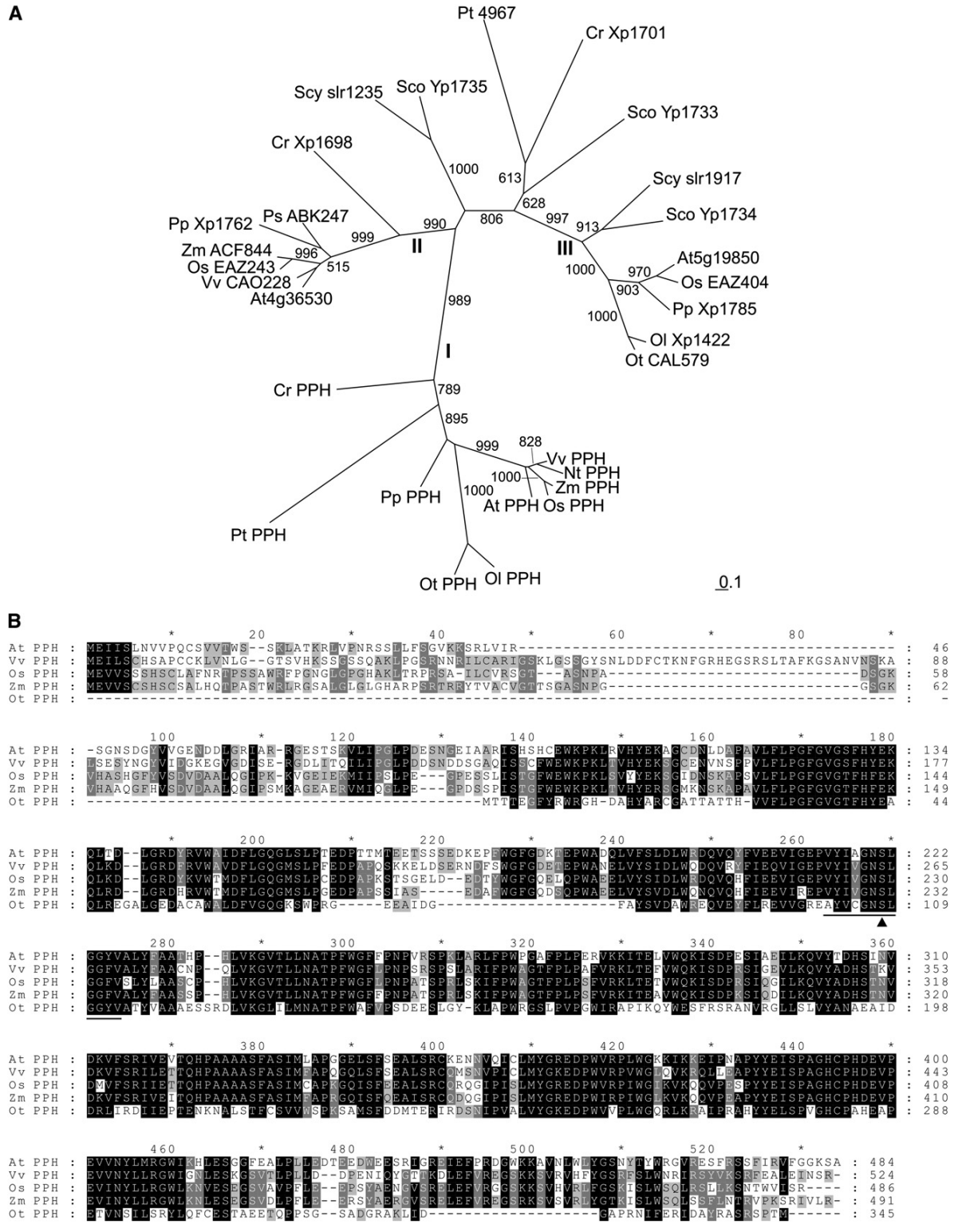

Figure 8. Phylogenetic Analysis and Sequence Alignment of PPH Homologs.

that *PPHs* are single-copy genes. Figure 8B shows an alignment of selected proteins from the PPH clade shown in Figure 8A. The proteins exhibited sequence identities between 38.6% (Ot PPH versus Os PPH) and 79.1% (Zm PPH versus Os PPH). Except for *Ostreococcus taurii*, all shown PPH proteins contained chloroplast transit peptides as predicted by ChloroP. An α/β hydrolase fold (InterPro IPR000120; Pfam PF00561) was present in all PPH proteins, but a screen in the InterPro database (http://www.ebi.ac.uk/Tools/InterProScan/) did not identify other known conserved motifs. However, a novel motif with the consensus sequence [AV]-x-[LIV]-x-G-N-S-[LIV]-G-G-[YF]-[LIV] (underlined in Figure 8B) was present, which we tentatively named the PPH motif and which was most similar to, but distinct from, the lipase GDSL motif of the PROSITE database (PS01098). The core sequence of the PPH motif (G-N-S-[LIV]-G-G) was also conserved in the proteins of clade II, but not clade III (see Supplemental Figure 7A online), indicating a possible related function of clade II proteins. To the best of our knowledge, none of the proteins in the tree have functionally been characterized. The active site of many hydrolytic enzymes is composed of a catalytic triad with a Ser residue that carries out the nucleophilic attack of the substrate (Dodson and Wlodawer, 1998). In analogy to PS01098 (see Supplemental Figure 7B online) and because PPH catalyzes the ester bond hydrolysis reaction from phein *a* to pheide *a* and phytol, the Ser residue of the PPH motif (marked with an arrowhead in Figure 8B) is likely the active-site Ser of PPHs. As shown above (Figures 2E and 7D), Ser-221 of *Arabidopsis* PPH was required for both in vitro PPH activity and *pph-1* complementation.

DISCUSSION

A Novel Candidate Protein for Chlorophyll Dephytylation in Senescent Leaves

The need for a phytol-cleaving reaction in chlorophyll breakdown is rationalized by the fact that the final breakdown products, NCCs, are water soluble and are located inside the vacuole (Matile et al., 1988). Phytol removal had been considered as an early reaction of the pathway, and mutants defective in either PAO (*pao1*) or red chlorophyll catabolite reductase (*acd2*) accumulate dephytylated pigments (Pružinská et al., 2003, 2007; Tanaka et al., 2003; Pružinská et al., 2005). Whereas red chlorophyll catabolites found in *acd2-2* during senescence are (partially) localized inside the vacuole (Pružinská et al., 2007), pheide *a* accumulating in *pao1* is retained in the plastid (S. Aubry and S. Hörtensteiner, unpublished results). These data indicate that phytol cleavage occurs rather early in the pathway and that the activity resides in the chloroplast. Nevertheless, the molecular identification of chlorophyllases questioned the exclusive location of dephytylation inside the plastid because several of the genes cloned so far indicated localization of the deduced proteins in the cytosol or vacuole (Takamiya et al., 2000). Experimental evidence for subcellular CLH localization using GFP fusions was ambiguous (Okazawa et al., 2006; Schenk et al., 2007), and in only one case, namely, *Citrus* Chlase1, has chloroplast localization been established immunologically (Harpaz-Saad et al., 2007; Azoulay Shemer et al., 2008). Nevertheless, the role of CLH in chlorophyll breakdown during leaf senescence remained elusive until our recent report, in which we demonstrated that CLHs are not essential for senescence-related chlorophyll breakdown in *Arabidopsis* (Schenk et al., 2007). We based our assumption on the analysis of *clh* single and double mutants, which were marginally affected in chlorophyll breakdown. In addition, CLH expression was not correlated with senescence (Liao et al., 2007; Schenk et al., 2007), and overexpression of CLHs in *Arabidopsis* did not accelerate leaf senescence (Benedetti and Arruda, 2002; Kariola et al., 2005). Here, we show that despite the presence of CLHs in *pph-1*, only small quantities of chlorophyll are converted to phytol-free NCCs. This supports our earlier finding of CLHs playing only a minor role in chlorophyll breakdown (Schenk et al., 2007), but the data presented here prompted us to suggest that PPH is a major chlorophyll-dephytylating enzyme during leaf senescence. By contrast, during fruit ripening of *Citrus limon*, levels of Chlase1 (a member of the CLH protein family) negatively correlated with chlorophyll amounts at the cellular level. Moreover, expression of the gene was increased by ethylene treatment, which also considerably accelerated chlorophyll breakdown (Azoulay Shemer et al., 2008). This implied that Chlase1 is involved in chlorophyll breakdown during *Citrus* fruit ripening (Azoulay Shemer et al., 2008), but further analysis is required to elucidate whether PPH might also have a role in fruits.

We identified PPH using a functional genomic approach, a powerful tool that has previously been used to identify the enzymes involved in chlorophyll breakdown at the molecular level (Pružinská et al., 2003). Deficiency of PPH resulted in a cosmetic stay-green phenotype (see below). In addition, *PPH* was highly coexpressed with and embedded within a network of genes involved in chlorophyll breakdown, namely, *PAO*, *NYC1*, and *SGR1*. The two other candidates obtained by this approach, namely, At1g54570 and At3g26840, were homologous to each other and had been shown in proteomic studies to localize to

Figure 8. (continued).

(A) Maximum likelihood phylogenetic tree of PPH and related proteins from plants, algae, and cyanobacteria. Branch support values obtained from 1,000 bootstraps are indicated when higher than 50%. Three clades (I, II, and III) are distinguished. For protein accession numbers, see Methods. At, *Arabidopsis thaliana*; Cr, *Chlamydomonas reinhardtii*; Nt, *Nicotiana tabacum*; Ol, *Ostreococcus lucimarinus*; Os, *Oryza sativa*; Ot, *Ostreococcus taurii*; Pp, *Physcomitrella patens*; Ps, *Picea sitchensis*; Pt, *Phaeodactylum tricornutum*; Sco, *Synechococcus* sp PCC 7002; Scy, *Synechocystis* sp PCC 6803; Vv, *Vitis vinifera*; Zm, *Zea mays*.

(B) Sequence alignment of PPH proteins from different species. Black shading with white letters, gray shading with white letters, and gray shading with black letters reflect 80, 60, and 40% sequence conservation, respectively, with Blosum62 similarity group enabled. A conserved domain (named the PPH domain) containing the proposed active-site Ser residue (arrowhead) is underlined.

plastoglobules (Vidi et al., 2006; Ytterberg et al., 2006). During leaf senescence, plastoglobules increase in size and number (Matile et al., 1999), and using electron tomography they were shown to form a continuum with the outer leaflet of the thylakoid membrane (Austin et al., 2006). Furthermore, plastoglobules contain large amounts of phytol and fatty acid phytyl esters (Gaude et al., 2007), and a salvage pathway of chlorophyll-derived phytol for tocopherol biosynthesis was recently established (Ischebeck et al., 2006). However, using single and double mutants, a direct role for At1g54570/At3g26840 in chlorophyll breakdown was not obvious.

PPH Is a Pheophytinase but Not a Chlorophyllase

The analysis of in vitro PPH activity after expression in *E. coli* yielded surprising results (Figure 7). The enzyme accepted phein as substrate, thereby both phein *a* and *b* were converted to the respective phytol-free pigments, pheide *a* and pheide *b*. By contrast, chlorophyll was not a substrate for the enzyme and did not inhibit pheophytinase activity in a competitive manner. In vitro–expressed CLH proteins, however, are much less specific and accept different porphyrinic substrates (see Supplemental Figure 5 online; Fiedor et al., 1992) but also unrelated hydrophobic esters, such as *p*-nitrophenyl decanoate (Arkus et al., 2005). The phein specificity of PPH was in agreement with the observation that *pph-1* accumulated substantial amounts of phein during leaf senescence. However, compared with the *pao1* mutant, which accumulates up to 150 μg pheide *a* g^{-1} leaf material (Pružinská et al., 2005), the amounts of phein found in *pph-1* (Figure 6D) were considerably smaller (~28 μg phein *a* g^{-1} leaf material). We speculated that PAO could act on phein *a*, yet phein *a* levels were not increased in a *pph-1 pao1* double mutant. Alternatively, an efficient (unknown) feedback mechanism might prevent further chlorophyll breakdown if the pathway is blocked. However, the fact that small quantities of NCCs accumulated in *pph-1* (Figure 6E) indicated some leakage, possibly the result of a limited participation of other hydrolases, such as CLHs.

Based on our results, we conclude that the order of the early reactions in chlorophyll breakdown during senescence is likely different than commonly assumed so far (Hörtensteiner, 2006). Thus, Mg release seems to precede phytol cleavage, resulting in the formation of intermediates in the following order: chlorophyll → phein → pheide. As a consequence, we propose a changed major route of chlorophyll metabolism, in which the reactions of chlorophyll biosynthesis and degradation are no longer linked through chlide as suggested earlier (Rüdiger, 2002) (Figure 9A). Instead, the anabolic and catabolic pathways are largely metabolically separated, but are connected through the chlorophyll cycle (Rüdiger, 2002). Thereby, the oxidative steps, catalyzed by chlorophyll *a* oxygenase (Tanaka et al., 1998), mainly occur at the level of phytol-free chlide, whereas *b* to *a* reduction, involving NYC1/NOL, mainly occurs at the level of chlorophyll.

Several published reports have described accumulation of various green intermediates of chlorophyll breakdown, including phein and pyropheophytin (Schoch et al., 1981; Schoch and Vielwerth, 1983; Amir-Shapira et al., 1987). However, dephytylated pigments, such as chlide, pheide, and pyropheophorbide, have been found as well (Amir-Shapira et al., 1987; Ziegler et al., 1988; Shimokawa et al., 1990; Shioi et al., 1991; Roca et al., 2004). Identification of Mg-free pheo intermediates is in agreement with the proposed route, but accumulation of chlide would argue against it. Chlide has been found both in fruits, such as *Citrus*, where chlorophyllase indeed seems to be involved in vivo (Azoulay Shemer et al., 2008), and in systems exhibiting rather high levels of in vitro chlorophyllase activity. Historically, chlorophyllase activity is determined in the presence of high concentrations of acetone or detergent (i.e., similar conditions as used for extraction of chlorophyll pigments from plant tissues). Thus, to determine in vivo quantities of chlide, care must be taken during pigment extraction to avoid artificial activation of chlorophyllases. As an example, in *Arabidopsis*, the fraction of chlide does not exceed 0.5% of total chlorophyll (Schenk et al., 2007), yet reports have been published claiming chlide fractions between 10 and 40% (Benedetti and Arruda, 2002; Kariola et al., 2005). Likewise, the occurrence of chlide in some stay-green mutants, such as *F. pratensis* Bf993 (Vicentini et al., 1995b), is correlated with advanced senescence, likely due to tissue rupture and subsequent nonphysiological chlorophyll hydrolysis (Aubry et al., 2008). In this work, only negligible amounts of chlide were found in the wild type or *pph-1* (Figure 6). In conclusion, we argue that the proposed route of chlorophyll breakdown during leaf senescence via phein instead of chlide does not conflict with data from the literature. However, the pathway involving PPH might be accompanied by additional, minor activities that convert some chlorophyll to chlide.

pph-1 Is a Nonfunctional Stay-Green Mutant Deficient in Chlorophyll Breakdown

The absence of PPH in *pph* mutants caused a stay-green phenotype, in which senescence parameters were uncoupled from chlorophyll breakdown. Thus, *pph* mutants can be classified as cosmetic, nonfunctional type C stay-greens (Thomas and Howarth, 2000). Despite the accumulation of phein *a* (see above), *pph* mutants did not exhibit a lesion-mimic phenotype. This is in contrast with *pao1* and *acd2*, which were shown to accumulate pheide *a* and red chlorophyll catabolites, respectively (Pružinská et al., 2005, 2007). Two hypotheses might explain this fact. First, the amount of phein accumulating in *pph* is not sufficient to cause cell death, or, second, phototoxicity of phein is prevented through its binding to LHCs. The latter is supported by the observation that, despite the loss of photosynthetic activity during senescence in *pph-1*, it is assumed that the mutant is able to dissipate light energy absorbed by the retained pigments. This is most likely achieved through the binding of chlorophyll to its apoproteins, but, as in the case of other nonfunctional stay-green mutants, the mechanism of energy quenching in *pph-1* remains unknown. Furthermore, even though senescence-regulated genes of chlorophyll breakdown, such as *PAO* and *SGR1*, are upregulated in *pph-1* (Figure 3), as they are in the wild type, chlorophyll breakdown is prevented. It is likely that the porphyrin pigments remain attached to their apoproteins as long as they carry the phytol moiety and are thus not accessible to further downstream catabolic enzymes. This view is supported by the fact that in *pph-1* or other stay-green mutants, such as

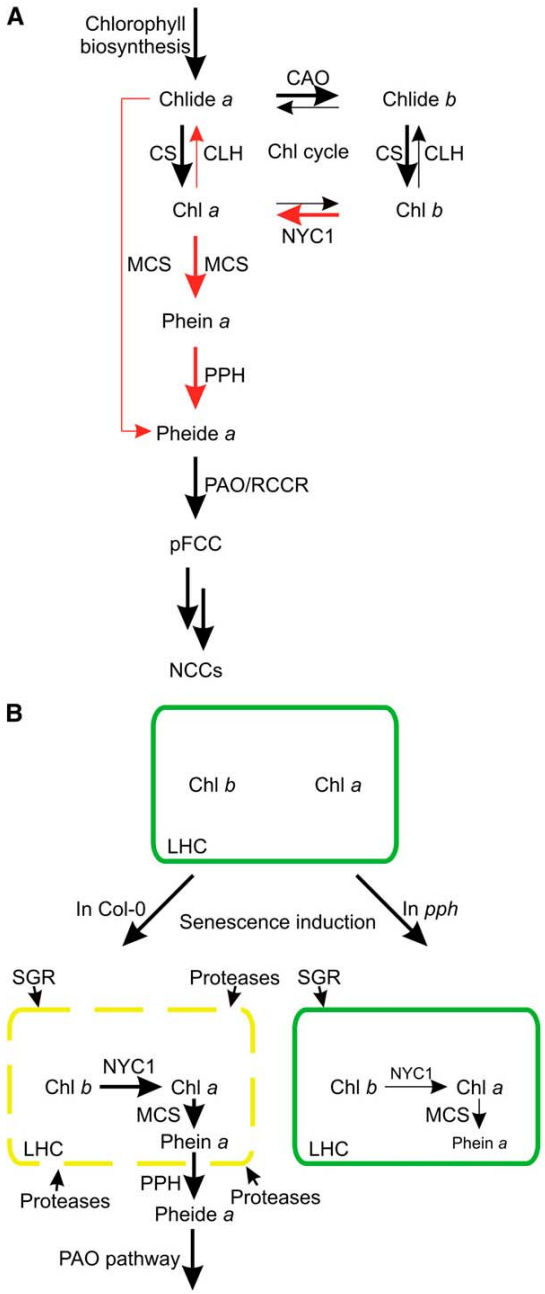

Figure 9. Tentative Models for Chlorophyll Metabolism and for Chlorophyll-Apoprotein Degradation.

(A) Schematic drawing of chlorophyll biosynthesis and degradation, integrating the findings of this work. In this model, anabolic and catabolic steps do not have overlapping activities but are interconnected through the chlorophyll cycle. Thickness of arrows within the cycle reflects relative activities of respective enzymes as suggested by Rüdiger (2002). CLHs might marginally contribute to chlorophyll degradation (thin red arrows), but the bulk of chlorophyll seems to be catabolized via phein *a* and PPH (thick red arrows).

nye1 or *nyc1* (Kusaba et al., 2007; Ren et al., 2007), no increase in free chlorophyll has been observed. In this respect, it is important to note that *pph-1* is particularly defective in chlorophyll *b* degradation, and it thus has a phenotype that greatly resembles that of *nyc1*. However, *NYC1* and *NOL* expression were not altered in *pph-1* compared with the wild type, and further analysis is required to elucidate whether chlorophyll *b* reductase activity is affected in *pph-1*. *pph-1* accumulated phein *a* but not phein *b*, indicating that the *b* to *a* conversion occurs before phytol hydrolysis. A tentative model of reactions required for chlorophyll-apoprotein degradation can be drawn, integrating published data and the results obtained in this work (Figure 9B). In this model, the concerted activity of (at least) three proteins (i.e., SGR, NYC1, and PPH) is required for the initiation of LHC protein degradation. The stromal localization of PPH implies that phein would be released from the complex before hydrolysis; however, PPH more likely transiently associates with components of the thylakoid membrane during catalysis. Similar interactions have been shown between envelope-bound PAO and stromal red chlorophyll catabolite reductase (Pružinská et al., 2007) and between LHC subunits and stroma-localized SGR (Park et al., 2007). LHCs are largely retained in *pph-1*; thus, it seems reasonable to assume that dephytylation (through PPH) is required for pigment release from the complexes as a prerequisite for the subsequent proteolytic degradation of the apoproteins. Alternatively, stabilization of LHC in *pph-1* could be achieved by preventing further chlorophyll *b* to chlorophyll *a* conversion as a consequence of phein *a* retention in the mutant.

PPH Is a Member of a Novel Subclass of α/β Hydrolases

From the distribution of PPH and PPH-like proteins in a phylogenetic tree (Figure 8), it can be hypothesized that they are all derived from an ancestral bacterial esterase gene that was duplicated twice. After endosymbiosis, one gene copy was recruited as PPH. This view is supported by the fact that each of the eukaryotic genomes analyzed contained a single copy of PPH, which was significantly distinct from the two other clades of the tree. In addition, the PPH clade did not contain a bacterial ortholog, indicating that PPH is absent from cyanobacteria. This is in agreement with recent labeling studies for chlorophyll

(B) Tentative model for the degradation of LHC-chlorophyll complexes during senescence in Col-0 and *pph-1*. Upon senescence induction in the wild type, SGR, NYC1, and PPH are activated. Acting independently or in concert, these induced proteins cause structural changes and/or partial destabilization of the LHC-chlorophyll complexes, at least in part through chlorophyll *b* to chlorophyll *a* conversion catalyzed by NYC1. By contrast, the function of SGR in this process is not resolved yet. These changes allow proteases to access and degrade the apoproteins. In the absence of PPH in *pph* mutants, LHC complexes are stabilized and not accessible for proteases, possibly because of the retention of phytylated pigments within the complexes. Alternatively, LHCs could be stabilized by preventing/slowing down further chlorophyll *b* to *a* conversion as a consequence of phein *a* accumulation.

CAO, chlide *a* oxygenase; Chl, chlorophyll. CS, chl synthase; MCS, metal-chelating substance; RCCR, red chlorophyll catabolite reductase.

synthesis and degradation in *Synechocystis* sp PCC 6803, demonstrating that a continuous chlorophyll dephytylation/chlide rephytylation cycle operates in cyanobacteria (Vavilin and Vermaas, 2007). However, *Synechocystis* sp PCC 6803 does not contain a gene with significant homology to CLHs; therefore, the nature of the phytol cleaving activity remains unknown (Vavilin and Vermaas, 2007). The presence of PPH proteins in evolutionary divergent plant species substantiates the likelihood of a common, important function for these proteins.

The primary amino acid sequences of PPH proteins exhibited several domains that are highly conserved between the members. Among these was a motif (named the PPH domain) with a conserved Ser residue, which, based on homology to nearly 500 hydrolases from bacteria to humans, most likely represents the active-site residue (see Supplemental Figure 7C online). Site-directed mutagenesis of the Ser residue seemed to confirm this, although we cannot exclude that the mutation might have impaired proper PPH folding, thereby causing the observed loss of function. The PPH domain was most similar to, but distinct from, a lipase domain (PROSITE PS01098) containing the core sequence G-D-S-[LIVM]. In PPHs, Asp is replaced by an invariant Asn residue, which could be involved in defining substrate specificity. By contrast, CLH proteins contain another PROSITE domain (PS00120) with the core consensus G-[HYVW]-S-x-G (see Supplemental Figure 7B online). The active site of many α/β hydrolases, including proteases and lipases, is composed of a catalytic triad that, in addition to the active Ser residue, involves a His and Asp residue (Dodson and Wlodawer, 1998). Several of these residues are conserved within PPH proteins; which of them are essential for PPH activity remains to be elucidated by site-directed mutagenesis.

In conclusion, we have identified an esterase, named PPH, that is involved in chlorophyll breakdown during leaf senescence. Our data demonstrate that the absence of PPH causes indefinite retention of greenness. We furthermore provide in vitro and in vivo evidence that PPH specifically cleaves the phytol ester of phein, but not chlorophyll. We propose that PPH is the major dephytylating activity in chlorophyll breakdown and is active downstream of chlorophyll *b* reductase (NYC1). Hence, the sequence of early reactions in chlorophyll breakdown has to be reconsidered and very likely proceeds in the following order: chlorophyll *b* → chlorophyll *a* → phein *a* → pheide *a*. Further analysis will be required to analyze whether PPH might also be involved in other instances of chlorophyll metabolism, such as chlorophyll turnover at the steady state level or during fruit ripening.

METHODS

Plant Material and Senescence Induction

Arabidopsis thaliana ecotype Col-0 was used as the wild type. T-DNA insertion lines were from the following collections: SALK (Alonso et al., 2003): *at5g13800-1* (*pph-1*), SALK_000095; *at1g54570-1*, SALK_034549; *at3g26840-1*, SALK_071769; JIC SM lines (Tissier et al., 1999): *pph-2*, SM_3_15198, and GABI lines (Rosso et al., 2003): *pph-3*, GABI_453A08. SALK and SM lines were obtained from the European Arabidopsis Stock Center, Nottingham, UK. The GABI line was obtained from GABI Kat, MPI for Plant Breeding Research, Cologne, Germany. Homozygous plants were identified by PCR using T-DNA-, transposon-, and gene-specific primers as listed in Supplemental Table 1 online. Likewise, homozygous *at1g54570-1 at3g26840-1* and *pph-1 pao1* double mutants were identified by PCR. Plants were grown on soil in long-day conditions in a greenhouse with fluence rates of 100 to 200 μmol photons m^{-2} s^{-1} at 22°C. For senescence induction, detached leaves of 3- to 4-week-old plants were incubated on wet filter paper for up to 7 d in the dark. Alternatively, individual attached leaves were covered with aluminum foil.

Biocomputational Methods and Phylogenetic Analysis

We screened the TAIR8 protein database (http://www.Arabidopsis.org) for hits containing the phrase "alpha/beta." Using the BULK PROTEIN ANALYSIS tool, a subset of 462 proteins was analyzed for proteins containing a putative plastid-targeting sequence. Screening for known protein function was done with the GENE ONTOLOGY ANNOTATION tool.

Homologs of PPH were identified by BLASTP searches (Altschul et al., 1997) with databases of the National Center for Biotechnology Information (http://www.ncbi.nlm.nih.gov) and the Joint Genome Institute (http://www.jgi.doe.gov). For phylogenetic analysis, multiple sequence alignment of PPH amino acid sequences was generated with PROMALS3D (Pei et al., 2008) using default settings. The alignment was curated using Gblocks 0.91b (Talavera and Castresana, 2007) with the following parameters: 15, minimum number of sequences for conserved and flanking positions: 120, maximum number of continuous nonconserved positions; 2, minimum length of a block; all, gap positions. The maximum likelihood tree was obtained with PhyML 3.0 (http://www.atgc-montpellier.fr/phyml; Guindon and Gascuel, 2003) using the LG+I+Γ model (Le and Gascuel, 2008) with four substitution rate categories and estimated gamma shape parameter and proportion of invariant sites. Default settings were used for other parameters. Branch support values are based on 1000 nonparametric bootstrap replicates.

For Figure 8B and Supplemental Figure 7 online, sequences were aligned using the programs DIALIGN (Morgenstern, 2004), GENEDOC (http://www.psc.edu/biomed/genedoc), and WebLogo (http://weblogo.threeplusone.com).

pph-1 Complementation

A full-length cDNA sequence of *PPH* was obtained from the RIKEN resource (Seki et al., 2002). In a two-step PCR amplification using Pfu polymerase (Promega) and the primers listed in Supplemental Table 1 online, Gateway BP recombination sites were added to the *PPH* cDNA. *PPH* was cloned behind the 35S promoter of the destination vector pMDC32 (Curtis and Grossniklaus, 2003) using Gateway technology (Invitrogen). Likewise, a *PPH* $S_{221}A$ missense mutation was produced in pMDC32. Two overlapping PCR fragments containing the mutation were produced by PCR using Pfu polymerase, attB1, and gene-specific primers as listed in Supplemental Table 1 online. In a second PCR reaction, the fragments were combined to yield PPH_{S221A} that, after verification by sequencing, was introduced behind the 35S promoter of pMDC32 (*35S:*PPH_{S221A}) using Gateway technology. *pph-1* was transformed with the flower dip method (Clough and Bent, 1998). Transformants were selected on hygromycin, and homozygous T2 plants were used for further analysis.

GFP Fusion Protein Analysis

PPH cDNA was PCR amplified using the primers listed in Supplemental Table 1 online and cloned into pMDC84 (Curtis and Grossniklaus, 2003) by Gateway technology, thereby producing an N-terminal fusion of PPH

with GFP (PPH-GFP). *Arabidopsis* mesophyll protoplasts were isolated from 6-week-old short-day-grown plants according to published procedures (Endler et al., 2006). Cell numbers were quantified with a Neubauer chamber and adjusted to a density of 2×10^6 protoplasts mL^{-1}. Protoplasts were transformed by 20% polyethylene glycol transformation according to published procedures (Meyer et al., 2006). Transformed cells were incubated for 48 h in the dark at room temperature before laser scanning confocal microscopic analysis (DM IRE2; Leica Microsystems). GFP fluorescence was imaged at an excitation wavelength of 488 nm, and the emission signal was recovered between 495 and 530 nm. TIC110-GFP expressed from pCL60-TIC110-GFP (Schenk et al., 2007) was used as a control for plastid envelope localization.

Protein Import Experiments

[^{35}S]-Met–labeled PPH was synthesized from *Arabidopsis* full-length *PPH* cloned in pBluescript with the TNT T7 Quick Coupled Transcription/Translation System (Promega). Intact chloroplasts of 4-week-old in vitro–grown *Arabidopsis* plants (ecotype Col-2) were isolated as published (Kubis et al., 2008) with the following modifications. The chloroplast isolation buffer was composed of 50 mM HEPES-KOH, pH 7.5, 2 mM EDTA, 1 mM $MnCl_2$, 1 mM $MgCl_2$, 330 mM sorbitol, 100 mM Na-ascorbate, 0.25% BSA, and 0.05% protease inhibitor cocktail (Sigma-Aldrich). Chloroplasts were purified on a 40/85% step gradient of Percoll (GE Healthcare) in 300 mM sorbitol, 20 mM Tricine-KOH, pH 8.5, 5 mM $MgCl_2$, and 2.5 mM EDTA. PPH import assays were performed as published (Fitzpatrick and Keegstra, 2001). For each import reaction, chloroplasts corresponding to 15 μg of chlorophyll and 6.5 μL of in vitro–translated PPH preprotein were used. Lysis of chloroplasts, separation of stroma from membranes, and alkaline membrane treatment were done as described (Smith et al., 2002). All samples were resolved by SDS-PAGE and visualized using a phosphor imager (Bio-Rad).

RNA Isolation and RT-PCR

RNA was isolated using the Plant RNeasy kit (Qiagen). After DNA digestion with RQ1 DNase (Promega), first-strand cDNA was synthesized using the RETROscript kit (Ambion). PCR was performed with a non-saturating number of amplification cycles as shown in the figures using gene-specific primers as listed in Supplemental Table 1 online.

Analysis of Chlorophyll and Chlorophyll Catabolites

For spectrophotometric determination of chlorophyll concentrations (Strain et al., 1971), chlorophyll was extracted from leaf tissue by homogenization in liquid nitrogen and subsequent threefold extraction into 80% (v/v) acetone containing 1 μM KOH. After centrifugation (2 min; 16,000*g*), supernatants were combined and used for analysis.

For HPLC analysis of green chlorophyll catabolites (chlorophyll, chlide, pheide, and phein), liquid nitrogen-homogenized tissue was extracted in 10% (v/v) 0.2 M Tris-HCl, pH 8, in acetone, cooled to −20°C (20 mL g^{-1} fresh weight), and incubated at −20°C for 2 h in the dark. After removal of insoluble material by centrifugation, supernatants were analyzed by reverse-phase HPLC as described (Pružinská et al., 2005). Pigments were identified by their absorption spectra, peak ratios, and comigration with authentic standards (Roca et al., 2004). For quantification, chlorophyll solutions of defined concentrations were analyzed by HPLC, and peak areas at A_{665} referred to the injected quantities. Likewise, pheo pigments obtained after acidification of chlorophyll solutions (see below) were quantified spectrophotometrically (Porra, 1991) and used to calibrate HPLC peak areas.

NCCs were extracted from leaf tissue and analyzed as described (Pružinská et al., 2005).

Chlorophyll Fluorescence and CO_2 Assimilation Rate

Senescence was induced by darkening attached leaves with aluminum foil. Maximum quantum yield of PSII (F_v/F_m) was measured with a portable photosynthesis system LI-COR 6400 (Li-Cor). Rates of CO_2 assimilation were determined at a flux density of 0 to 1000 μmol m^{-2} s^{-1} and a CO_2 concentration of 380 μmol mol^{-1}.

Analysis of Recombinant PPH

For heterologous expression of PPH in *Escherichia coli*, a truncated fragment of *PPH* cDNA, lacking the 46 5′-terminal amino acids encoding the predicted chloroplast transit peptide, was produced by PCR using Pfu polymerase and the primers listed in Supplemental Table 1 online. After restriction digest with *Bam*HI/*Sal*I, the fragment was cloned into pMAL-c2 (New England Biolabs), producing an MBP-truncated PPH (ΔPPH) fusion (MBP-ΔPPH). Likewise, a $S_{221}A$ missense mutation was introduced into ΔPPH by PCR as described above and cloned into pMAL-c2 (MBP-ΔPPH_{S221A}). After verification of constructs by sequencing, recombinant proteins were allowed to accumulate after chemical induction of gene expression for 3 h as described (Wüthrich et al., 2000). Cells were lysed by lysozyme treatment and sonication as described (Wüthrich et al., 2000) using 0.1 M MOPS-KOH, pH 7.0, as buffer. Crude cell extracts were supplemented with 10% (v/v) glycerol and either directly used for assays or frozen in liquid nitrogen, which did not affect enzyme activity. For MBP fusion protein cleavage, *E. coli* extracts were treated for 24 h with factor XA (50 mg g^{-1} protein) according to the manufacturer's protocol (New England Biolabs). Recombinant *Citrus* Chlase1 was expressed as a thioredoxin fusion protein as described (Jakob-Wilk et al., 1999). Crude Chlase1 extracts were produced as above.

The assays (total volume 200 μL) consisted of 10 μL crude cell extracts (corresponding to 0.36 mL of original cell culture at $OD_{600} = 1.5$) and 20 μL of pigment substrates dissolved in acetone (final concentration of pigment substrates, 29 μM; final acetone concentration, 10%). After incubation at 25°C for various time periods as indicated in the figures, the reaction was stopped by the addition of acetone to a final concentration of 66%. After centrifugation (2 min at 18,000*g*), samples were analyzed by HPLC as described above. Chlorophyll used as substrate was isolated from coffee (*Coffea arabica*) leaves as described (Vicentini et al., 1995a) and quantified photometrically (Strain et al., 1971). For the production of phein, the chlorophyll solution was acidified by the addition of HCl to a final concentration of 20 mM. After 2 min, 20 mM NaOH (final concentration) was added to neutralize the solution, which was then employed as substrate in the assays.

Extraction and Analysis of Photosystem Subcomplexes

Chloroplast membranes were isolated according to established procedures (Oh et al., 2003). Membranes were subsequently solubilized on ice for 30 min with 0.8% (w/v) dodecylmaltoside in 1× PBS. After centrifugation (5 min, 15,000*g*, 4°C), complexes were separated on a linear gradient of 1.0 to 0.1 M sucrose in 50 mM Tris-HCl, pH 8 (0.05%, w/v) dodecylmaltoside. After centrifugation at 4°C (197,000*g* for 16 h), 0.5 mL fractions were withdrawn with a gradient former (AutoDensiFlow II; Buchler) and analyzed by immunoblotting (see below).

Protein Extraction and Immunoblot Analysis

Total leaf protein and soluble and membrane fractions were prepared essentially as described (Pružinská et al., 2003; Schenk et al., 2007). SDS-PAGE and subsequent immunoblot analysis were performed as described (Pružinská et al., 2007). The following antibodies were used: monoclonal antibodies against PAO (1:500; Gray et al., 2004) and polyclonal antibodies against LHCa1, LHCa2, LHCb1, LHCb2, PsbA

(1:2000; AgriSera), PsaA (1:5000; J.D. Rochaix, Geneva, Switzerland), and Rubisco large subunit (1:2000; S. Gepstein, Haifa, Israel).

Transmission Electron Microscopy

Leaf segments (2 × 20 mm) were fixed at room temperature in 2.5% (v/v) glutaraldehyde and 1% (w/v) formaldehyde (freshly prepared from paraformaldehyde) in 0.1 M sodium cacodylate buffer, pH 7.3. After washing in buffer, the samples were postfixed in buffered 1% osmium tetroxide, washed, dehydrated in a graded series of ethanol, and embedded in LR white resin. The resin was polymerized at 60°C. Ultrathin sections were cut with a diamond knife in an Ultracut UCT ultramicrotome (Leica). The sections were stained with saturated uranyl acetate in water and lead citrate (Reynolds, 1963) and observed using a Philips CM10 transmission electron microscope.

Accession Numbers

Protein sequences used in this work are as follows. GenBank identification numbers: *Arabidopsis thaliana* (At): At PPH, 15240707 (At5g13800); At4g36530, 15234433; At5g19850, 26450541; SGR1, 18416035 (At4g22920); PAO, 15230543 (At3g44880); NYC1, 18413962 (At4g13250); NOL, 18414726 (At5g04900); CLH1, 18394772 (At1g19670); CLH2, 15240020 (At5g43860); *Chlamydomonas reinhardtii* (Cr): Cr PPH, 159490010; Cr XP1701, 159486857; Cr XP1698, 159480594; *Citrus sinensis* (Cs): Chlase1, 7328567; *Nicotiana tabacum* (Nt): Nt PPH, 156763846; *Ostreococcus lucimarinus* (Ol): Ol PPH, 145340970; Ol XP1422, 145355583; *Oryza sativa* (Os): Os PPH, 115467988 (Os06g0354700); Os EAZ404, 125600825; Os EAZ243, 125583397; *Ostreococcus taurii* (Ot): Ot PPH, 116000661; Ot CAL579, 116055845; *Physcomitrella patens* (Pp): Pp PPH, 168018382; Pp XP1785, 168067769; Pp XP1762, 168019983; *Picea sitchensis* (Ps): Ps ABK247, 116788178; *Synechococcus* sp PCC 7002 (Sco): Sco YP1733, 170076657; Sco YP1734, 170077791; Sco YP1735, 170078876; *Synechocystis* sp PCC 6803 (Scy): Scy slr1917, 16329733; Scy slr1235, 16330114; *Vitis vinifera* (Vv): Vv PPH, 157350650; Vv CAO228, 157348115; *Zea mays* (Zm): Zm PPH, 194706646; Zm ACF844, 194,700,822. *Phaeodactylum tricornutum* (Pt) protein IDs are from the Joint Genome Initiative (http://jgi.doe.gov): Pt PPH, 41648; Pt 4967, 4967.

Supplemental Data

The following materials are available in the online version of this article.

Supplemental Figure 1. Natural Senescence of Col-0 and *pph-1*.

Supplemental Figure 2. Changes in Net Photosynthesis during Senescence in *pph-1*.

Supplemental Figure 3. Immunoblot Analysis of Photosynthetic Complexes after Sucrose Density Gradient Centrifugation.

Supplemental Figure 4. Accumulation of Chlorophyll *a* Derivatives in *pph-1*.

Supplemental Figure 5. Activity Determination of Recombinant *Citrus* Chlorophyllase.

Supplemental Figure 6. Activity Determination of Recombinant PPH.

Supplemental Figure 7. Sequence Alignment of the Active-Site Domain of PPH and PPH-Like Proteins.

Supplemental Table 1. Primers Used in This Work.

Supplemental Data Set 1. Sequences Used to Generate the Phylogenetic Tree Presented in Figure 8A.

ACKNOWLEDGMENTS

For the supply of antibodies, we thank John Gray (University of Toledo) (PAO), Shimon Gepstein (Israel Institute of Technology) (Rubisco large subunit), and Jean-David Rochaix (University of Geneva, Switzerland) (PsaA). Smadar Harpaz-Saad and Yoram Eyal (Volcani Center, Israel) kindly provided a bacterial strain expressing recombinant *Citrus* chlorophyllase. We thank Maria Mulisch (University of Kiel, Germany) for electron microscopy analysis. Support by grants from the Swiss National Science Foundation (3100A0-117940) to S.H., the National Center of Competence in Research Plant Survival, the research program of the Swiss National Science Foundation to S.H. and F.K., and the Global Research Laboratory program of the Ministry of Science and Technology of Korea to B.B. is acknowledged.

Received October 30, 2008; revised February 12, 2009; accepted March 8, 2009; published March 20, 2009.

REFERENCES

Alonso, J.M., et al. (2003). Genome-wide insertional mutagenesis of *Arabidopsis thaliana*. Science **301:** 653–657.

Altschul, S.F., Madden, T.L., Schaffer, A.A., Zhang, J.H., Zhang, Z., Miller, W., and Lipman, D.J. (1997). Gapped BLAST and PSI-BLAST: A new generation of protein database search programs. Nucleic Acids Res. **25:** 3389–3402.

Amir-Shapira, D., Goldschmidt, E.E., and Altman, A. (1987). Chlorophyll catabolism in senescing plant tissues: *In vivo* breakdown intermediates suggest different degradative pathways for *Citrus* fruit and parsley leaves. Proc. Natl. Acad. Sci. USA **84:** 1901–1905.

Arkus, K.A.J., Cahoon, E.B., and Jez, J.M. (2005). Mechanistic analysis of wheat chlorophyllase. Arch. Biochem. Biophys. **438:** 146–155.

Armstead, I., et al. (2006). From crop to model to crop: identifying the genetic basis of the staygreen mutation in the *Lolium/Festuca* forage and amenity grasses. New Phytol. **172:** 592–597.

Armstead, I., et al. (2007). Cross-species identification of Mendel's *I* locus. Science **315:** 73.

Aubry, S., Mani, J., and Hörtensteiner, S. (2008). Stay-green protein, defective in Mendel's green cotyledon mutant, acts independent and upstream of pheophorbide *a* oxygenase in the chlorophyll catabolic pathway. Plant Mol. Biol. **67:** 243–256.

Austin, J.R., Frost, E., Vidi, P.A., Kessler, F., and Staehelin, L.A. (2006). Plastoglobules are lipoprotein subcompartments of the chloroplast that are permanently coupled to thylakoid membranes and contain biosynthetic enzymes. Plant Cell **18:** 1693–1703.

Azoulay Shemer, T., Harpaz-Saad, S., Belausov, E., Lovat, N., Krokhin, O., Spicer, V., Standing, K.G., Goldschmidt, E.E., and Eyal, Y. (2008). *Citrus* chlorophyllase dynamics at ethylene-induced fruit color-break; a study of chlorophyllase expression, post-translational processing kinetics and *in-situ* intracellular localization. Plant Physiol. **148:** 108–118.

Barry, C.S., McQuinn, R.P., Chung, M.Y., Besuden, A., and Giovannoni, J.J. (2008). Amino acid substitutions in homologs of the STAY-GREEN protein are responsible for the *green-flesh* and *chlorophyll retainer* mutations of tomato and pepper. Plant Physiol. **147:** 179–187.

Benedetti, C.E., and Arruda, P. (2002). Altering the expression of the chlorophyllase gene *ATHCOR1* in transgenic Arabidopsis caused changes in the chlorophyll-to-chlorophyllide ratio. Plant Physiol. **128:** 1255–1263.

Borovsky, Y., and Paran, I. (2008). Chlorophyll breakdown during pepper fruit ripening in the *chlorophyll retainer* mutation is impaired at

the homolog of the senescence-inducible stay-green gene. Theor. Appl. Genet. **117:** 235–240.

Clough, S.J., and Bent, A.F. (1998). Floral dip: A simplified method for *Agrobacterium*-mediated transformation of *Arabidopsis thaliana*. Plant J. **16:** 735–743.

Curtis, M.D., and Grossniklaus, U. (2003). A gateway cloning vector set for high-throughput functional analysis of genes in planta. Plant Physiol. **133:** 462–469.

Dodson, G., and Wlodawer, A. (1998). Catalytic triads and their relatives. Trends Biochem. Sci. **23:** 347–352.

Emanuelsson, O., Nielsen, H., and Von Heijne, G. (1999). ChloroP, a neural network-based method for predicting chloroplast transit peptides and their cleavage sites. Protein Sci. **8:** 978–984.

Endler, A., Meyer, S., Schelbert, S., Schneider, T., Weschke, W., Peters, S.W., Keller, F., Baginsky, S., Martinoia, E., and Schmidt, U.G. (2006). Identification of a vacuolar sucrose transporter in barley and Arabidopsis mesophyll cells by a tonoplast proteomic approach. Plant Physiol. **141:** 196–207.

Fiedor, L., Rosenbach-Belkin, V., and Scherz, A. (1992). The stereospecific interaction between chlorophylls and chlorophyllase - Possible implication for chlorophyll biosynthesis and degradation. J. Biol. Chem. **267:** 22043–22047.

Fitzpatrick, L.M., and Keegstra, K. (2001). A method for isolating a high yield of Arabidopsis chloroplasts capable of efficient import of precursor proteins. Plant J. **27:** 59–65.

Fojan, P., Jonson, P.H., Petersen, M.T.N., and Petersen, S.B. (2000). What distinguishes an esterase from a lipase: A novel structural approach. Biochimie **82:** 1033–1041.

Gaude, N., Brehelin, C., Tischendorf, G., Kessler, F., and Dörmann, P. (2007). Nitrogen deficiency in Arabidopsis affects galactolipid composition and gene expression and results in accumulation of fatty acid phytyl esters. Plant J. **49:** 729–739.

Gray, J., Wardzala, E., Yang, M., Reinbothe, S., Haller, S., and Pauli, F. (2004). A small family of LLS1-related non-heme oxygenases in plants with an origin amongst oxygenic photosynthesizers. Plant Mol. Biol. **54:** 39–54.

Guindon, S., and Gascuel, O. (2003). A simple, fast, and accurate algorithm to estimate large phylogenies by maximum likelihood. Syst. Biol. **52:** 696–704.

Harpaz-Saad, S., Azoulay, T., Arazi, T., Ben-Yaakov, E., Mett, A., Shiboleth, Y.M., Hörtensteiner, S., Gidoni, D., Gal-On, A., Goldschmidt, E.E., and Eyal, Y. (2007). Chlorophyllase is a rate-limiting enzyme in chlorophyll catabolism and is posttranslationally regulated. Plant Cell **19:** 1007–1022.

Hinder, B., Schellenberg, M., Rodoni, S., Ginsburg, S., Vogt, E., Martinoia, E., Matile, P., and Hörtensteiner, S. (1996). How plants dispose of chlorophyll catabolites. Directly energized uptake of tetrapyrrolic breakdown products into isolated vacuoles. J. Biol. Chem. **271:** 27233–27236.

Horn, R., and Paulsen, H. (2004). Early steps in the assembly of light-harvesting chlorophyll *a/b* complex - Time-resolved fluorescence measurements. J. Biol. Chem. **279:** 44400–44406.

Hörtensteiner, S. (2006). Chlorophyll degradation during senescence. Annu. Rev. Plant Biol. **57:** 55–77.

Hörtensteiner, S., Vicentini, F., and Matile, P. (1995). Chlorophyll breakdown in senescent cotyledons of rape, *Brassica napus* L.: Enzymatic cleavage of phaeophorbide *a in vitro*. New Phytol. **129:** 237–246.

Hörtensteiner, S., Wüthrich, K.L., Matile, P., Ongania, K.-H., and Kräutler, B. (1998). The key step in chlorophyll breakdown in higher plants. Cleavage of pheophorbide *a* macrocycle by a monooxygenase. J. Biol. Chem. **273:** 15335–15339.

Ischebeck, T., Zbierzak, A.M., Kanwischer, M., and Dörmann, P. (2006). A salvage pathway for phytol metabolism in *Arabidopsis*. J. Biol. Chem. **281:** 2470–2477.

Jakob-Wilk, D., Holland, D., Goldschmidt, E.E., Riov, J., and Eyal, Y. (1999). Chlorophyll breakdown by chlorophyllase: Isolation and functional expression of the *Chlase1* gene from ethylene-treated *Citrus* fruit and its regulation during development. Plant J. **20:** 653–661.

Jiang, H., Li, M., Liang, N., Yan, H., Wei, Y., Xu, X., Liu, J., Xu, Z., Chen, F., and Wu, G. (2007). Molecular cloning and function analysis of the *stay green* gene in rice. Plant J. **52:** 197–209.

Kariola, T., Brader, G., Li, J., and Palva, E.T. (2005). Chlorophyllase 1, a damage control enzyme, affects the balance between defense pathways in plants. Plant Cell **17:** 282–294.

Kräutler, B. (2003). Chlorophyll breakdown and chlorophyll catabolites. In The Porphyrin Handbook, vol. 13, K.M. Kadish, K.M. Smith, and R. Guilard, eds (Oxford, UK: Elsevier Science), pp. 183–209.

Kräutler, B., and Hörtensteiner, S. (2006). Chlorophyll catabolites and the biochemistry of chlorophyll breakdown. In Chlorophylls and Bacteriochlorophylls: Biochemistry, Biophysics, Functions and Applications, B. Grimm, R. Porra, W. Rüdiger, and H. Scheer, eds (Dordrecht, The Netherlands: Springer), pp. 237–260.

Kräutler, B., Jaun, B., Bortlik, K.-H., Schellenberg, M., and Matile, P. (1991). On the enigma of chlorophyll degradation: the constitution of a secoporphinoid catabolite. Angew. Chem. Int. Ed. Engl. **30:** 1315–1318.

Kreuz, K., Tommasini, R., and Martinoia, E. (1996). Old enzymes for a new job. Herbicide detoxification in plants. Plant Physiol. **111:** 349–353.

Kubis, S.E., Lilley, K.S., and Jarvis, P. (2008). Isolation and preparation of chloroplasts from *Arabidopsis thaliana* plants. Methods Mol. Biol. **425:** 171–186.

Kusaba, M., Ito, H., Morita, R., Iida, S., Sato, Y., Fujimoto, M., Kawasaki, S., Tanaka, R., Hirochika, H., Nishimura, M., and Tanaka, A. (2007). Rice NON-YELLOW COLORING1 is involved in light-harvesting complex II and grana degradation during leaf senescence. Plant Cell **19:** 1362–1375.

Le, S.Q., and Gascuel, O. (2008). An improved general amino acid replacement matrix. Mol. Biol. Evol. **25:** 1307–1320.

Liao, Y., An, K., Zhou, X., Chen, W.-J., and Kuai, B.-K. (2007). *AtCLH2*, a typical but possibly distinctive chlorophyllase gene in *Arabidopsis*. J. Integr. Plant Biol. **49:** 531–539.

Matile, P., Ginsburg, S., Schellenberg, M., and Thomas, H. (1988). Catabolites of chlorophyll in senescing barley leaves are localized in the vacuoles of mesophyll cells. Proc. Natl. Acad. Sci. USA **85:** 9529–9532.

Matile, P., Hörtensteiner, S., and Thomas, H. (1999). Chlorophyll degradation. Annu. Rev. Plant Physiol. Plant Mol. Biol. **50:** 67–95.

Matile, P., Schellenberg, M., and Peisker, C. (1992). Production and release of a chlorophyll catabolite in isolated senescent chloroplasts. Planta **187:** 230–235.

Meyer, A., Eskandari, S., Grallath, S., and Rentsch, D. (2006). AtGAT1, a high affinity transporter for γ-aminobutyric acid in *Arabidopsis thaliana*. J. Biol. Chem. **281:** 7197–7204.

Morgenstern, B. (2004). DIALIGN: Multiple DNA and protein sequence alignment at BiBiServ. Nucleic Acids Res. **32:** W33–W36.

Mühlecker, W., Ongania, K.-H., Kräutler, B., Matile, P., and Hörtensteiner, S. (1997). Tracking down chlorophyll breakdown in plants: Elucidation of the constitution of a 'fluorescent' chlorophyll catabolite. Angew. Chem. Int. Ed. Engl. **36:** 401–404.

Müller, T., Moser, S., Ongania, K.-H., Pružinská, A., Hörtensteiner, S., and Kräutler, B. (2006). A divergent path of chlorophyll breakdown in the model plant *Arabidopsis thaliana*. ChemBioChem **7:** 40–42.

Oberhuber, M., Berghold, J., Breuker, K., Hörtensteiner, S., and

Kräutler, B. (2003). Breakdown of chlorophyll: A nonenzymatic reaction accounts for the formation of the colorless "nonfluorescent" chlorophyll catabolites. Proc. Natl. Acad. Sci. USA **100:** 6910–6915.

Oh, M.H., Moon, Y.H., and Lee, C.H. (2003). Increased stability of LHCII by aggregate formation during dark-induced leaf senescence in the *Arabidopsis* mutant, *ore10*. Plant Cell Physiol. **44:** 1368–1377.

Okazawa, A., Tang, L., Itoh, Y., Fukusaki, E., and Kobayashi, A. (2006). Characterization and subcellular localization of chlorophyllase from *Ginkgo biloba*. Z. Naturforsch. [C] **61:** 111–117.

Park, J.H., Oh, S.A., Kim, Y.H., Woo, H.R., and Nam, H.G. (1998). Differential expression of senescence-associated mRNAs during leaf senescence induced by different senescence-inducing factors in *Arabidopsis*. Plant Mol. Biol. **37:** 445–454.

Park, S.-Y., et al. (2007). The senescence-induced staygreen protein regulates chlorophyll degradation. Plant Cell **19:** 1649–1664.

Pei, J., Kim, B.-H., and Grishin, N.V. (2008). PROMALS3D: A tool for multiple protein sequence and structure alignments. Nucleic Acids Res. **36:** 2295–2300.

Porra, R.J. (1991). Recent advances and re-assessments in chlorophyll extraction and assay procedures for terrestrial, aquatic, and marine organisms, including recalcitrant algae. In Chlorophylls, H. Scheer, ed (Boca Raton, FL: CRC Press), pp. 31–57.

Pružinská, A., Anders, I., Aubry, S., Schenk, N., Tapernoux-Lüthi, E., Müller, T., Kräutler, B., and Hörtensteiner, S. (2007). In vivo participation of red chlorophyll catabolite reductase in chlorophyll breakdown. Plant Cell **19:** 369–387.

Pružinská, A., Anders, I., Tanner, G., Roca, M., and Hörtensteiner, S. (2003). Chlorophyll breakdown: Pheophorbide *a* oxygenase is a Rieske-type iron-sulfur protein, encoded by the *accelerated cell death 1* gene. Proc. Natl. Acad. Sci. USA **100:** 15259–15264.

Pružinská, A., Tanner, G., Aubry, S., Anders, I., Moser, S., Müller, T., Ongania, K.-H., Kräutler, B., Youn, J.-Y., Liljegren, S.J., and Hörtensteiner, S. (2005). Chlorophyll breakdown in senescent Arabidopsis leaves: Characterization of chlorophyll catabolites and of chlorophyll catabolic enzymes involved in the degreening reaction. Plant Physiol. **139:** 52–63.

Ren, G., An, K., Liao, Y., Zhou, X., Cao, Y., Zhao, H., Ge, X., and Kuai, B. (2007). Identification of a novel chloroplast protein AtNYE1 regulating chlorophyll degradation during leaf senescence in Arabidopsis. Plant Physiol. **144:** 1429–1441.

Reynolds, E.S. (1963). The use of lead citrate at high pH as an electron-opaque stain in electron microscopy. J. Cell Biol. **17:** 208–212.

Roca, M., James, J., Pružinská, A., Hörtensteiner, S., Thomas, H., and Ougham, H. (2004). Analysis of the chlorophyll catabolism pathway in leaves of an introgression senescence mutant of *Lolium temulentum*. Phytochemistry **65:** 1231–1238.

Rodoni, S., Mühlecker, W., Anderl, M., Kräutler, B., Moser, D., Thomas, H., Matile, P., and Hörtensteiner, S. (1997). Chlorophyll breakdown in senescent chloroplasts. Cleavage of pheophorbide *a* in two enzymic steps. Plant Physiol. **115:** 669–676.

Rosso, M.G., Li, Y., Strizhov, N., Reiss, B., Dekker, K., and Weisshaar, B. (2003). An *Arabidopsis thaliana* T-DNA mutagenized population (GABI-Kat) for flanking sequence tag-based reverse genetics. Plant Mol. Biol. **53:** 247–259.

Rüdiger, W. (2002). Biosynthesis of chlorophyll *b* and the chlorophyll cycle. Photosynth. Res. **74:** 187–193.

Sato, Y., Morita, R., Katsuma, S., Nishimura, M., Tanaka, A., and Kusaba, M. (2009). Two short-chain dehydrogenase/reductases, NON-YELLOW COLORING 1 and NYC1-LIKE, are required for chlorophyll *b* and light-harvesting complex II degradation during senescence in rice. Plant J. **57:** 120–131.

Sato, Y., Morita, R., Nishimura, M., Yamaguchi, H., and Kusaba, M. (2007). Mendel's green cotyledon gene encodes a positive regulator of the chlorophyll-degrading pathway. Proc. Natl. Acad. Sci. USA **104:** 14169–14174.

Schenk, N., Schelbert, S., Kanwischer, M., Goldschmidt, E.E., Dörmann, P., and Hörtensteiner, S. (2007). The chlorophyllases AtCLH1 and AtCLH2 are not essential for senescence-related chlorophyll breakdown in *Arabidopsis thaliana*. FEBS Lett. **581:** 5517–5525.

Schoch, S., Scheer, H., Schiff, J.A., Rüdiger, W., and Siegelman, H.W. (1981). Pyropheophytin *a* accompanies pheophytin *a* in darkened light grown cells of *Euglena*. Z. Naturforsch. [C] **36c:** 827–833.

Schoch, S., and Vielwerth, F.X. (1983). Chlorophyll degradation in senescent tobacco cell culture (*Nicotiana tabacum* var. "Samsun"). Z. Pflanzenphysiol. **110:** 309–317.

Seki, M., et al. (2002). Functional annotation of a full-length Arabidopsis cDNA collection. Science **296:** 141–145.

Shimokawa, K., Hashizume, A., and Shioi, Y. (1990). Pyropheophorbide *a*, a catabolite of ethylene-induced chlorophyll *a* degradation. Phytochemistry **29:** 2105–2106.

Shioi, Y., Tatsumi, Y., and Shimokawa, K. (1991). Enzymatic degradation of chlorophyll in *Chenopodium album*. Plant Cell Physiol. **32:** 87–93.

Smith, M.D., Schnell, D.J., Fitzpatrick, L., and Keegstra, K. (2002). In vitro analysis of chloroplast protein import. In Current Protocols in Cell Biology, J.S. Bonifacino, M. Dasso, J.B. Harford, J. Lippincott-Schwartz, and K.M. Yamada, eds (New York: Wiley Interscience), pp. 11.16.1–11.16.21.

Strain, H.H., Cope, B.T., and Svec, W.A. (1971). Analytical procedures for the isolation, identification, estimation and investigation of the chlorophylls. Methods Enzymol. **23:** 452–476.

Suzuki, T., Kunieda, T., Murai, F., Morioka, S., and Shioi, Y. (2005). Mg-dechelation activity in radish cotyledons with artificial and native substrates, Mg-chlorophyllin *a* and chlorophyllide *a*. Plant Physiol. Biochem. **43:** 459–464.

Takamiya, K., Tsuchiya, T., and Ohta, H. (2000). Degradation pathway (s) of chlorophyll: What has gene cloning revealed? Trends Plant Sci. **5:** 426–431.

Talavera, G., and Castresana, J. (2007). Improvement of phylogenies after removing divergent and ambiguously aligned blocks from protein sequence alignments. Syst. Biol. **56:** 564–577.

Tanaka, A., Ito, H., Tanaka, R., Tanaka, N.K., Yoshida, K., and Okada, K. (1998). Chlorophyll *a* oxygenase (*CAO*) is involved in chlorophyll *b* formation from chlorophyll *a*. Proc. Natl. Acad. Sci. USA **95:** 12719–12723.

Tanaka, R., Hirashima, M., Satoh, S., and Tanaka, A. (2003). The *Arabidopsis-accelerated cell death* gene *ACD1* is involved in oxygenation of pheophorbide *a*: Inhibition of pheophorbide *a* oxygenase activity does not lead to the "stay-green" phenotype in *Arabidopsis*. Plant Cell Physiol. **44:** 1266–1274.

Thomas, H. (1987). *Sid*: A Mendelian locus controlling thylakoid membrane disassembly in senescing leaves of *Festuca pratensis*. Theor. Appl. Genet. **73:** 551–555.

Thomas, H., and Hilditch, P. (1987). Metabolism of thylakoid membrane proteins during foliar senescence. In Plant Senescence: Its Biochemistry and Physiology, W.W. Thomson, E.A. Nothnagel, and R.C. Huffaker, eds (Rockville, MD: American Society of Plant Physiologists), pp. 114–122.

Thomas, H., and Howarth, C.J. (2000). Five ways to stay green. J. Exp. Bot. **51:** 329–337.

Tissier, A.F., Marillonnet, S., Klimyuk, V., Patel, K., Torres, M.A., Murphy, G., and Jones, J.D. (1999). Multiple independent defective *suppressor-mutator* transposon insertions in Arabidopsis: a tool for functional genomics. Plant Cell **11:** 1841–1852.

Tsuchiya, T., Ohta, H., Okawa, K., Iwamatsu, A., Shimada, H., Masuda, T., and Takamiya, K. (1999). Cloning of chlorophyllase,

the key enzyme in chlorophyll degradation: Finding of a lipase motif and the induction by methyl jasmonate. Proc. Natl. Acad. Sci. USA **96:** 15362–15367.

Vavilin, D., and Vermaas, W. (2007). Continuous chlorophyll degradation accompanied by chlorophyllide and phytol reutilization for chlorophyll synthesis in *Synechocystis* sp PCC 6803. Biochim. Biophys. Acta **1767:** 920–929.

Vicentini, F., Hörtensteiner, S., Schellenberg, M., Thomas, H., and Matile, P. (1995b). Chlorophyll breakdown in senescent leaves: identification of the biochemical lesion in a *stay-green* genotype of *Festuca pratensis* Huds. New Phytol. **129:** 247–252.

Vicentini, F., Iten, F., and Matile, P. (1995a). Development of an assay for Mg-dechelatase of oilseed rape cotyledons, using chlorophyllin as the substrate. Physiol. Plant. **94:** 57–63.

Vidi, P.A., Kanwischer, M., Baginsky, S., Austin, J.R., Csucs, G., Dörmann, P., Kessler, F., and Brehelin, C. (2006). Tocopherol cyclase (VTE1) localization and vitamin E accumulation in chloroplast plastoglobule lipoprotein particles. J. Biol. Chem. **281:** 11225–11234.

Willstätter, R., and Stoll, A. (1913). Die Wirkungen der Chlorophyllase. In Untersuchungen über Chlorophyll, R. Willstätter and A. Stoll, eds (Berlin: Verlag Julius Springer), pp. 172–187.

Wüthrich, K.L., Bovet, L., Hunziker, P.E., Donnison, I.S., and Hörtensteiner, S. (2000). Molecular cloning, functional expression and characterisation of RCC reductase involved in chlorophyll catabolism. Plant J. **21:** 189–198.

Ytterberg, A.J., Peltier, J.B., and van Wijk, K.J. (2006). Protein profiling of plastoglobules in chloroplasts and chromoplasts. A surprising site for differential accumulation of metabolic enzymes. Plant Physiol. **140:** 984–997.

Ziegler, R., Blaheta, A., Guha, N., and Schönegge, B. (1988). Enzymatic formation of pheophorbide and pyropheophorbide during chlorophyll degradation in a mutant of *Chlorella fusca* SHIRIA et KRAUS. J. Plant Physiol. **132:** 327–332.

Zimmermann, P., Hirsch-Hoffmann, M., Hennig, L., and Gruissem, W. (2004). GENEVESTIGATOR. Arabidopsis microarray database and analysis toolbox. Plant Physiol. **136:** 2621–2632.

4.2 Kinetic properties of pheophytinase

4.2.1 Introduction

Recently, we discovered a so far unknown esterase playing a crucial role in chl breakdown during leaf senescence in *Arabidopsis*, pheophytin pheophorbide hydrolase (pheophytinase, PPH) (Schelbert et al., 2009; see 4.1.2). PPH is a plastid-localized α/β hydrolase-fold family protein with an esterase/ lipase motif. The absence of the gene product led to a non functional stay-green phenotype during senescence with an indefinite high retention of chlorophyll up to 80%. While recombinant *Citrus* chlorophyllase (*Cs*Chlase1) accepted both, pheophytin (phein) and chlorophyll (chl) as substrates, *At*PPH displayed a clear and only pheophytin-hydrolyzing activity *in vitro* employing *E. coli* crude extracts of soluble proteins. A phylogenetic analysis of PPH-related proteins displayed that *At*PPH clustered with one protein each from eukaryotic plant species. The distribution within the tree indicated that *PPH*s are single-copy genes. The only *PPH*-homolog characterised in the meantime is the ortholog in rice, non yellowing coloring 3 (NYC3, Morita et al., 2009). Due to the fact that PPH is a single copy gene and exhibits rather narrow substrate specificity, heterologously expressed PPH was purified and its kinetic properties studied. The results are presented in this chapter.

4.2.2 Material and methods

4.2.2.1 Protein expression in Escherichia coli and purification process

Protein expression and purification was performed with the pMAL Protein Fusion and Purification System (New England BioLabs). Recombinant proteins were expressed and cells were lysed as described (Schelbert et al., 2009). All chromatographic steps were performed on a Pharmacia chromatography system at 4 °C with a flow of 0.5 ml/min.

Step I: Affinity chromatography An amylose resin column of 15 ml volume was washed with 5 vol of buffer A (0.1 M Mops-KOH pH 7). A total amount of 45 mg (2.5 mg/ml) soluble fusion protein (MBP-Δ*At*PPH; Schelbert et al., 2009) was loaded. After loading of the sample, the column was washed with 10 vol of buffer A and the fusion protein was eluted with buffer B (0.1 M Mops-KOH pH 7, 10 mM maltose). 0.5ml fractions were collected individually for determining fusion protein elution by Bradford Protein Assay (BioRad). Fractions containing the highest protein quantities were pooled.

Step II: Cleavage with Factor Xa Factor Xa (New England BioLabs) cleavage was carried out at a w/w ratio of 2 % the amount of fusion protein (MBP-Δ*At*PPH) according to the manufacturers` instructions. The reaction mixture (7.5 ml) was incubated for 88 h at 4 °C. Complete cleavage of MBP from Δ*At*PPH was controlled by SDS-PAGE.

Step III: Anion exchange chromatography (AEX) A 1 ml HiTrap Q HP column (GE Healthcare) was washed with 5 vol of buffer C (0.1M Mops-KOH pH 7, 25 mM NaCl). After loading the sample, the column was washed with 5 vol of buffer C. The elution of MBP and Δ*At*PPH was carried out using a step gradient of NaCl in buffer C (25 mM; 200 mM; 500 mM). For each step 5 column volumes were applied. 0.5 ml fractions were collected individually for determining MBP and Δ*At*PPH protein elution using the Bradford Protein Assay (BioRad). Fractions containing Δ*At*PPH were pooled. Aliquots of Δ*At*PPH were supplemented with 10 % (v/v) glycerol and either directly used for assays or frozen in liquid nitrogen and stored at -80 °C until further use. Storage did not affect enzyme activity.

4.2.2.2 Substrate purification

Chl used to produce the phein substrate was isolated from coffee (*Coffea arabica*) leaves as described (Vicentini et al., 2005) and quantified photometrically (Strain et al., 1971). Phein production was carried out by acidifying chl *a/b* mixtures by adding HCL to a final concentration of 20 mM. After 2 min, 20 mM NaOH (final concentration) was added to neutralize the solution. The phein a*/b* mixtures were separated by reversed-phase HPLC. Pigments were identified by their absorption spectra and comigration with authentic standards (Roca et al., 2004) and were collected manually. Respective substrate fractions were pooled and elution buffer was removed by flushing under nitrogen atmosphere. Dried substrate was resuspended in 100 % acetone, quantified photometrically (Strain et al., 1971) and stored at -80 °C until further use.

4.2.2.3 In vitro assays for studying kinetic properties of pheopyhtinase

Temperature and pH: The assay (total volume of 40 µl) consisted of 2 µl Δ*At*PPH (corresponding to 2 µg protein) and 4 µl of phein *a/b* mixtures (1.4 mg/ml) dissolved in acetone (final acetone concentration, 10 %) in 0.1 M Hepes-KOH pH 8. After incubation of 30 min in various temperatures as indicated in the figures, the reaction was stopped and analysed by HPLC as described (Schelbert et al., 2009). Product production and quantification was performed according to Schelbert et al. (2009). 0.1 M Hepes-KOH (pH 7-8) and 0.1 M Bicine-HCL (pH 8-9) buffers were used to adjust the pH of the assay.

***K_m* determination:** The assay (total volume of 40 µl) consisted of 1 µl Δ*At*PPH (corresponding to 1 µg protein) and 4 µl of pigment substrate (phein *a*, 4-20 µmol; phein *b*, 0.6-9 µmol) dissolved in acetone (final acetone concentration, 10 %) in 0.1 M Hepes-KOH pH 8. After incubation for 10 min at 34 °C the reaction was stopped and analyzed as described above. Calculation of the apparent K_m was performed according to Lineweaver and Burk (Lineweaver and Burk, 1934).

Transesterification: The assay (total volume of 40 µl) consisted of 2 µl MBP-Δ*At*PPH or *Cs*Chlase1 crude extract, 4 µl of phein *a/b* mixtures (1.4 mg/ml) dissolved in acetone (final acetone concen-

tration, 10 %) and 4 µl MeOH in 0.1 M Hepes-KOH pH 8. After incubation for 30 min at 34 °C, the reaction was stopped and analysed by HPLC as described above. *Cs*Chlase1 was expressed and cells were lysed as described (Schelbert et al., 2009).

4.2.3 Results

4.2.3.1 Purification of pheophytinase

Three consecutive steps were necessary to obtain a protein fraction that was pure enough to study the biochemical features of PPH (Figure 5). In the first step, I used an amylose resin column to purify the fusion protein (MBP-Δ*At*PPH) from *E. coli* soluble proteins present in the crude extract. Thereby, the fusion protein was eluted with 0.1 M Mops-KOH buffer pH 7 containing 10 mM maltose. In the second step, the fusion protein (MBP-Δ*At*PPH) was cleaved into MBP and Δ*At*PPH by Factor Xa, which cleaves at the specific cleavage site located between the two proteins. The resulting fraction was directly used for the third step, separating MBP and Δ*At*PPH by anion-exchange chromatography. Elution was performed by a step gradient of buffer containing increasing amounts of NaCl. MBP was eluted at 200 mM whereas the truncated version of pheophytinase (Δ*At*PPH) was eluted at 500 mM NaCl. Commassie blue-stained SDS-PAGE of the purified enzyme showed a major protein band at 49 kD and faintly stained unspecific bands (Figure 5, lane 8). Visual judgement indicated approximately 90 % purity of the enzyme preparation.

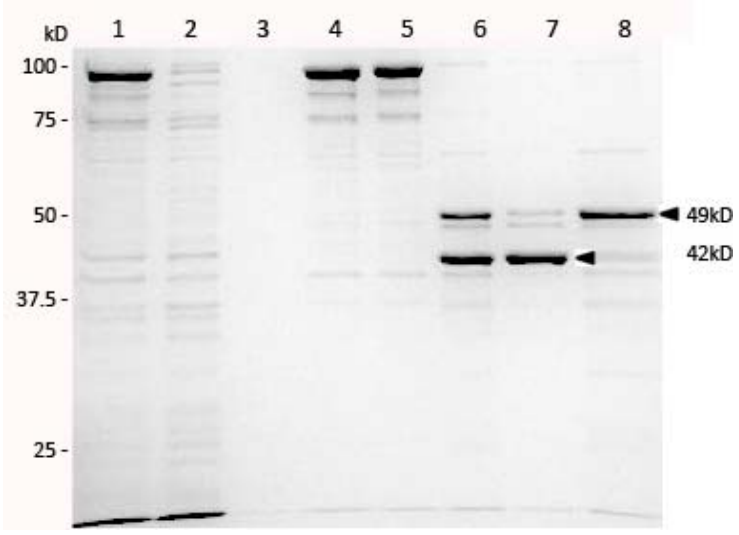

Figure 5 PPH purification summary. Commassie blue-stained SDS-PAGE gel of various fractions from the purification process. **1** *E. coli* crude extract of soluble proteins loaded onto the amylose column, **2** flow-through of the amylose column, **3** last wash of the amylose column, **4** pooled MBP-Δ*At*PPH eluted from the amylose column, **5** 88 h digest at 4 °C without Factor Xa, **6** 88 h digest at 4 °C with 2 % Factor Xa, **7** and **8** MBP and purified Δ*At*PPH protein eluted by anion exchange chromatography. Arrowheads indicate positions of MBP (42 kD) and Δ*At*PPH (49 kD). Molecular size markers (kD) are indicated at the left.

4.2.3.2 Kinetic properties of pheophytinase

Maximum activity of the enzyme was found at pH 8. The enzyme exhibited a rather narrow pH range of maximal activity, with only 36 % of maximal activity retained at pH 7.0 (Figure 6 B). In addition, purified Δ*At*PPH showed highest activity at the temperature of 34 °C and activity was significantly decreased below 25 °C and above 45 °C (Figure 6 A). PPH had been shown to accept both phein *a* and phein *b* as substrate (Schelbert et al., 2009). To determine K_m values, both substrates were analyzed separately. Pheide *a* resp. *b* formation as a function of phein *a* resp. *b* concentrations followed Michaelis-Menten kinetics with apparent K_m values of 3.3 µM for phein *a* and 4.4 µM for phein *b* (Figure 7). Thus, hydrolytic activities for both substrates were in comparable ranges, indicating equal substrate specificity of PPH for both phein *a* and phein *b*.

The study of the biochemical properties of *At*PPH was extended by the determination of a possible transesterase activity. Under certain conditions *Cs*Chlase1 can act as a transesterase (Matile et al., 1999) and, therefore, was used as control. Methanol was added to the assay in order to analyze if these two esterases are able to form the methylester of pheide (pheide *a*-Me) under the applied conditions. Surprisingly, 63 % of the product produced by *Cs*Chlase1 was esterified whereas in the assay with *At*PPH only a marginal amount of 2 % was esterified (Figure 8). Moreover, *At*PPH trans-esterase activity did not increase over time (data not shown). These data indicate that the *At*PPH most probably does not function as a transesterase.

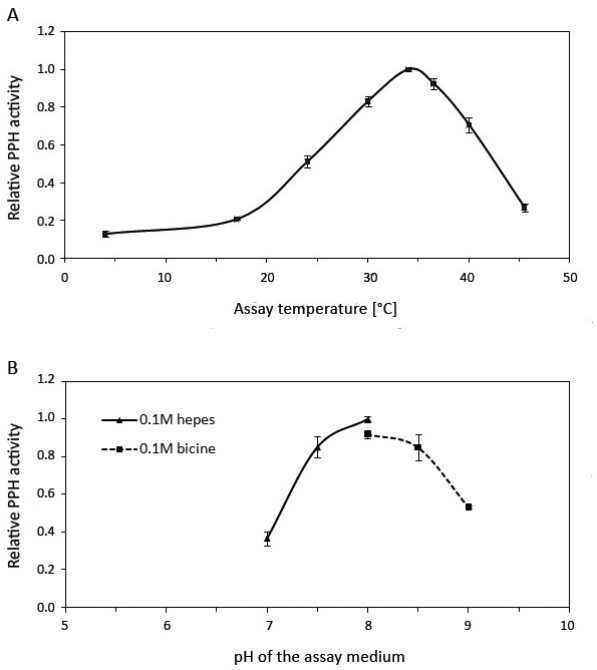

Figure 6 Kinetic properties of *At*PPH. Effects of reaction temperature **(A)** and pH **(B)** on the activity of pheophytinase with pheophytin *a*/*b* mixtures as the substrate. The buffer used in **(A)** was Hepes-KOH pH 8 and in **(B)** Hepes-KOH (pH 7-pH 8) and Bicine-HCL (pH 8- pH 9). All data were adjusted relative to maximum activity. Data are mean values of a representative experiment with three replicates. Error bars indicate SD.

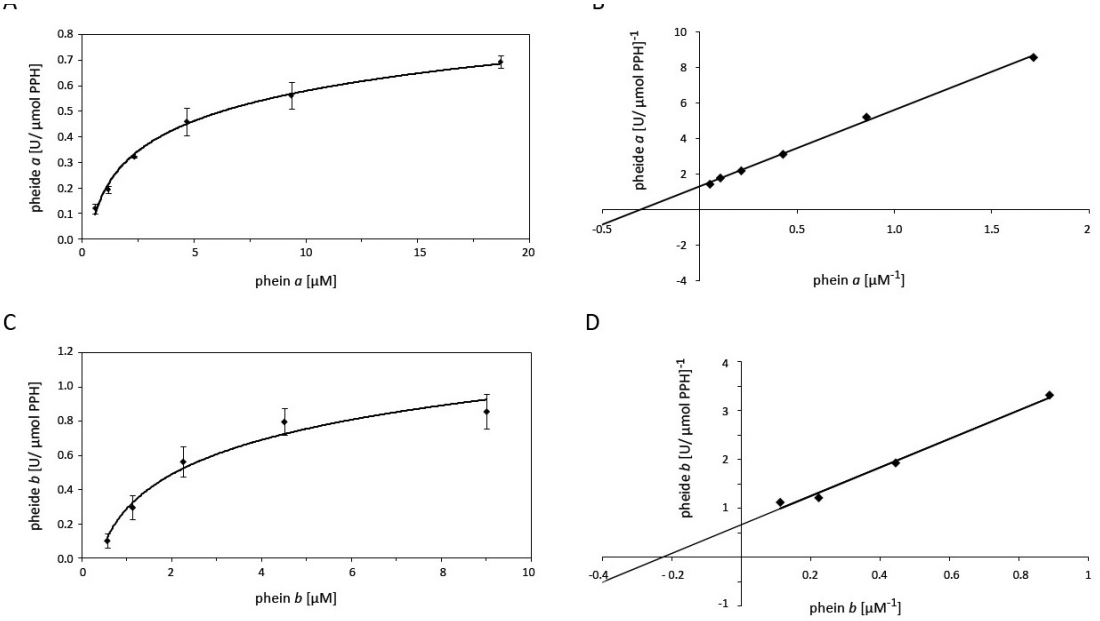

Figure 7 Pheophytinase is a high affinity pheophytin hydrolase. Hydrolase velocities were measured at different pheophytin concentrations, as indicated **(A** and **C)**. Data are mean values of a representative experiment with three replicates. Error bars indicate SD. A double reciprocal plot was used to determine the K_m values of *At*PPH **(B** and **D)** (Lineweaver and Burk, 1934). Product formation followed Michaelis-Menten kinetics with an apparent K_m of 3.3 µM for phein *a* and 4.4 µM for phein *b*.

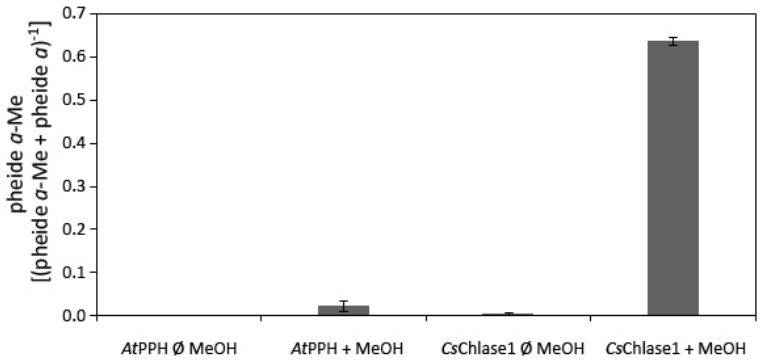

Figure 8 Transesterase activity of *At*PPH and *Cs*Chlase1. Proportion of pheide *a*-Me to the overall product formation was determined. Note that 63 % of the product produced by *Cs*Chlase1 was esterified whereas in *At*PPH only about 2 % were esterified. Data are mean values of a representative experiment with three replicates. Error bars indicate SD.

4.2.4 Discussion

In the present study we have investigated the biochemical properties of recombinant AtPPH which is known for the hydrolysing activity on phein, Mg-free chl, during senescence-related chl breakdown. Purified recombinant protein displayed highest activity at pH 8. This is highly reasonable since *At*PPH was shown to be located in the stromal fraction of chloroplasts (Schelbert et al., 2009) exhibiting pH values around 8. Further, *At*PPH hydrolysing activity is highly specific for phein *a* and *b* with apparent K_m values in the low µM-range. Substrate specificity for phein *a* and *b* at comparable ranges indicates that methyl or formyl residues at C_7 on the porphyrin-ring do not affect phytol hydrolysing activity *in vitro*. However, it is highly likely that *in vivo* phein *b* is not a substrate of PPH, since PAO, catalyzing the following step during chl breakdown, is highly specific for pheide *a* and *pao* mutants accumulate pehide *a*, but not pheide *b* (Hörtensteiner et al., 1995; Pružinská et al., 2005). Moreover, chl *b* to *a* conversion is perfomed by chl *b* reductase while entering the catabolic pathway (Kusaba et al., 2007; Sato et al., 2009). *At*PPH did not display transesterase activity under the applied conditions (Figure 8) which indicates that the *At*PPH most probably does not have an additional function as a trans-esterase.

These analyses provide first insights into kinetic properties of *At*PPH but at the same time raise new issues for further work to be done on the biochemical characterization of *At*PPH. For example, an assay providing pheide *a*-Me as substrate could reveal, whether substrate specificity towards phein is only determined by the porphyrin-ring. In addition, inhibitory effects of chl on the phein hydrolyzing activity could be examined. Finally, studies on the crystal structure of the PPH alone or in its sub-strate-bound form would facilitate the elucidation of the PPH reaction mechanism.

4.3 Role of pheophytinase in fruit ripening of *Solanum lycopersicum*

4.3.1 Introduction

Colour-break is the most obvious sign of fruit ripening. This process involves the biosynthesis of large amounts of carotenoids and flavanoids accompanied by massive degradation of chl (Kato et al., 2004). Both metabolic processes occur within the plastids of the flavedo tissue, the pigmented outer part of the peel and are the visible appearance of the transition of photosynthetically active chloroplasts into chromoplasts (Thomson and Whatley, 1980). Thereby, degradation of chl is a fundamental process that is of central importance concerning changes in pigment composition that typically occurs in fleshy fruits at the onset of ripening (Barry, 2009). Besides the functional similarities between senescing leaves and ripening fruits, the evolutionary significance of chl breakdown in these systems seems to be different. Whereas in senescing leaves chl breakdown appears to be a component of the retrieval of nitrogen from dying organs, in fleshy fruits the disappearance of chl exposes the bright pigments which render the fruit attractive for seed dispersing animals (Goldschmidt, 2001).

Colour variants of many fleshy fruit-bearing species such as tomato and bell pepper have been selected during domestication and through breeding in respect to altered carotenoid biosynthesis (Paran and van der Knaap, 2007). Colour variations in respect to chl degradation also occur in mutations such as at the tomato *green-flesh* (*gf*) and bell pepper *chlorophyll retainer* (*cl*) loci (Efrati et al., 2005; Roca and Minquez-Mosquera, 2006). Fruits harbouring these mutations ripen to a brown colour due to the deficiency in chl breakdown at the onset of fruit ripening. Moreover, leaf senescence in these mutants is also affected (Akhtar et al., 1999). Together, published data indicate that *gf* and *cl* display a cosmetic, non functional type C stay-green phenotype (reviewed by Hörtensteiner, 2009). In both cases, the mutations were shown to affect the orthologues stay-green genes (SGR) (Barry et al., 2008). Recently, a new type of stay-green mutant has been described in *Citrus sinensis* (Alos et al., 2008). The *navel negra* (*nan*) mutant displayed a stay-green phenotype in the flavedo of fruits with no accumulation of known chl catabolites. Sequence analysis of the *SGR* locus responsible for chl retention in diverse species, was not altered from the wild type sequence. This was also the case for the *PPH* gene of *nan* (unpublished results). Thus, *nan* displays a novel stay-green mutant with unknown molecular basis.

Mutants deficient in chl catabolism allow studies on the impact of chl breakdown on fruit quality including taste and aroma. Indeed, reduced rates of carotenoid biosynthesis were observed in *gf* and *cl* (Roca et al., 2006), while *nan* accumulated carotenoid levels comparable to wild type in ripe fruits (Alos et al., 2008). Altered aroma compounds and antioxidative capacity might be due to a delay in the transition of chloroplasts to chromoplasts. Thus, many aroma compounds derive from essential

amino acids, carotenoids or from fatty acid metabolism (Goff and Klee, 2006). Beside these known pigments functioning as visual indicators for seed dispersing fauna, a recent study on ripening banana peels proposed chl catabolites serving as visual indicators of the ripening stage (Moser et al., 2008). Ripe bananas exhibited intense blue luminescence under UV light due to *Mc*-FCC-56, a fluorescent chl catabolite esterified at the C_{17^3} position. High levels of *Mc*-FCC-56 were detected just before the over-ripe stage where FCCs are being converted to NCCs. These findings raised the hypothesis that chl catabolites may serve as distinct ripening signals to insects and birds which have a larger window of vision in the UV range. An additional role of chl catabolites has been proposed by Müller et al. (2007). Thus, NCCs accumulating in the fruit peel of ripe apples and peers displayed effective antioxidant properties.

Although the majority of literature on chl breakdown has been focused on leaf senescence processes, some work was performed on *Citrus*, tomato and bell pepper fruit degreening (Goldschmidt et al., 1993; Trebitsh et al., 1993; Akhtar et al., 1999; Spassieva and Hille, 2002; Efrati et al., 2005; Roca et al., 2006; Alos et al., 2008; Azoulay-Shemer et al. 2008). Additionally, FCCs and NCCs, whose formation can be attributed to PAO activity, were identified in ripe apples, pears and bananas (Müller et al., 2007; Moser et al., 2008). Although these findings provide structural insight into the fate of chl during fruit ripening and support the view that chl breakdown in senescing leaves and ripening fruits is identical (Moser & Matile, 1997), controversial findings on the phytol-hydrolysis step of the passway stresses this assumption (Thomas et al., 2009). Recently, we could convincingly demonstrate that *At*CLHs are not essential for leaf senescence but a new type of esterase, PPH, plays an important role in chl breakdown during leaf senescence (Schenk et al., 2007; Schelbert et al., 2009). Interestingly, a proteome analysis on red fruit chromoplasts of tomato revealed the presence of PPH (Barsan et al., 2010). By contrast, there are studies on *Citrus* fruit colour-break demonstrating that Chlase was located in the plastid of ethylene-treated fruit peel tissue in *Citrus limon* (Harpaz-Saad et al., 2007; Azoulay-Shemer et al., 2008). Chlase accumulation was negatively correlated with chl quantity at the cellular level.

Thus, it needs to be demonstrated whether various tissues evolved different types of chl degradation, *i.e.* fruits comprising enzyme activities that are different from leaves. This demand led to this project where I attempted to elucidate the role of PPH during fruit ripening of *Solanum lycopersicum* (*Sl*PPH) by biochemical and molecular approaches.

4.3.2 Materials and methods

4.3.2.1 Plant material and growth conditions

Solanum lycopesicum ecotype Ailsa Craig wild type and green flesh (*gf*) were obtained from Yoram Eyal, Volcani Center, Israel. Plants were grown on soil in long-day conditions (16 h/8 h) in a green house with fluence rates of 100-200 µmol photons m^{-2} s^{-1} at 25 °C and 60 % humidity. Plants were grown until they showed different leaf senescence and fruit ripening stages. Leaves and fruits were harvested and immediately frozen in liquid nitrogen, and stored at -80 °C. Plants under sterile conditions were grown in ½ MS media containing 1.5 % sucrose in long-day conditions (16 h/8 h) in a culture room with fluence rates of 50 µmol photons m^{-2} s^{-1} at 23 °C.

4.3.2.2 Cloning strategy

Full-lenght cDNA sequence of mature green tomato fruit was obtained from from Yoram Eyal, Volcani Center, Israel. For heterologous expression of *Sl*PPH in *Escherichia coli*, a truncated cDNA fragment, lacking the 61 5`-terminal amino acids encoding the predicted chloroplast transit peptide, was produced by PCR using Extender polymerase (5Prime) with the following primers:

SlPPH_EcoRI_LP 5`-GGAATTCGCTTCTGTTAAGGGGGTTGAC-3`
SlPPH_EcoRI_RP 5`-GGAATTCTTATGGAGAGTAAACTCCATCTTG-3`

After restriction digest with *Eco*RI, the fragment was cloned into pMAL-c2 (New England Biolabs), producing a MBP-truncated *Sl*PPH fusion (MBP-Δ*Sl*PPH). After verifying the insert by sequencing, constructs were transformed into BL21(DE3).

For silencing of *Sl*PPH by RNA interference, a pHannibal-derived (Wesley et al., 2001) construct was used which harboured a *Sl*PPH sense and antisense cDNA fragment of 400bp amplified with Pfu polymerase (Promega) and the following primer combinations:

SlPPH_XhoISacII_LP 5`-CCCTCGAGCCGCGGACAACTAAATTTTAAAGAG-3`
SlPPH_KpnI_RP 5`-GGGGTACCAGATTTTAGAAACATGGAAAG-3`
SlPPH_BamHI_LP 5`-CGGGATCCGGACAACTAAATTTTAAAGAG-3`
SlPPH_ClaI _RP 5`-CCATCGATAGATTTTAGAAACATGGAAAG-3`

Two different silencing constructs, driven by the CaMV 35S promoter or the fruit-specific 2A11 promotor (Pear et al., 1989) were produced. The gene constructs were excised from the pHannibal constructs by *Not*I and cloned into pGreen0029 (Hellens et al., 2000). For the overexpression construct, *Sl*PPH full-length cDNA was cloned into pGreen0029 by *Nde*I and *Eco*RI harbouring the CaMV 35S promoter and CaMVpolyA terminator. After verifying inserts by sequencing, constructs were transformed into *Agrobacterium* strain GV3101 together with pSOUP (Hellens et al. 2000).

4.3.2.3 Plant transformation

Seed sterilization was performed with 1.2 % sodium hypochlorite for 15 min. Seeds were rinsed 3 times with sterile distilled water and planted in 10 cm high sterile glass pots. After 9-12 days of growth in the culture room, cotyledons were cut at 2-3 mm from the proximal- and distal ends of the blade. Cotyledons were placed upside down in Petri dishes containing D1 medium (4.4 g/l MS salts including B5 vitamins, 30 g/l glucose, 1 mg/l zeatin, 0.1 mg/l NAA, 1mg/l folic acid, 2mM MES-KOH pH 5.6-5.7 and 8 g/l agar) and incubated in the culture room for 2 d. 20 ml of *Agrobacterium* harbouring the respective plasmids were grown overnight at 28 °C. Cells were collected by centrifugation (4000 rpm, 15 min), and pellets resuspended in MSO-KOH pH 5.6 (4.4 g/l MS salts including B5 vitamins, 20 g/l sucrose) to an OD_{600} of 0.4-0.5. 100 µM acetosyringone was added and the culture was grown for another 2 h at 28 °C. For transformation bacterial cultures were incubated with cotyledons for 2 h in the dark. After 2-3 d of co-cultivation on D1 medium, the cotyledons were transferred to D1 medium containing kanamycin (75 mg/l) and timenten (100 mg/l). Shoot regeneration was detected after 30 d and respective plantlets were transferred to DL medium (4.4 g/l MS salts including B5 vitamins, 20 g/l glucose, 0.1 mg/l zeatin, 1 mg/l folic acid, 2 mM MES-KOH pH 5.6-5.7 and 8g/l agar) for shoot elongation. Well developed shoots were transferred to DR medium (4.4 g/l MS salts including B5 vitamins, 20 g/l glucose, 2 mg/l IBA, 1 mg/l folic acid, 2 mM MES-KOH pH 5.6-5.7 and 8g/l agar) for root induction. Rescued transformants were then transferred to soil.

4.3.2.4 RNA isolation and RT-PCR

Total RNA was extracted from leaf tissues and the flavedo of fruits using TRIzol according to the manufacturer`s protocol (Invitrogen). After DNA digestion with RQ1 DNase (Promega), first-strand cDNA was synthesized using the RETROscript kit (Ambion). PCR was performed with a non-saturating number of amplification cycles using the following gene-specific primers:

SlPPH_S	5`-GTGTCGAATGAACAATGTACC-3`
SlPPH_AS	5`-CCATTGAGAAGTCATTGATCC-3`
TIP41_S	5`-GCTGCGTTTCTGGCTTAGG-3`
TIP41_AS	5`-ATGGAGTTTTTGAGTCTTCTGC-3`, control gene as published (Exposito-Rodriguez et al., 2008)

4.3.2.5 Chlorophyll extraction

For spectrophotometric determination of chlorophyll concentrations (Strain et al., 1971), chlorophyll was extracted from tomato leaf tissue by homogenization in liquid nitrogen and subsequent extraction into 90 % (v/v) acetone, 10 % (v/v) Tris-HCL pH 8 for 24 h at -20 °C. After centrifugation (2 min, 16 000 g), the supernatant was used for analysis.

4.3.2.6 Analysis of recombinant SlPPH

Recombinant *Sl*PPH protein was expressed and cells were lysed as described (Schelbert et al., 2009). The assay (200 µl) consisted of 10 µl protein crude extract (~100 µg soluble protein), 15 ul phein *a/b* mixtures (1.4 mg/ml) dissolved in 100 % acetone and 175 µl 0.1 M Hepes-KOH pH 8 containing 1 mM EDTA. After incubation at 34 °C for various time periods the reaction was stopped and analysed by HPLC as described (Schelbert et al., 2009). Substrate production and quantification was performed according (Schelbert et al., 2009).

4.3.2.7 Protein import experiment

[^{35}S]-Met-labeled PPH was synthesized from full-lenght *SlPPH* cloned in pBluescript with the TNT T7 Quick Coupled Transcription/Translation System (Promega). Intact chloroplasts of 3-week-old in vitro-grown *Arabidopsis* plants (ecotype Col-0) were isolated as published (Schelbert et al., 2009). PPH import assays were performed as published (Fitzpatrick and Keegstra, 2001). For each import reaction, chloroplasts corresponding to 16 µg chl and 7 µl of in vitro-translated *Sl*PPH preprotein were used. Lysis of chloroplasts was performed according to Smith et al. (2002). All samples were resolved by SDS-PAGE and visualized by autoradiography.

4.3.2.8 Biocomputational methods and phylogenetic analysis

*Sl*PPH was identified by tblastn searches (Altschul et al., 1997) with databases of the National Centre for Biotechnology Information (http://www.ncbi.nlm.nih.gov) using *At*PPH as query and choosing EST database in *Solanum lycopersicum* (taxid:4081) organism. Whole sequence coverage was reached by the following ESTs (in brackets positions of the coding sequence): BW689698 (1-483), BP887030 (484-830), BP881587 (831-1237) and AW930541 (1238-1770). Homologs of PPH were identified by blastp searches at NCBI. Sequence alignment was performed by ClustalW using the program BioEdit (http://www.mbio.ncsu.edu/bioedit/bioedit.html). The phylogenetic tree was estimated using the maximum likelihood method (http://www.phylogeny.fr/). Protein sequences used in this work are as follows. GeneBank identification numbers: *Arabidopsis thaliana* (At): AtPPH, 15240707 (At5g13800); *Chlamydomonas reinhardtii* (Cr): CrPPH, 159490010; *Micromonas pusilla* (Mp): MpPPH, 226463090; *Nicotiana tabacum* (Nt): NtPPH, 156763846; *Ostreococcus lucimarinus* (Ol): OlPPH, 145340970; *Oryza sativa* (Os): OsPPH, 115467988 (Os06g0354700); *Ostreococcus tauri* (Ot): OtPPH, 116000661; *Physcomitrella patens* (Pp): PpPPH, 168018382; *Populus trichocarpa* (Pt): PtPPH, 224106163; *Ricinus communis* (Rc): RcPPH, 255545291; *Vitis vinifera* (Vv): VvPPH, 225449963; *Zea mays* (Zm): ZmPPH, 226530215.

4.3.3 Results

4.3.3.1 Tomato PPH expression correlates with loss of chl

Tomato (*Solanum lycopersicum*) was used to allow analysis of chl breakdown in leaves and fruits. Stages of natural leaf senescence and fruit ripening in wild type (Ailsa Craig) and a stay-green mutant (*green flesh*) were analyzed (Figure 9A and B). The senescence status of leaves was evaluated on the basis of chl content (Figure 9C) whereas the fruit ripening status was evaluated by eye. While wild-type tomato fruits ripened to a bright red colour, tomatoes of the *gf* mutant ripened to a brown colour due to the deficiency in chl breakdown at the onset of fruit ripening (Figure 9B). Chl content declined with senescence progression in wild type leaves but not in *gf* where chl was retained at high levels (Figure 9C). Semi quantitative RT-PCR was performed on natural senescing leaves and the flavedo of tomato fruits. *SlPPH* expression was up-regulated at the onset of leaf senescence in wild type and *gf* (Figure 9D). This data is in line with *PPH* expression analysis in *Arabidopsis* leaves (Schelbert et al., 2009). *SlPPH* expression in fruit ripening showed a clear up-regulation starting at the breaker state (Figure 9E). *PPH* gene expression in fully ripe fruits was again lowered due to the finish of chl breakdown in this stage. Comparable results were obtained for wild type and *green flesh*.

4.3.3.2 SlPPH is localized in the chloroplast

The ortholog of tomato PPH in *Arabidopsis* (*At*PPH) was shown to be located in the soluble fraction of chloroplasts (Schelbert et al. 2009). Although ChloroP prediction for an N-terminal chloroplast transit peptide in *Sl*PPH was not as clear as for the *At*PPH, gene expression analysis and *in vitro* PPH activity (see below) strongly promoted chloroplast localization of *Sl*PPH. I performed import experiments of [^{35}S]-Met labeled *Sl*PPH into isolated *Arabidopsis* mesophyll chloroplasts. The tomato PPH was indeed imported into chloroplasts (Figure 10). After thermolysin treatment to digest surface-bound and nonimported precursor, the mature PPH signal was clearly visible at 50kD. Thus, it is highly likely that the *Sl*PPH is located in the chloroplast.

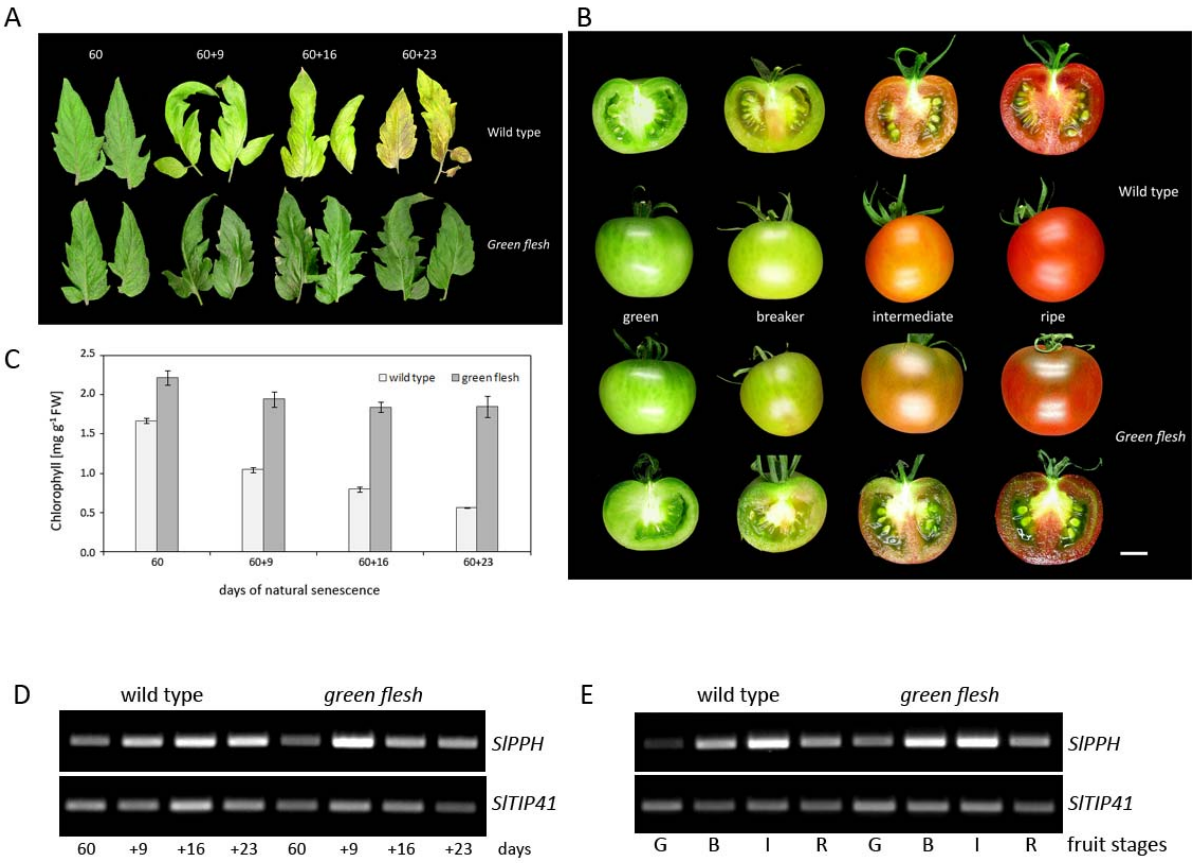

Figure 9 *PPH* expression is related to leaf senescence and fruit ripening of tomato. (A) Progression of natural senescence starting at 60 d old tomato leaves of wild type and *green flesh* mutant plants. Leaf tissue at different time points was collected from first true leaves. **(B)** Progression of ripening stages of tomato wild type (upper) and *green flesh* (lower) fruits**.** Retention of chl in *gf* gives it a rusty red phenotype. Bar= 1cm. **(C)** Chl degradation during natural senescence of wild type and *gf* leaves in tomato. Data are mean values of a representative experiment with three replicates. Error bars indicate SD. **(D** and **E)** *PPH* gene expression during **(D)** natural senescence of leaves and **(E)** fruit ripening stages of wild type and *green flesh* tomato. *TIP41* was used as control (Exposito-Rodriguez et al., 2008). Expression was analyzed with nonsaturating numbers of PCR cycles. PCR products were separated on agarose gels and visualized with ethidium bromide.

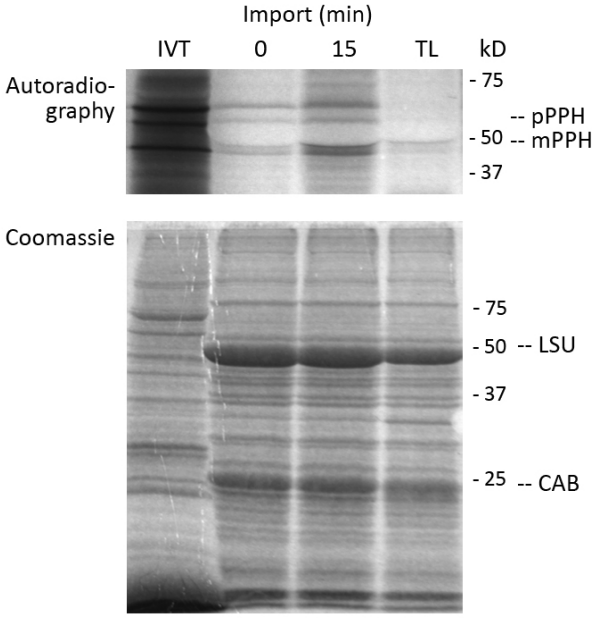

Figure 10 Import of [^{35}S]-Met-labeled precursor of PPH (pPPH) in *Arabidopsis* chloroplasts. Import proceeded for 15 min and mature PPH (mPPH) accumulated. After import, chloroplasts were treated with thermolysin (TL) to digest surface-bound and nonimported precursor. Molecular size markers (kDa) are indicated at the right. IVT, in vitro translation product; LSU, large subunit of Rubisco; CAB, chlorophyll *a/b* binding protein.

4.3.3.3 SlPPH shows pheophytinase activity in vitro

The enzymatic activity of *Sl*PPH was examined with a truncated version, devoid of the predicted chloroplast transit peptide (Δ*Sl*PPH), as a maltose binding protein fusion (MBP-Δ*Sl*PPH) in *E. coli*. The recombinant protein was expressed in large amounts and was located in the soluble cell fraction (Figure 11A). Crude soluble cell extracts were used in assays containing chlorophyll *a/b* and/or pheophytin *a/b* as possible substrates. Assay conditions were applied as described to be optimal for the purified *At*PPH, 34 °C at a pH of 8 (see 4.2.3.2) We expected the tomato PPH to act on the Mg-free pigment, phein, since the *At*PPH also displayed this specificity. Indeed, recombinant MBP-Δ*Sl*PPH converted phein *a/b* to pheide *a/b* by cleaving of the lipophilic phytol chain (Figure 11B and C). The hydrolytic activity was time- dependent and highly specific for phein. Only small amounts of dephytylated chl (chlide *a/b*) were formed although chl was present in large excess in the assay mixture. In contrast, the vector control (MBP) did not act on chl or phein.

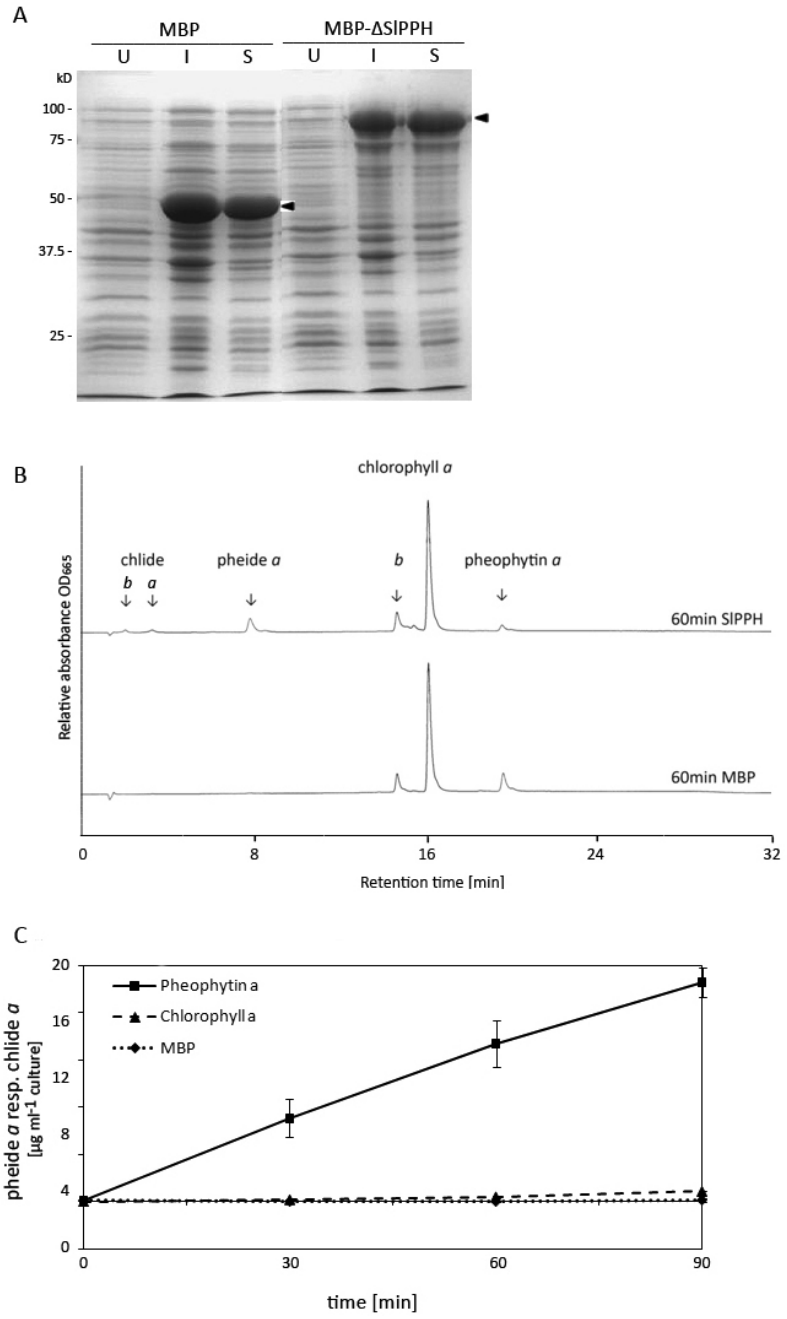

Figure 11 Analysis of recombinant PPH of tomato. (A) Coomassie blue-stained SDS-PAGE gel of *E. coli* cells [BL21(DE3)] expressing an N-terminal truncated version of *Sl*PPH fused to MBP (MBP-Δ*Sl*PPH). A strain expressing free MBP was used as control. After induction with IPTG for 3 h (I), cells were lysed, and soluble protein (S) were isolated as described in Methods. U, cells before IPTG induction. Gel loadings are based on equal amounts of cell cultures at OD_{600}= 1.5. Arrowheads indicate position of recombinant proteins. Molecular size markers (kD) are indicated at the left. **(B)** HPLC analysis of assays employing soluble *E. coli* lysates expressing MBP-Δ*Sl*PPH with chl as major substrate. Small amounts of phein *a* that are present in the assay, are due to chl that has lost the central Mg atom. HPLC traces at A_{665} after 60 min of incubation at 34 °C are shown. Note that only small amounts of dephytylated chl (chlide *a/b*) were formed although chl was present in large excess. Arrows indicate substrates and respective dephytylated products. **(C)** Formation of pheide *a* and chlide *a* from phein or chl used as substrate in assays with MBP-Δ*Sl*PPH in a time- dependent manner. Assays were performed under identical conditions and protein quantity was based on equal amounts of cell culture at OD_{600}= 1.5. Data are mean ± SD of three independent assays.

4.3.3.4 SlPPH-silencing lines

To study the role of PPH during fruit ripening in tomato, *PPH* expression was increased and decreased, respectively, with the aim to accelerate and suppress the kinetics of chl breakdown. For this purpose, tomato cotyledons were transformed and plants regenerated from calli that harboured either an *PPH* over-expression construct under the control of the CaMV 35S promotor (35S::SlPPH) or a silencing construct with either the CaMV 35S promotor (35S::SlPPH_HPPIS) or the fruit specific 2A11 promotor (2A11::SlPPH_HPPS). Levels of *PPH* gene expression of transgenic tomato lines used for further analysis was determined by semiquantitative RT-PCR analysis. Respective lines displayed altered *PPH* expression compared to wild type or *gf* (Figure 12). Whether respective silencing lines show a brown-fruited, stay-green phenotype, remains to be demonstrated. This analysis is underway. Likewise, transgenic lines harbouring the 2A11::SlPPH_HPPlS construct have at present not been tested and are not fruiting yet.

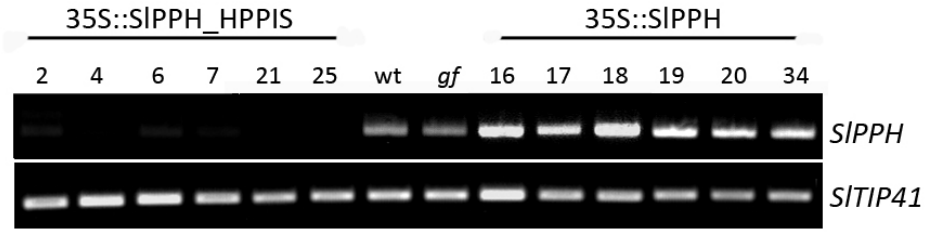

Figure 12 Analysis of transgenic tomato lines with altered *PPH* expression. (A) Analysis of *PPH* expression in green leaf tissue of different transgenic tomato lines by RT-PCR. (35S::SlPPH_HPPlS), silencing lines harbouring the 35S promotor; (35S::SlPPH), overexpression lines harbouring a full length *SlPPH* cDNA driven by the 35S promoter. *TIP41* was used as control (Exposito-Rodriguez et al., 2008). Expression was analyzed with nonsaturating numbers of PCR cycles. PCR products were separated on agarose gels and visualized with ethidium bromide. Note that silencing lines harbouring the fruit-specific promotor (2A11::SlPPH_HPPlS) are under development.

4.3.3.5 Phylogenetic analysis and sequence alignment of PPH orthologs

*Sl*PPH and homologous PPH protein sequences from higher and lower plant species were identified by blastp searches as described in Methods. To investigate the relationship between these proteins, I performed a phylogenetic analysis on selected proteins within the blast hits. The tomato PPH clustered into a clade with PPH proteins of higher plants (Figure 13A). A sequence alignment of selected proteins from the PPH clade of higher plants and *Ostreococcus taurii* was performed by using the program BioEdit (Figure 13B). The *Sl*PPH versus the *At*PPH exhibited a protein sequence identity of 56 %. Except for *Ostreococcus taurii*, all shown PPH protein sequences contained chloroplast transit peptides, as predicted by ChloroP (Emanuelsson et al., 1999). A conserved domain, named PPH do-

main (Schelbert et al., 2009) containing the proposed active-site serine residue of these serine-esterase was present in all PPH proteins.

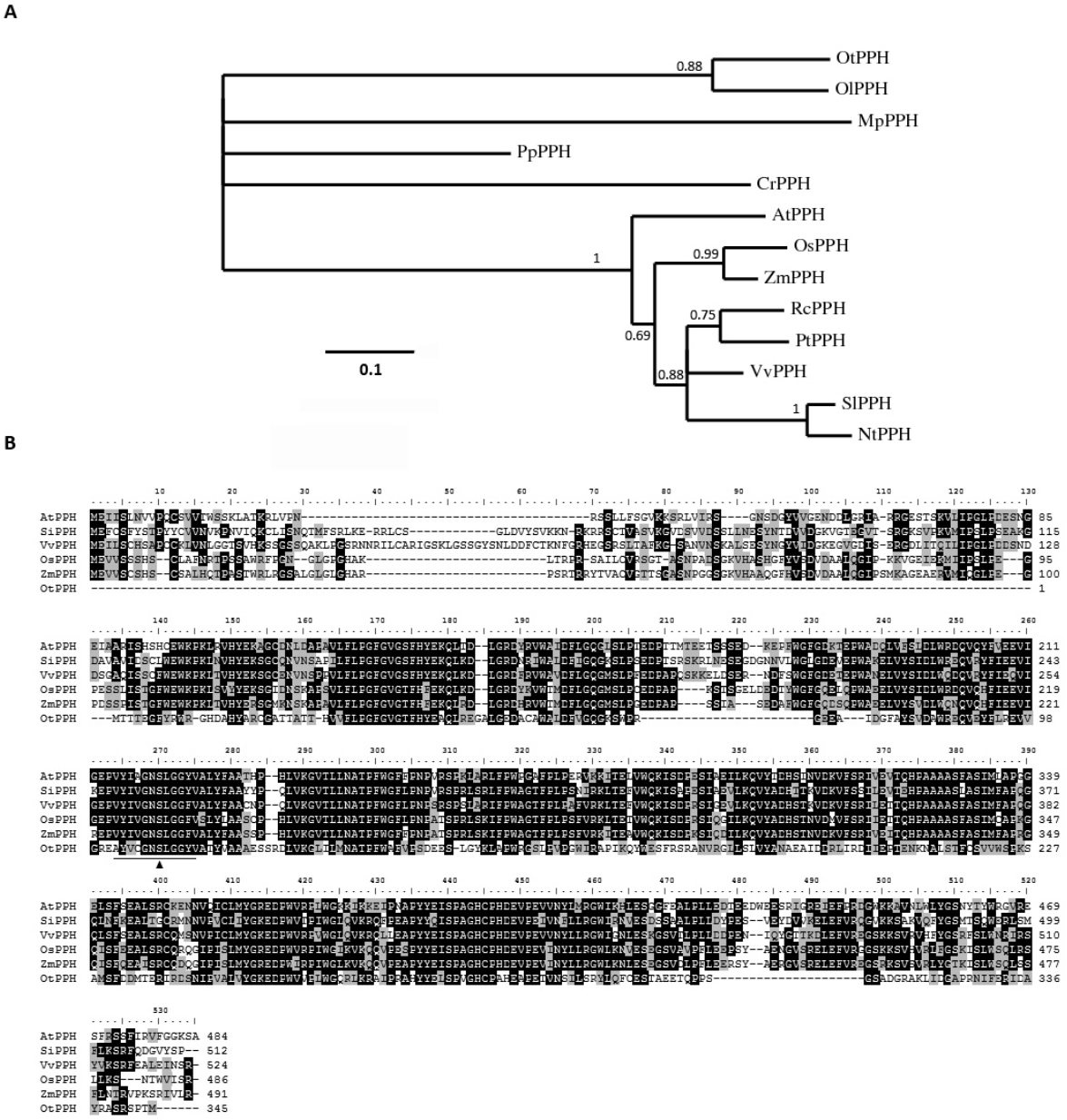

Figure 13 Phylogenetic analysis and sequence alignment of PPH homologs. (A) Phylogenetic tree of 13 proteins with high similarity to *Sl*PPH. Sequences were aligned using ClustalW and the phylogenetic tree estimated using the maximum likelihood method (http://www.phylogeny.fr/). Bootstrap values are shown at branchpoints with a cut-off of 0.5. At, *Arabidopsis thaliana*; Cr, *Chlamydomonas reinhardtii*; Mp, *Micromonas pusilla*; Nt, *Nicotiana tabacum*; Ol, *Ostreococcus lucimarinus*; Os, *Oryza sativa*; Ot, *Ostreococcus tauri*; Pp, *Physcomitrella patens*; Pt, *Populus trichocarpa*; Rc, *Ricinus communis*; Sl, *Solanum lycopersicum*; Vv, *Vitis vinifera*; Zm, *Zea mays*. For protein accession numbers, see Methods. **(B)** Sequence alignment of PPH proteins from different species. The sequences were aligned using the BioEdit software. Black shading with white letters reflects identical amino acids; grey shading with black letters reflects similar amino acids, according to Blosum62 similarity groups. The PPH domain containing the proposed active-site Ser residue (arrowhead) is underlined.

4.3.4 Discussion

There are studies on *Citrus* fruit colour-break demonstrating that Chlase was located in the plastid of ethylene-treated fruit peel (flavedo) tissue in *Citrus limon* (Harpaz-Saad et al., 2007; Azoulay Shemer et al. 2008). Chlase accumulation was negatively correlated with chl quantity at the cellular level. But these studies on Chlase of *Citrus limon* challenged the recently proposed new route of chl breakdown pathway in leaves which excludes chlorophyllases (Schenk et al., 2007; Schelbert et al., 2009). It raises the question whether various tissues evolved different types of chl degradation, *i.e.* fruits comprising enzyme activities that are different from leaves. To address these questions I studied the impact of PPH in tomato fruit ripening, while Y. Eyal and co-workers attempted to modulate Chlase in tomato.

In this study I confirmed that *PPH* expression correlates with loss of chl in leaf senescence and fruit ripening of tomato. PPH is located in the chloroplast and recombinant protein shows pheophytinase activity *in vitro*, with intriguing substrate specificity towards the Mg-free pigment, phein. Whether silencing of *PPH* expression results in a stay-green leaf phenotype with fruits that ripen to a brown colour, remains to be demonstrated. From our data we conclude that PPH most probably is involved in the loss of chl during fruit ripening beside the reported role in leaf senescence (Schelbert et al., 2009). Thus, chl breakdown in leaves and fruits shows similarities, but whether the pathway follows the route by Chlase or PPH remains to be demonstrated.

4.4 Chl breakdown occurs by a senescence-specific multi-protein complex

4.4.1 Introduction

Identification of protein interactions often provides insight into protein function, and many cellular processes are performed by the formation of both stable or transient protein complexes and networks. For instance, complex formation has been reported for porphyrin channelling during different reactions of tetrapyrrole biosynthesis (Koch et al., 2004; Nogaj et al., 2005). These complexes might facilitate substrate channelling between different enzymes, thereby reducing the possibility that potentially dangerous intermediates will accumulate. Thus, it is highly feasible that proteins functioning in chl breakdown might also act together in protein complexes to avoid accumulation of photodynamic chl catabolites which are known to lead to oxidative damage upon exposure to light. In line with this possibility, biochemical interaction between PAO and RCCR was demonstrated in a bacterial two-hybrid screen, although attempts to confirm interactions using other approaches were unsuccessful (Pružinská et al., 2007). However, subcellular co-localization of individual protein components would be a prerequisite for possible *in vivo* interactions. RCCR, PPH and SGR were demonstrated to localize to the stroma fraction of chloroplasts (Mach et al., 2001; Jiang et al., 2007; Ren et al., 2007; Schelbert et al., 2009). For many years, PAO was suggested to be associated with the envelope of gerontoplasts (Matile and Schellenberg, 1996), but recently, PAO localization was re-addressed using PAO-GFP fusion analysis and immunoblot analysis of chloroplast membrane fractions. Thereby, the data show that PAO localizes to the thylakoid membrane not the envelope (Hörtensteiner lab, unpublished results). NYC1 and NOL encoding chl *b* reductases were shown to co-localize in thylakoid membranes facing the stromal side where they act in the form of a complex (Sato et al., 2009). Furthermore, co-immunoprecipitation experiments displayed that rice SGR specifically interacts with LHCII subunits *in vivo* (Park et al., 2007).

In the present investigation I attempted to define, if individual protein components that function in chl breakdown act together in a multi-protein complex and how this complex is assembled and located *in vivo*. Thereby, interaction studies were employed using the bimolecular fluorescence complementation (BiFC) technique in *Arabidopsis* protoplasts.

4.4.2 Materials and methods

4.4.2.1 Plant material and growth conditions

Arabidopsis thaliana ecotype Col-0 was used. Plants were grown on soil in short-day conditions (8h/16h) in a growth chamber with fluence rates of 100-200 µmol photons m^{-2} s^{-1} at 21 °C and 60 % humidity. For senescence induction, detached leaves of 5-week-old plants were incubated on wet filter paper for up to 4 d in the dark.

4.4.2.2 Cloning strategy

Full-length cDNA sequences were obtained from the RIKEN resource (Seki et al., 2002). Full length cDNAs of respective proteins *i.e.* PPH (At5g13800), PAO (At3g44880), SGR1 (At4g22920), RCCR (At4g37000), NYC1 (At4g13250) and NOL (At5g04900), were PCR-amplified using Pfu polymerase (Promega) and the following primers:

PPHfor_BspHI	5` CGTTCATGAAGATAATCTCACTGAACGTTG 3`
PPHrev_Not	5` TAAAGCGGCCGCGCAGACTTCCCTCCAAACAC 3`
PAOfor_BspHI	5` CGTTCATGACAGTAGTTTTACTCTCTTCTAC 3`
PAOrev_Not	5` TAAAGCGGCCGCTCGATTTCAGAATGTACAT 3`
SGRfor_BspHI	5` CGTTCATGAGTAGTTTGTCGGCGATTATG 3`
SGRrev_Not	5` TAAAGCGGCCGCAGTTTCTCCGGATTTGGA 3`
RCCRfor_BspHI	5` CGTTCATGACGATGATATTTTGCAACACTC 3`
RCCRrev_Not	5`TAAAGCGGCCGCAGAACACCGAAAGCTTCTTT 3`
AtNYC1_BspHI	5` CGTTCATGACTACTTTAACGAAGATTCAAG 3 `
AtNYC1rev_Not	5` TAAAGCGGCCGCGTGCCTGGAAAAGAGCTAGG 3`
AtNOL_BspHI	5` CGTTCATGACTACTTGGAGTGGTTTCAACG 3`
AtNOLrev_Not	5` TAAAGCGGCCGCTCTTCAGTAACATACCTGTT 3`

PCR fragments were cloned into pSY728 and pSY738, respectively (Bracha-Drori et al., 2004). Thereby, producing C-terminal fusions of chl catabolic proteins with respectively, the N- and C-terminal halves of YFPs (termed protein-YFP_n and protein-YFP_c, respectively). After verifying the inserts by sequencing, constructs were used for BiFC study.

4.4.2.3 Protoplast transformation and BiFC analysis

Arabidopsis mesophyll protoplasts were isolated from 5-week-old short day-grown plants according to published procedures (Endler et al., 2006). Cell numbers were quantified with a Neubauer chamber and adjusted to a density of 2 x 10^6 protoplasts ml^{-1}. Protoplasts were co-transformed with each two constructs by 20 % polyethylene glycol transformation according to published procedures (Meyer et al., 2006). Twenty µg plasmid of each construct was used. Transformed cells were incubated for 12 h in the dark at room temperature before laser scanning confocal microscopic analysis (DM IRE2; Leica Microsystems). YFP fluorescence was imaged at an excitation wavelength of 512 nm,

and the emission signal was recovered between 525 and 565 nm. CP12-YFP$_n$ and phosphoribulokinase (PRK-YFP$_c$) constructs where used as a control for plastid co-localization. Both proteins participate in the Calvin cycle and were shown to interact in a yeast two-hybrid system (Wedel et al., 1997). *In vivo* interaction using these constructs was demonstrated in the stroma of *Arabidopsis* mesophyll chloroplasts (R. Scheibe, personal communication).

4.4.3 Results

4.4.3.1 In vivo interaction study

The bimolecular fluorescence complementation (BiFC) assay provides an approach for the visualization of protein interactions in living cells. This approach relies on the formation of a fluorescent complex by two non-fluorescent fragments of the yellow fluorescent protein (YFP) brought together by association of interacting proteins fused to these fragments (Figure 14A) (Hu et al., 2002). To enable BiFC analyses in plant cells, I used a complementary set of expression vectors (pSY728 and pSY738) which are especially designed to enable protein interaction studies in transient plant cell transformation approaches (Figure 14B) (Bracha-Drori et al., 2004). The advantage of this approach is that protein interaction can be visualized in the native environment of a plant cell. In my experiments I used mesophyll protoplasts from both green and senescent leaves of *Arabidopsis.* Senescent protoplasts (4ddi) contained smaller and less chloroplasts, which often localized to one pole of the cells, where in nonsenescent protoplasts (0ddi) they were more evenly distributed (Figure 14 C). Interaction between proteins of chl breakdown was not detected in protoplasts of green plant material (data not shown). This observation in nonsenescing cells might be explained by the absence of additional unknown elements or structural changes which are needed for the proper complex formation. By contrast, protein interaction was detected in senescing chloroplasts for different combinations of enzymes involved in chl breakdown (Figure 15). All interactions found by this study were confirmed in three independent experiments. Moreover, interaction could be shown for different protoplasts within one experiment. CP12 and PRK interaction shown by R. Scheibe and co-workers (personal communication) could be confirmed in senscing protoplasts and was used as positive control (Figure 15 B). By this approach, PAO and RCCR interaction which was shown in a two-hybrid study in bacteria (Pružinská et al., 2007) could be confirmed (Figure 15A). PAO and RCCR interaction signal was partially overlapping with chl fluorescence in senescing chloroplasts. Furthermore, PAO interacted with SGR and PPH (Figure 15 A), whereas cells co-transformed with PAO and functional unrelated stromal proteins such as CP12 or PRK, produced no or only background fluorescence (data not shown).Further, PPH displayed interaction with RCCR but not with SGR (Figure 15B). Additionally,

NYC1 and NOL interaction as reported by Sato et al. (2009) could be confirmed (Figure 15C). A summary of all protein interactions tested by BiFC analysis is presented in Figure 16.

Interestingly, the overall interaction signal negatively correlated with the intensity of the chl autofluorescence at the cellular level. For PAO-YFPn/SGR-YFPc (Figure 15 A) and NYC-YFPn/NOL-YFPc (Figure 15 C) each two representative examples are shown, which support this negative correlation between the protein interaction level (YFP fluorescence, line 1) and chl levels (red fluorescence, line 2). This result indicates that chl breakdown is not synchronous within the entire thylakoid membrane structure but occurs successively at specific sites that exhibited chl catabolic protein interaction.

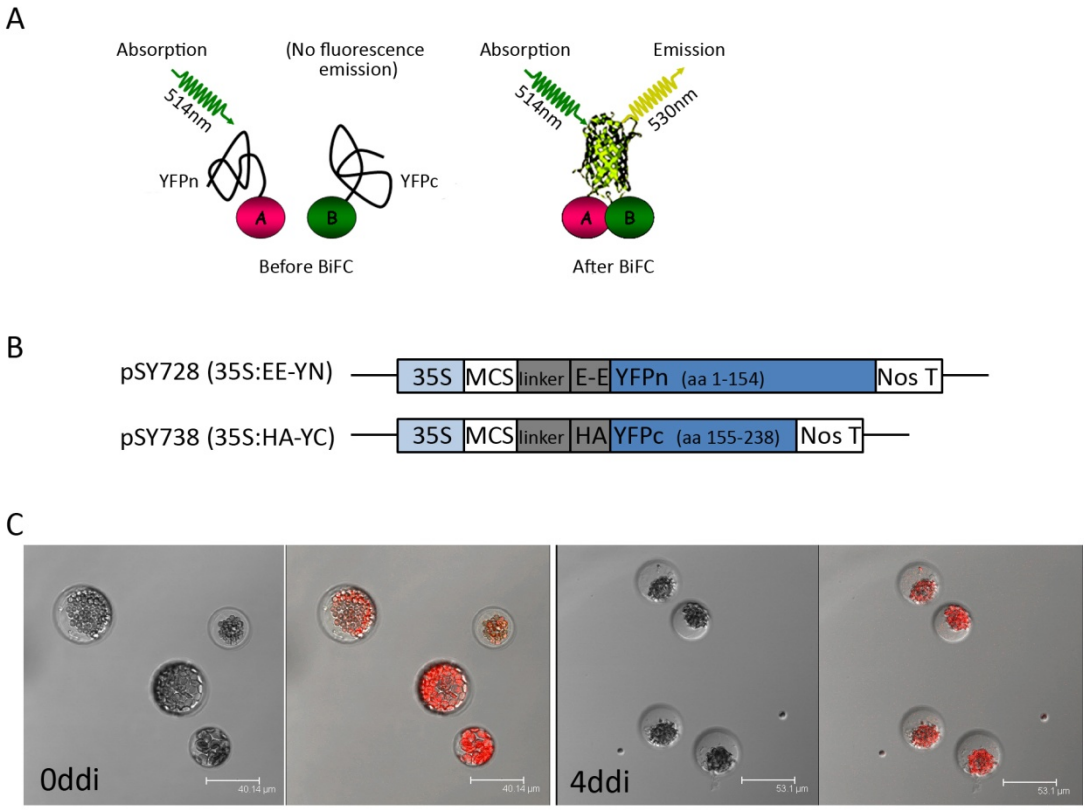

Figure 14 Setup of the BiFC experiments using *Arabidopsis* mesophyll protoplasts. (A) The principle of BiFC. Under physiological conditions reconstitution of a fluorescent YFP molecule can only take place following interaction between proteins that are fused to YN and YC fragments, from Bhat (2006) Plant methods **(B)** Schematic representation of the complementary plant-compatible BiFC vectors used for this study. E-E, Glu-Glu tag; HA, haemaglutinin tag; MCS, multiple cloning site; 35S, 35S promoter of the cauliflower mosaic virus; NosT, terminator of the *Nos* gene; YFPn, N-terminal fragment of YFP covering amino acids (aa) 1 to 154; YFPc, C-terminal fragment of YFP covering amino acids 156 to 238. **(C)** *Arabidopsis* mesophyll protoplasts used for co-transformation before (0ddi) and after 4 d of dark-induced senescence (4ddi). Note that at 4ddi, protoplasts contained chloroplasts smaller in size and quantity. Bright field images alone (left) and merged with chl autofluorescence (right).

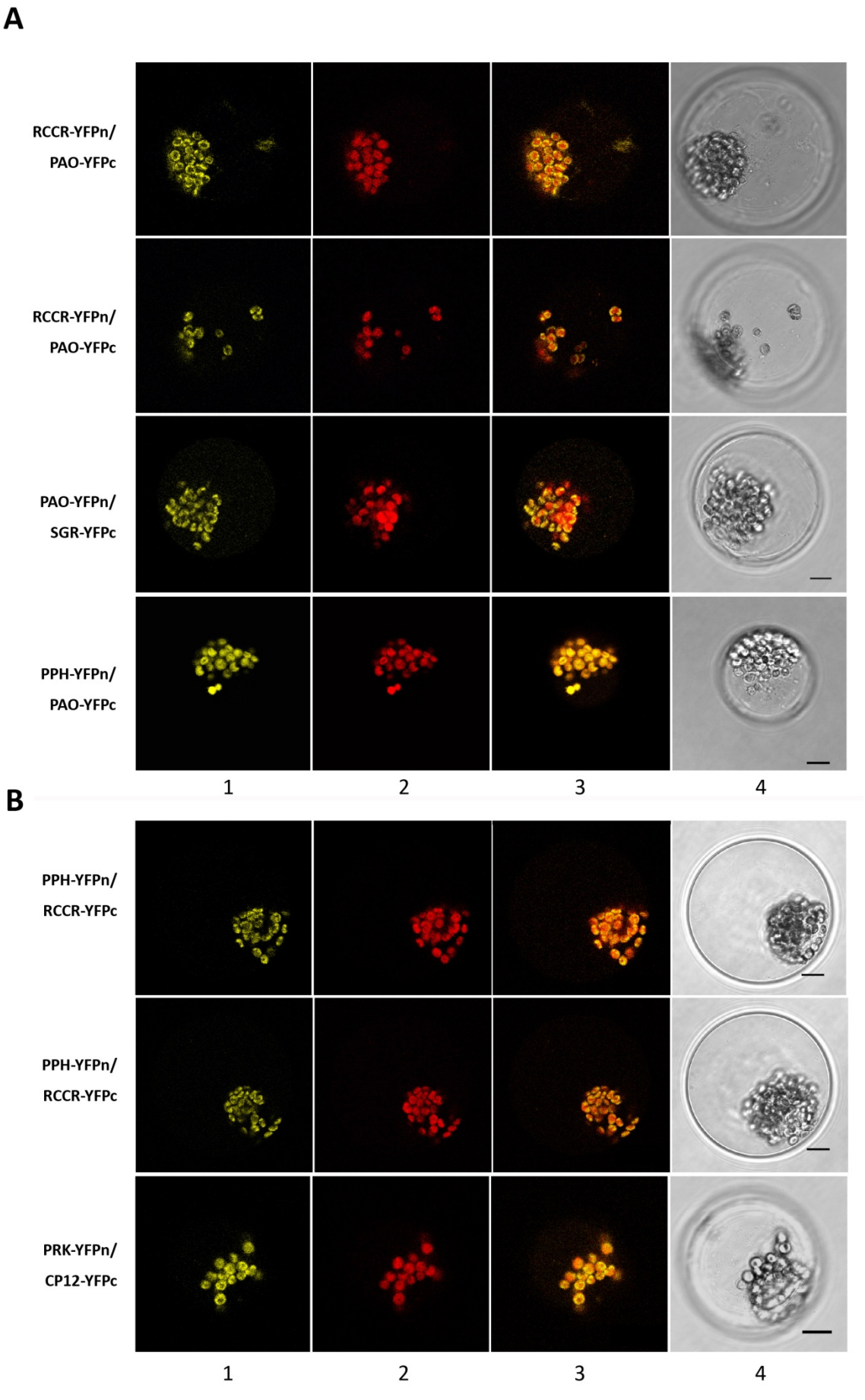
A
RCCR-YFPn/
PAO-YFPc
RCCR-YFPn/
PAO-YFPc
PAO-YFPn/
SGR-YFPc
PPH-YFPn/
PAO-YFPc
1
2
3
4
B
PPH-YFPn/
RCCR-YFPc
PPH-YFPn/
RCCR-YFPc
PRK-YFPn/
CP12-YFPc
1
2
3
4

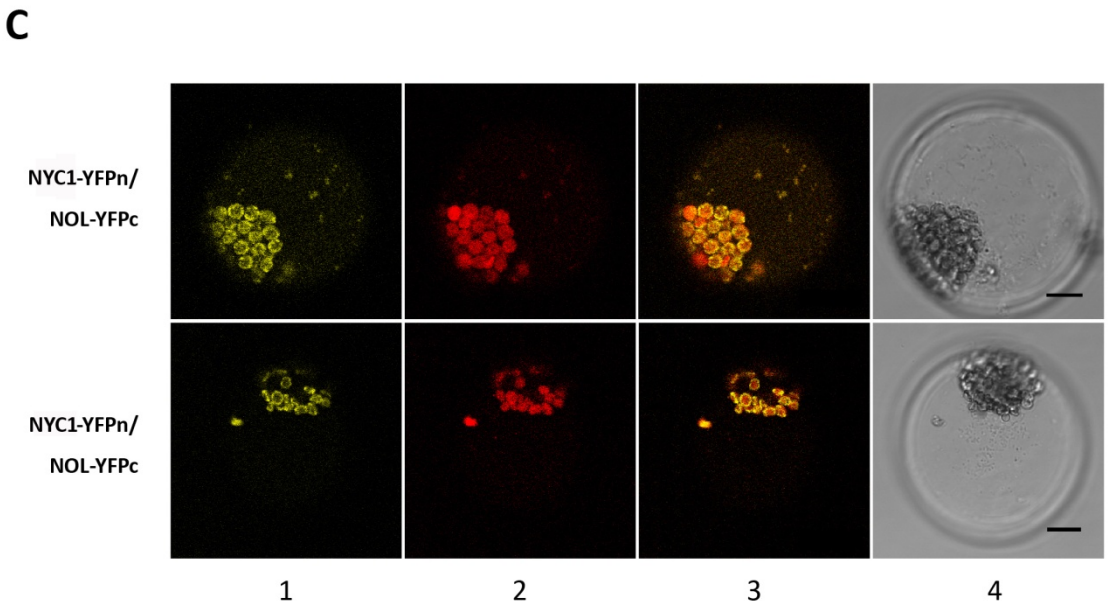

Figure 15 Detection of subcellular localization of protein complexes by BiFC. BiFC visualization of **(A)** PAO/RCCR, PAO/SGR and PAO/PPH, in transiently transformed *Arabidopsis* mesophyll protoplasts after 4 d of dark-induced senescence. **(B)** PPH/RCCR and PRK/CP12 and **(C)** NYC1/NOL interactions. For some interactions, two representative protoplasts are shown. YFP fluorescence (column 1) and chl autofluorescence (column 2) were examined by confocal laser scanning microscopy; column 3, merge of YFP and autofluorescence; column 4, bright field image. Bars = 10µm.

RCCR	SGR	PPH	NYC1	NOL	
✓	✓	✓	X	X	PAO
	weak	✓	n.d.	n.d.	RCCR
		X	n.d.	X	SGR
				✓	NYC1

Figure 16 Summary of the examined protein-protein interactions by BiFC. Hook, interaction detected by BiFC; red cross, no interaction detected; n.d., interaction not tested.

4.4.4 Discussion

The idea about the need to shield potentially phototoxic intermediates of chl breakdown from light excitation indicated that chl catabolic enzymes might act in complexes. For analyzing such complexes in living cells, several methods have been developed. Among them, the yeast two-hybrid system has significantly advanced the speed and extent of protein interaction studies. However, this system bears intrinsic limitations as for example systematic 'false-positive' and 'false-negative' interactions and, moreover, usually combines protein pairs in a heterologous environment (Fields and Song, 1989; Stephens and Banting, 2000). The most widely used approach for the visualization of protein interactions in living cells is fluorescence resonance energy transfer (FRET) between spectral variants of the green fluorescence protein (GFP) fused to the associating proteins (Chen et al., 2003). However, to enable observation of small alterations in fluorescence emission by energy transfer intensive methodical training is required. By contrast, the BiFC technique bears several significant advantages (Hu et al., 2002). Protein interactions using BiFC can be visualized in the native environment of the plant cell. Several restrictions inherent to interaction approaches in heterologous systems (e.g. yeast), as for instance missing plant-specific post-translational protein modifications or incorrect subcellular localization, are overcome by BiFC.

The present investigation applying BiFC technique confirms previously described interactions between PAO and RCCR (Pružinská et al., 2007) as well as between NYC1 and NOL (Sato et al., 2009). Moreover, the present study demonstrates the existence of a transient multi-protein complex occurring in senescing *Arabidopsis* chloroplasts. The following model illustrates the results of this project (Figure 17). From these findings, it can be assumed that a multi-protein complex consisting of SGR, PAO, RCCR and PPH formed at sites of active chl breakdown at the thylakoid membrane provides catabolite channelling between different enzymes of early chl breakdown reactions. Thus, green chl catabolites are only released from the complex after being catabolyzed to linear, fluorescing chl catabolites which are no longer phototoxic for the cell. In this model the function of SGR could be the recruitment of catabolic enzymes to LHC complexes. Further analysis is needed to elucidate whether the multi-protein complex contains further enzymes such as NYC1/NOL. So far, interaction with the chl *b* reductase complex is not demonstrated. However, our results obtained by applying BiFC could be substantiated by further studies using other techniques such as a yeast two-hybrid analysis or a *in vivo* pull down assays of mildly solubilized protein complexes.

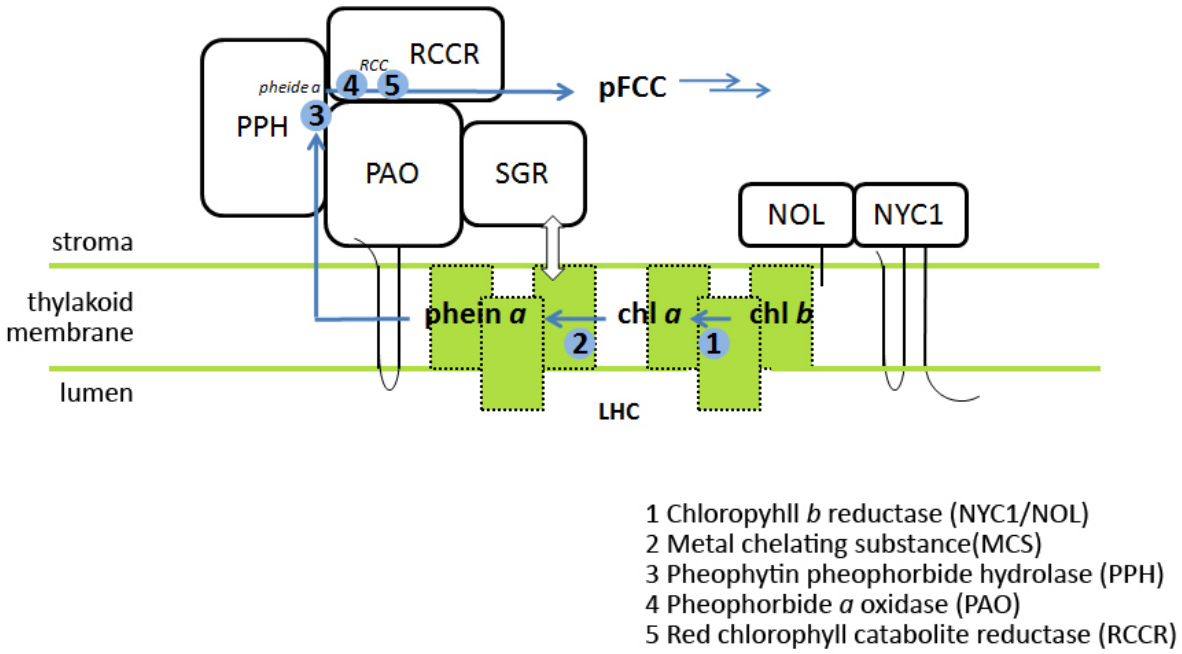

Figure 17 Proposed model for chl catabolite channelling during chl breakdown. The scheme is based on the findings of this project. A putative multi-protein complex is composed of four proteins, SGR, PAO, RCCR and PPH, acting at LHC complexes in the thylakoid membrane. A second complex consisting of NYC1 and NOL probably acts independently. The route of chl breakdown is indicated by blue arrows and involved enzymatic steps are labelled by numbers. Note that the chl catabolite intermediates formed during breakdown are either embedded in the thylakoid structure or retained in the multi-protein complex until nontoxic, linear primary fluorescent chl catabolites (pFCCs) are formed. For PAO and NYC1, predicted transmembrane domains are indicated. The white arrow indicates recruitment of the complex to LHCs through SGR.

4.5 The role of chlorophyllase in plant development

4.5.1 Indroduction

Phytol hydrolysis is an early step of chl breakdown where the lipophilic phytol residue is removed from the phorphyrin-ring moiety to increase water solubility of further chl catabolites. It was widely accepted that this hydrolysis is conducted by chlorophyllase (Chlase, CLH) which was first discovered by Willstätter and Stoll (1913). In the past, chlorophyllase genes were cloned from different species such as *Citrus sinensis*, *Chenopodium album* and *Arabidopsis thaliana* (Jakob-Wilk et al., 1999; Tsuchiya et al., 1999). However, conflicting data concerning localization led to the suggestion of an alternative pathway of chl breakdown operating outside the plastid (Takamiya et al., 2000), or questioned the involvement of Chlase in chl breakdown (Hörtensteiner, 2006). Moreover, our recent work provided reliable evidence that the *Arabidopsis* CLH1 and CLH2 are not essential during dark induced leaf senescence *in vivo* (Schenk et al., 2007). *At*CLHs displayed cytosolic localization when fused to GFP. Additionally, *clh1* and *clh2* single and double knockout lines degraded chl similar to wild type during dark induced senescence. More recently, we identified an alternative hydrolase, pheophytinase (PPH) (Schelbert et al., 2009). PPH is a chloroplast-located and senescence-induced esterase catalyzing the hydrolysis of the ester bond of the Mg-free chl pigment, phein, producing pheide and phytol. An *Arabidopsis* mutant (*pph1*) was unable to degrade chl and thus, displayed a stay-green phenotype. In conclusion, a new route of chl breakdown during leaf senescence via phein and not chlide was proposed (Schelbert et al., 2009). Nevertheless, the new pathway involving PPH might be accompanied by additional minor activities that convert some chl to chlide.

In the present study we examined the possibility of esterases other than PPH being involved in the hydrolytic step at early chl breakdown during leaf senescence. Thereby, we focussed on CLH1 and CLH2. Double and triple mutants being impaired at early reactions of chl breakdown were generated and the pigment composition of these mutant lines, including a *pph-1 pao-1 clh1-1* triple mutant, was analyzed. In a further attempt *At*CLH1 was mis-localized to the chloroplast with the aim to shed light on the *in vivo* function of CLH1.

4.5.2 Materials and methods

4.5.2.1 Plant material and growth conditions

Arabidopsis thaliana ecotype Col-0 was used as the wild type. T-DNA insertion lines were from the SALK collections (Alonso et al., 2003): *pph-1* (At5g13800), SALK_000095; *pao-1* (At3g44880), SALK_111333; *clh1-1* (At1g19670), SALK_124978. SALK lines were obtained from the European Arabidopsis Stock Center, Nottingham, UK. Homozygous plants were identified by PCR using the following T-DNA- and gene-specific primers:

pph-1	000095RP	5`-TGTACAGGTTATCGGTGAGCC-3`
	000095LP	5`-CTACCAATCCTGGACTCCTCC-3`
pao-1	N14-RP	5`-GGCTCACCTGACGCTTGGTTA-3`
	N14-LP	5`-CGACGGTGACAATTCAAAGGG-3`
clh1-1	RP2	5`-ACGTTAAGATATGCGGATCGG-3`
	LP	5`-GCATGGTTACATTCTTGTAGC-3`
SALK	LBb1.3	5`-ATTTTGCCGATTTCGGAAC-3`

Likewise, *pph-1 pao-1* double and *pph-1 pao-1 clh1-1* triple mutants were identified by PCR. Plants were grown on soil in long-day conditions in a greenhouse with fluence rates of 100 to 200 µmol photons m^{-2} s^{-1} at 22 °C. For senescence induction, detached leaves of 4- to 5-week-old plants were incubated on wet filter paper for up to 5 d in the dark. Primary transformants (T1) expressing PPH_{TP}-$CLH1_{HA}$ under the control of the PPH promotor (see below) were grown in ½ MS media containing 1 % sucrose in long-day conditions (16 h/8 h) in a culture room with fluence rates of 50 µmol photons m^{-2} s^{-1} at 23 °C.

4.5.2.2 Ion leakage

For ion conductivity analysis, senescence was induced in detached leaves that were incubated in the dark for 2.5 d. Eight leaf discs (1-cm diameter) were excised and transferred to 6-well cell culture plates (Sarstedt) containing 5 ml water. After re-exposure to light (150 μmol photons m^{-2} s^{-1}) for up to 4 h, ion leakage from the leaf discs as a measure of cellular damage was determined by measuring the conductivity of the solution with a CDH-42 conductivity meter (Omega Engineering). Finally, leaf discs were re-measured after freezing and thawing in liquid nitrogen, to determine the maximal ion leakage of dead tissue.

4.5.2.3 Analysis of chl catabolites

For HPLC analysis of green chl catabolites (chl, chlide, pheide, and phein), liquid nitrogen-homogenized tissue was extracted in 10 % (v/v) 0.2 M Tris-HCl pH 8, in acetone, cooled to -20 °C (20 ml g^{-1} fresh weight), and incubated at -20 °C for 2 h in the dark. After removal of insoluble material by cen-

trifugation, supernatants were analyzed by reversed-phase HPLC as described (Pružinská et al., 2005). Pigments were identified by their absorption spectra, and comigration with authentic standards (Roca et al., 2004). For quantification, peak areas at A_{665} referring to injected quantities were determined.

4.5.2.4 AtCLH1 mistargeting gene construct

A full-length cDNA sequence of *CLH1* was obtained from the RIKEN resource (Seki et al., 2002). A genomic clone of PPH was available from a former cloning effort (pMDC99_Pro_{PPH}:$gDNA_{PPH}$). A chimeric construct, consisting of the PPH promotor (1.3 kb; Pro_{PPH}), the PPH chloroplast transit peptide (TP_{PPH}) and the *CLH1* coding sequence including an HA-tag ($CLH1_{HA}$) was produced by a two-step PCR method. In a first PCR reaction, two overlapping PCR fragments (Pro_{PPH}:TP_{PPH} and $CLH1_{HA}$) were produced using Pfu polymerase (Promega) and the following primers:

at5g13800_gDNAfor	5`-TGTGGAGGAGAGCTCCGAATTAGC-3`
at5g13800_gDNArev(TP)	5`-CTCTATCGCCGCTCCACTTCGAATCACAAGTC-3`(underlined= overlap with *at1g19670_for/ATG)*
at1g19670_for/ATG	5`-GATTCGAAGTGGAGCGGCGATAGAGGACAGTCC-3`
at1g19670_revHA	5`-GTCTAGGCATAGTCTGGGACGTCATATGGATAGACGAAGATACCAGAAGCTTC-3` (underlined =HAtag)

In a second PCR reaction, the fragments were combined to yield Pro_{PPH}:TP_{PPH}-$CLH1_{HA}$ that was introduced by TA cloning into pCR2.1 (Invitrogen). After verification by sequencing, the chimeric fragment was excised with *Kpn*I/*Xba*I and cloned into pHannibal containing the OCS terminator (Wesley et al., 2001). Subsequently, the chimeric fragment was excised with *Spe*I and cloned into pGreen0179 (Hellens et al., 2000). The construct was transformed into *Agrobacterium* strain GV3101 together with pSOUP. Col-0*, pph-1*, *pph-1 pao-1* and *pph-1 pao-1 clh1-1* mutant lines were transformed with the flower dip method (Clough and Bent, 1998). Transformants were selected on hygromycin, and T1 plants were used for further analysis.

4.5.2.5 Protein import experiment

A *Sac*I/*Eco*RI-fragment from the chimeric construct (pCR2.1_Pro_{PPH}:TP_{PPH}-$CLH1_{HA}$) was cloned into pBluescript. [^{35}S]-Met-labeled TP_{PPH}-$CLH1_{HA}$ was synthesized with the TNT T7 Quick Coupled Transcription/Translation System (Promega). Intact chloroplasts of 3-week-old *Arabidopsis* plants (ecotype Col-0) grown on ½ MS plates were isolated as published (Schelbert et al., 2009). PPH import assays were performed as published (Fitzpatrick and Keegstra, 2001). For each import reaction, chloroplasts corresponding to 20 µg chl and 6 µl of in vitro-translated TP_{PPH}-$CLH1_{HA}$ preprotein were used. Lysis of chloroplasts and separation of stroma from membranes were done as described (Smith et al., 2002). All samples were resolved by SDS-PAGE and visualized by autoradiography.

4.5.3 Results

4.5.3.1 Characterization of different mutant lines in Arabidopsis

To analyze the senescence behaviour of the double (*pph-1 pao-1*) and the triple mutant (*pph-1 pao-1 clh 1-1*), detached leaves of several mutant lines were incubated in permanent darkness. Under these conditions, *pph-1* and *pao-1* displayed a stay-green phenotype as previously been shown (Pružinská et al., 2003; Park et al., 2007; Schelbert et al., 2009) (Figure 18A). Senescence progression in the wild type and *clh1-1* lines was evident by a progressive yellowing of leaves (Schenk et al., 2007). The investigated double and triple mutants exhibited a stay-green phenotype with no lesions formed; confirming earlier data showing that light is required for lesion formation in *pao-1* mutants (Pružinská et al., 2005). Nevertheless, visible leaf integrity of double and triple mutant lines was much better compared to the *pao-1* single mutant (data not shown).

To examine whether *pao-1* and respective double and triple mutants displayed a different speed in cell death upon light exposure, ion conductivity analysis was performed. Detached leaves were incubated in the dark for 2.5 d to induce senescence. Excised leaf discs, floated in water, were then re-exposed to light for up to 4 h. Leaf discs stayed intact in wild type, *pph-1* and *clh1-1* (Figure 18B). By contrast, cell death was measured in *pao-1*, the double and the triple mutants. Under the applied conditions, *pao-1* reached entire cell death at 2 h after re-exposure to light, while the double mutant displayed a slight and the triple mutant an even more clear delay in cell death progression (Figure 18B). Pheide *a* content was shown to be responsible for cell death observed in *pao-1* (Pružinská et al., 2005). Thereby cell death, as measured by ion leakage of leaf discs, was positively correlated with pheide *a* content. This correlation was also detected in my study (Figure 18B and C). Lines exhibiting no cell death such as wild type, *pph-1* and *clh1-1* did not accumulate pheide *a* during the course of senescence (Figure 18B, C and D). By contrast, *pao-1* displaying the fastest cell death progression also exhibited the highest pheide *a* content. Although pheide *a* content in the double and the triple mutants was moderate at 3 and 5 d of dark induced senescence (Figure 18C and D), cell death was clearly measured in senescing leaf discs (2.5 d) after 2 h of light exposure (Figure 18B) indicating that a relatively small amount of pheide *a* is inducing the maximal ion leakage.

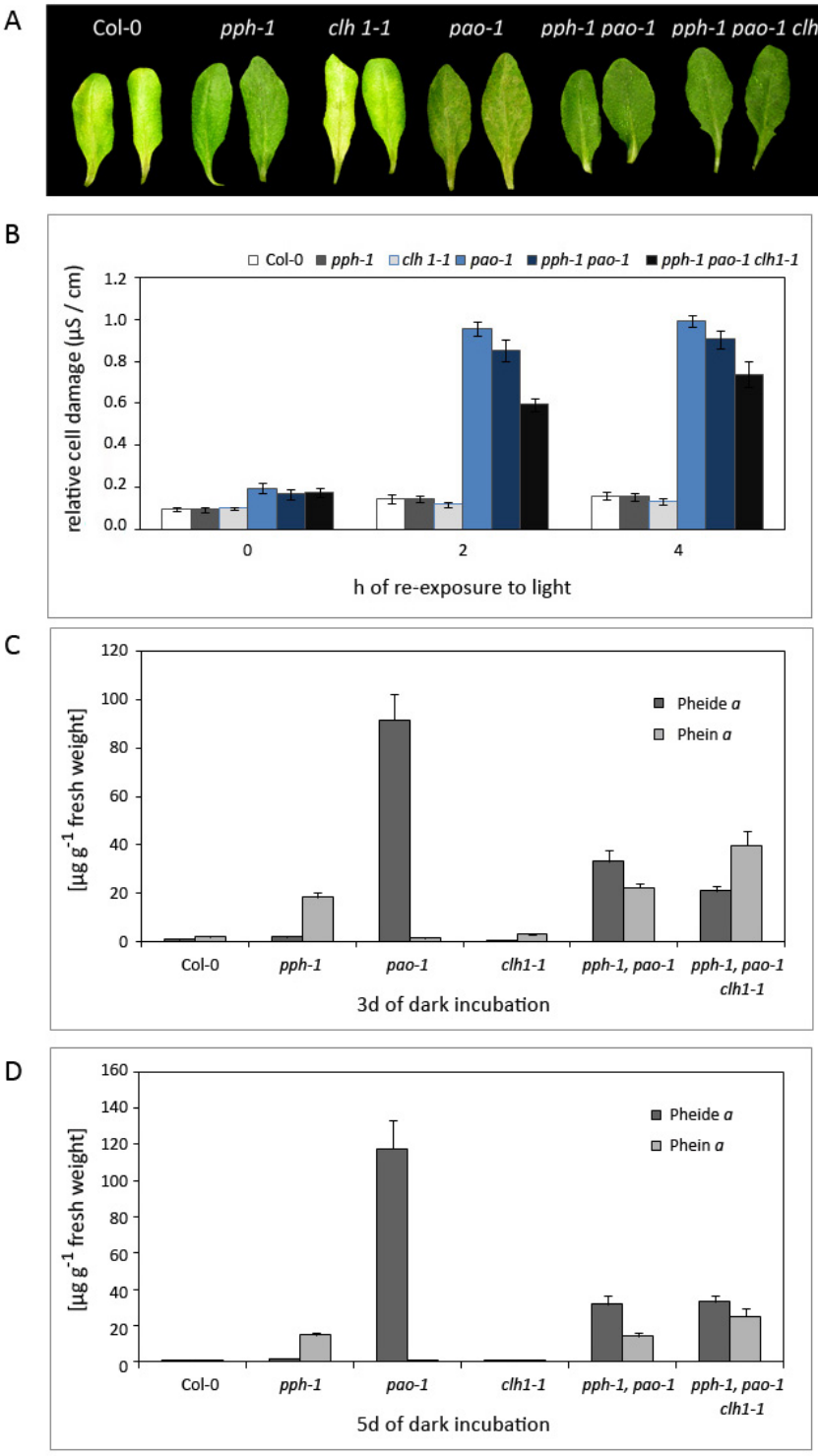

Figure 18 Impact of CLH1 in leaf senescence. (A) Phenotype in leaves of different mutant lines after 5 d of dark-induced senescence. **(B)** Determination of ion leakage as a measure of cell death in Col-0 and different mutant lines analyzed. Before exposure to light (150 µmol m^{-2} s^{-1}) up to 4 h, leaves were incubated in the dark for 2.5 d. **(C)** and **(D)** HPLC analysis of green chl catabolites during dark-induced senescence. Amount of total chl catabolites, phein *a* and pheide *a* respectively found in Col-0 and different mutant lines after **(C)** 3 d and after **(D)** 5 d of dark-induced senescence. Data in **(B)** to **(D)** are mean values ±SD of representative experiments with **(B)** eight, **(C)** and **(D)** three replicates.

4.5.3.2 Analysis of chl catabolites

Different stay-green mutants have been shown to accumulate green intermediates of chl breakdown such as chlide and/or pheide as well as phein (Roca et al., 2004; Park et al., 2007; Schelbert et al., 2009). To further investigate the role of CLH1 during chl breakdown, pigment composition of the *pph-1 pao-1 clh1-1* triple mutant compared to the wild type and corresponding single and double mutants was analyzed. Green pigments were extracted at 3 d and 5 d of dark induced senescence and separated by reversed-phase HPLC (Figure 18C and D). In order to study pigment composition of mutant lines which are deficient in early reactions, the chl breakdown pathway was blocked further downstream at the level of PAO *e.g.* a tight block at this level led to the accumulation of large quantities of pheide *a*. Thus, *pao-1* background served as an indicator of the level of catabolites accumulating.

No green chl catabolites were detected in the wild type (Col-0) and *clh1-1* where the breakdown pathway is not blocked (Figure 18C and D) (Schenk et al., 2007). By contrast, pheide *a* content in *pao-1* was fairly high at 3 d of dark induced senescence with no prominent increase after 5 d (Figure 18C and D), indicating that chl catabolite accumulation at 3 d is high enough to provoke maximal cell death. Thus, analysis of catabolites at 5 d is negligible. Surprisingly, pheide *a* was detected in the double and triple mutants although at smaller amounts compared to *pao-1*. Phein *a* accumulation was detected as expected in all mutants being deficient in PPH. Yet, levels were higher in the triple mutant indicating that CLH1 might converted some phein *a* to pheide *a* in *pph-1* and *pph-1 pao-1* (Figure 18C and D). These findings point to a limited participation of other hydrolases, such as CLH1 and CLH2, acting on chl and its derivatives.

4.5.3.3 Mistargeting of CLH1 in the chloroplast

The *Arabidopsis* CLH1 was previously shown to localize to the cytosol and not being involved in chl breakdown during leaf senescence (Schenk et al., 2007). To further emphasize the assumption that CLH1 is not essential for chl breakdown *in vivo*, CLH1 was mistargeted to the chloroplast. Thereby, a chimeric construct under the control of the PPH promoter was engineered (Figure 19A) and introduced into the plant expression vector pGreen0179. *Arabidopsis* wild type and different mutant lines were transformed with the flower dip method. Surprisingly, transgenic plants harbouring the chimeric gene construct were severely affected in growth and chl metabolism, demonstrated by a light-sensitive pale phenotype (Figure 19B). The pale phenotype was already present at early stages of development regardless of the genetic background most probably due to basal PPH promotor activity present almost throughout the entire above-ground plant development (Zimmermann et al. 2004). Transgenic plants were viable only under low light conditions and sucrose supplement. Plant growth was severely retarded with no development beyond an early rosette stage (data not shown). Yet,

whether the phenotype is due to the occurrence of phototoxic chl breakdown intermediates through CLH1 activity or whether *CLH1* expression inside the chloroplast somehow prevents chl biosynthesis and/or chloroplast synthesis remains to be demonstrated. In this respect, an inducible system would be advantageous for futher studies.

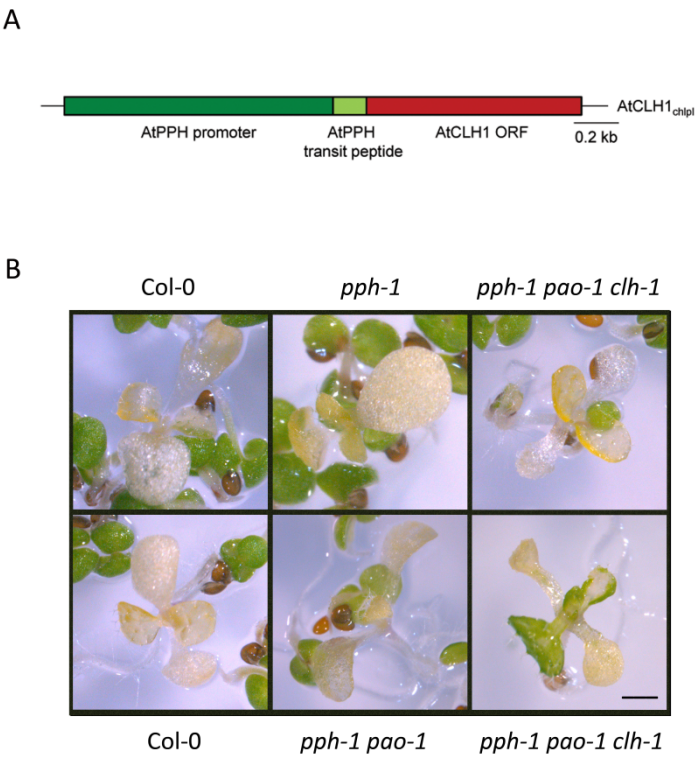

Figure 19 CLH1 mistargeting to the chloroplast. (A) Chimeric gene construct used for mistargeting; full length cDNA of *At*CLH1 without its start codon was cloned to the pGreen0179 vector, with an N-terminally added PPH chloroplast targeting signal and a C-terminally added HA taq cassette. The construct was under the control of the PPH promotor. (**B)** Transgenic plants harbouring the transgene. A light-sensitive pale phenotype was already present at early stages of development regardless of the genetic background. Note that pictures are taken from a primary transformant screen. Therefore, untransformed green seedlings died whereas transgenic pale plants survived under hygromycin selection. Bar = 0.2 cm.

4.5.3.4 TP_{PPH}-$CLH1_{HA}$ is imported into the chloroplast

We performed import experiments of [^{35}S]-Met labeled TP_{PPH}-$CLH1_{HA}$ into isolated *Arabidopsis* mesophyll chloroplasts, followed by chloroplast reisolation and subfractionation (Figure 20). $CLH1_{HA}$ was efficiently imported into the plastids and was detected in the soluble fraction. From these results, we conclude that also in the pale transgenic lines (Figure 19) $CLH1_{HA}$ is located inside the chloroplast, most likely as a soluble protein in the stroma.

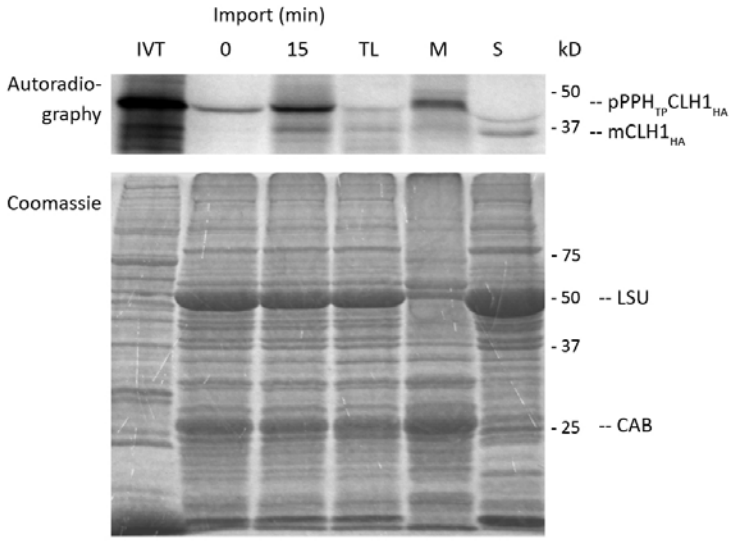

Figure 20 Import of [^{35}S]-Met-labeled TP_{PPH}-$CLH1_{HA}$ in *Arabidopsis* chloroplasts. Import proceeded for 15 min and mature $CLH1_{HA}$ ($mCLH1_{HA}$) accumulated. After import, chloroplasts were treated with thermolysin (TL) to digest surface-bound and nonimported precursor. To determine the subchloroplast $CLH1_{HA}$ localization, chloroplasts without TL treatment were lysed and separated into stroma (S) and membrane (M) fractions. kD, molecular size markers are indicated at the right. IVT, in vitro translation product; LSU, large subunit of Rubisco; CAB, chlorophyll *a/b* binding protein.

4.5.4 Discussion

4.5.4.1 Impact of CLHs on chl breakdown in leaves

Recent data demonstrated that dephytylation is catalyzed by PPH and not by CLHs as commonly accepted (Schenk et al., 2007; Schelbert et al., 2009) Nevertheless, the new pathway involving PPH might be accompanied by additional minor activities that convert some chl to pheide. We aimed to dissect this assumption by analyzing the pigment composition of different mutant lines including a *pph-1 pao-1 clh1-1* triple mutant. The most striking observation was the detection of pheide *a* in the double (*pph-1 pao-1)* and triple (*pph-1 pao-1 clh1-1*) mutant lines (Figure 18C and D). Although pheide *a* quantities were much smaller compared to *pao-1*, it was not expected to accumulate. However, this data support the hypothesis that additional minor activities, such as CLH1 and CLH2, could convert some chl to pheide, acting directly on chl or on phein *a* (Figure 21). Indeed, *c*hlorophyllases were shown to act on both, chl and phein in a respective *in vitro* assay (Schelbert et al., 2009). But this assumption is in contrast with the proposed localization of CLHs in the cytosol (Schenk et al., 2007). Moreover, retarded growth and affected chl metabolism in transgenic plants harbouring the chimeric gene construct (Figure 19B) strongly support that CLH1 has no physiological role in the chloroplast *in vivo*. Accordingly, CLHs would not have access to early chl breakdown reactions which occur within the chloroplast. Only for CLH2, a majority of available servers that predict subcellular localization of plant proteins (Schwacke et al., 2004) indicate a plastidial localization (Schenk et al., 2007). CLH2 was shown to be constitutively expressed at a low level throughout leaf development, unaffected by either stress or senescence (Tsuchiya et al., 1999; Benedetti and Arruda, 2002). Whether CLH2 is responsible for the remaining pheide *a* accumulation in the triple mutant (*pph-1 pao-1 clh1-1*) (Figure 21) or whether these findings are due to artefactual esterase activity occurring during tissue extraction needs to be demonstrated. A quadruple knockout line being deficient in PPH, PAO, CLH1 and CLH2 is under construction.

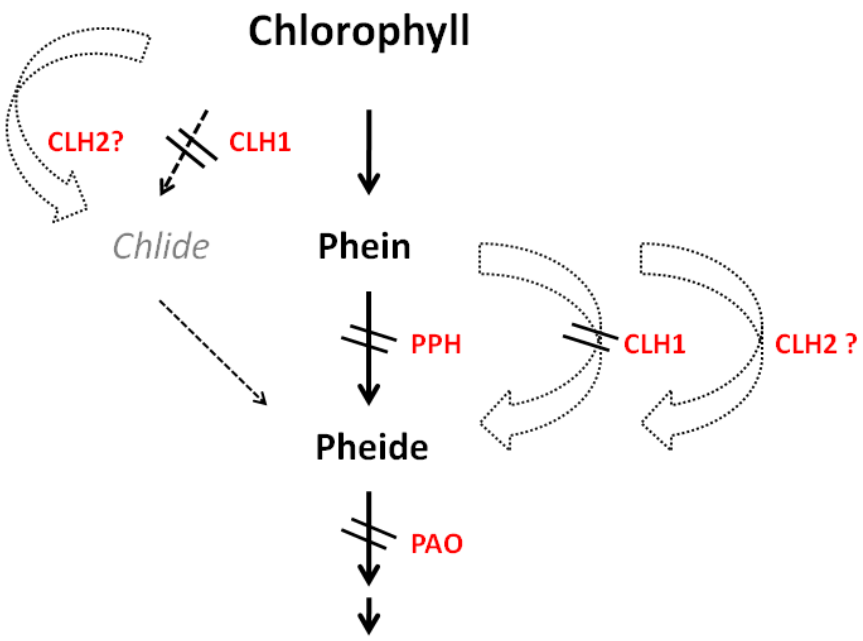

Figure 21 Schematic representations of possible early reactions of chl catabolism. Schematic drawing of chl breakdown integrating the findings of this project. Black solid arrows indicate the major route of chl breakdown as described (Schelbert et al., 2009). Dashed arrows indicate possible alternative routes of chl degradation. Forward slashes notify sites of blockage of the pathway in mutants used for this study. Involved enzymes are labeled in red and intermediates formed are indicated in black and grey. CLH1 and CLH2, chlorophyllase 1 and 2; PPH, pheophytin pheophorbide hydrolase; PAO, pheophorbide *a* oxygenase.

V Conclusion and outlook

During my PhD, I studied different aspects of chl catabolism. I focussed on the phytol hydrolyzing activity that is an early reaction of the chl breakdown pathway during leaf senescence and fruit ripening processes. Additionally, I investigated a possible degradation-complex consisting of several enzymes involved in early chl breakdown, demonstrating a possible way to channel phototoxic chl intermediates through several catabolic steps.

The chl breakdown pathway has been elucidated in recent years (Hörtensteiner, 2006) and most catabolites and enzymes involved in chl breakdown were already well described when I started my thesis. Nevertheless, a re-examination of *Arabidopsis* CLHs function revealed that CLHs are not essential for chl breakdown and own investigations proposed PPH to catalyze phytol hydrolysis during leaf senescence *in vivo* (Schenk et al., 2007; Schelbert et al., 2009). These findings questioned the long-proposed *in vivo* function of CLHs and suggested a revision of the route of early reactions of chl breakdown. However, the degradation path involving PPH is suggested to be accompanied by limited participation of other hydrolases that convert some chl to pheide. Own investigations on *At*CLH1 demonstrated cytosolic localization and transgenic lines harbouring a chimeric gene construct, which delivers CLH1 into the chloroplast, were severely affected in growth (Figure 19) indicating that *At*CLH1 most probably does not play a physiological role in early chl breakdown that is executed in the gerontoplast. On the other hand, *At*CLH1 is proposed to be involved in other instances of chl catabolism such as during pathogen defence (Kariola et al., 2005). Thereby, *At*CLH1 might be involved in a rapid detoxification of free chl occurring upon tissue damage. Whether *At*CLH2 or other unknown esterases contribute to phytol hydrolysis during leaf senescence is part of ongoing investigations (Figure 21).

While the majority of work on chl breakdown has focussed on leaf senescence, a few studies were done on fruit degreening. Among them, SGR protein was identified as being involved in chl breakdown at the onset of fruit ripening in different species (Akhtar et al., 1999; Efrati et al., 2005) and linear chl catabolites were detected in apples, pears and bananas (Müller et al., 2007; Moser et al., 2008). Although a study in *Citrus* fruit degreening described the involvement of chlase (Azoulay Shemer et al., 2008) my own investigations suggest that *Sl*PPH is involved in chl breakdown during fruit ripening of tomato besides the described role in chl catabolism during leaf senescence. These findings provide further evidence that chl breakdown in fruits follows the same route as in leaves. Nevertheless, further investigations on chl breakdown-related enzymes, such as PAO, could, in addition, substantiate the idea of the same pathway functioning in leaves and fruits.

The accumulation of free porphyrins during chl metabolism causes cell death and needs to be avoided. In this context, we examined the possible formation of a multi-protein complex during chl

breakdown. Indeed, my investigations revealed the occurrence of a multi-protein complex *in vivo* that is formed exclusively during senescence at sites of active chl breakdown at the thylakoid membrane. Based on these results, I assume that several consecutive enzymatic steps of early chl breakdown are assembled in the suggested chl-degradation super complex (Figure 17). This would allow channelling of the chl intermediates leading to a safer processing of the phototoxins and may also facilitate regulation of degradation. Even though my studies were performed in a native environment using the BiFC system, additional studies using other techniques such as yeast two-hybrid or pull down assays could substantiate my findings.

Although chl breakdown is well understood and most enzymes and intermediates functioning in the pathway are characterized, elucidation of the Mg-removing activity as well as knowledge on the function of SGR would improve the actual understanding on early chl breakdown.

Chl turnover at the steady state level represents a further area for future investigations. During the productive photosynthetic phase of a leaf, parts of photosystems are damaged and recycled. In addition, plants are adapting to different light conditions by changing the size of their antennae, and this might also require a degradation of chl-protein complexes. Chl biosynthesis genes are shown to keep basal expression levels during chl turnover. By contrast, no evidence has been reported for an involvement of the common chl breakdown pathway in this process. Genes involved in chl breakdown such as SGR, PPH and PAO are marginally expressed in green tissues and final chl breakdown products (NCCs) were not detected. Taking in consideration that chl does not turn over at the same rate as the D1 subunit (Vavilin et al., 2005) it is possible that chl is temporarily stored during PSII repair. Recent work from the Vermaas group has suggested, based on labeling studies for chl metabolism in *Synechocystis sp* PCC 6803, that during turnover the phytol tail of chl *a* is removed and that the tetrapyrrole headgroup is reused (Vavilin and Vermaas, 2007). Interestingly, a gene with significant homology to CLHs is missing in *Synechocystis* (Vavilin and Vermaas, 2007) and PPH-like proteins present in *Synechocystis* do not cluster into the PPH clade (Schelbert et al., 2009). Thus, the identity of the phytol hydrolyzing activity that is proposed to occur during chl turnover remains unknown. Further work will be required to analyze the fate of chl at the steady state level and whether enzymes functioning in the common chl catabolism pathway are involved during chl turnover as well.

In conclusion, chl pigments play a central role in absorbing light energy that is converted to chemical energy during photosynthesis, a process that is fundamental for life on earth. Yet, chl metabolism has to be highly coordinated to allow a safe processing of potentially phototoxic intermediates through several enzymatic steps. Here I show that this occurs during chl breakdown and it can be expected that similar complexes combined with metabolic channelling occur in chl biosynthesis.

VI References

Abbott BL (2003) ABCG2 (BCRP) expression in normal and malignant hematopoietic cells. Hematol. Oncol. **21:** 115-130

Ajioka RS, Phillips JD, Weiss RB, Dunn DM, Kushner JP (2006) HAMP and HVJ as candidate modifier genes in typel hereditary hemochromatosis with high iron burden and in porphyria cutanea tarda (PCT). Blood **108:** 444A

Akhtar MS, Goldschmidt EE, John I, Rodoni S, Matile P, Grierson D (1999) Altered patterns of senescence and ripening in *gf*, a stay-green mutant of tomato (*Lycopersicon esculentum* Mill.). J. Exp. Bot. **50:** 1115-1122

Alonso JM, Stepanova AN, Leisse TJ, Kim CJ, Chen H, Shinn P, Stevenson DK, Zimmermann J, Barajas P, Cheuk R, Gadrinab C, Heller C, Jeske A, Koesema E, Meyers CC, Parker H, Prednis L, Ansari Y, Chory N, Deen H, Geralt M, Hazari N, Hom E, Karnes M, Mulholland C, Ndubaku R, Schmidt I, Guzman P, Aguilar-Henonin L, Schmid M, Weigel D, Carter DE, Marchand T, Risseeuw E, Brogden D, Zeko A, Crosby WL, Berry CC, Ecker JR (2003) Genome-wide insertional mutagenesis of *Arabidopsis thaliana*. Science **301:** 653-657

Alos E, Roca M, Iglesias DJ, Minguez-Mosquera MI, Damasceno CMB, Thannhauser TW, Rose JKC, Talon M, Cercos M (2008) An evaluation of the basis and consequences of a stay-green mutation in the navel negra citrus mutant using transcriptomic and proteomic profiling and metabolite analysis. Plant Physiol. **147:** 1300-1315

Altschul SF, Madden TL, Schaffer AA, Zhang JH, Zhang Z, Miller W, Lipman DJ (1997) Gapped BLAST and PSI-BLAST: a new generation of protein database search programs. Nucl. Acids Res. **25:** 3389-3402

Armstead I, Donnison I, Aubry S, Harper J, Hörtensteiner S, James C, Mani J, Moffet M, Ougham H, Roberts L, Thomas A, Weeden N, Thomas H, King I (2007) Cross-species identification of Mendel's *I* locus. Science **315:** 73

Armstead IP, Turner LB, King IP, Cairns AJ, Humphreys MO (2002) Comparison and integration of genetic maps generated from F-2 and BC1-type mapping populations in perennial ryegrass. Plant Breeding **121:** 501-507

Aubry S, Mani J, Hörtensteiner S (2008) Stay-green protein, defective in Mendel's green cotyledon mutant, acts independent and upstream of pheophorbide a oxygenase in the chlorophyll catabolic pathway. Plant Mol. Biol. **67:** 243-256

Aubry S (2008) Biochemical and molecular analysis of chlorophyll degradation in higher plants. Ph. D. University of Zürich

Azoulay Shemer T, Harpaz-Saad S, Belausov E, Lovat N, Krokhin O, Spicer V, Standing KG, Goldschmidt EE, Eyal Y (2008) Citrus chlorophyllase dynamics at ethylene-induced fruit color-break: A study of chlorophyllase expression, posttranslational processing kinetics, and in situ intracellular localization. Plant Physiol. **148:** 108-118

Banala S, Moser S, Müller T, Kreutz C, Holzinger A, Lütz C, Kräutler B (2010) Hypermodified Fluorescent Chlorophyll Catabolites: Source of Blue Luminescence in Senescent Leaves. Angew. Chem. Int. Edit. **49**: 5174–5177

Barry CS (2009) The stay-green revolution: Recent progress in deciphering the mechanisms of chlorophyll degradation in higher plants. Plant Sci. **176:** 325-333

Barry CS, McQuinn RP, Chung MY, Besuden A, Giovannoni JJ (2008) Amino acid substitutions in homologs of the STAY-GREEN protein are responsible for the green-flesh and chlorophyll retainer mutations of tomato and pepper. Plant Physiol. **147:** 179-187

Barsan C, Sanchez-Bel P, Rombaldi C, Egea I, Rossignol M, Kuntz M, Zouine M, Latche A, Bouzayen M, Pech JC (2010) Characteristics of the tomato chromoplast revealed by proteomic analysis. J. Exp. Bot. **61:** 2413-2431

Benedetti CE, Arruda P (2002) Altering the expression of the chlorophyllase gene *ATHCOR1* in transgenic Arabidopsis caused changes in the chlorophyll-to-chlorophyllide ratio. Plant Physiol. **128:** 1255-1263

Benedetti CE, Costa CL, Turcinelli SR, Arruda P (1998) Differential expression of a novel gene in response to coronatine, methyl jasmonate, and wounding in the *Coi1* mutant of *Arabidopsis*. Plant Physiol. **116:** 1037-1042

Borovsky Y, Paran I (2008) Chlorophyll breakdown during pepper fruit ripening in the chlorophyll retainer mutation is impaired at the homolog of the senescence-inducible stay-green gene. Theor. Appl. Genet. **117:** 235-240

Bortlik K-H (1990) Chlorophyllabbau: Charakterisierung von Kataboliten in seneszenten Gerstenblättern. Ph. D. University of Zürich

Bracha-Drori K, Shichrur K, Katz A, Oliva M, Angelovici R, Yalovsky S, Ohad N (2004) Detection of protein-protein interactions in plants using bimolecular fluorescence complementation. Plant J. **40:** 419-427

Buchanan-Wollaston V, Page T, Harrison E, Breeze E, Lim PO, Nam HG, Lin JF, Wu SH, Swidzinski J, Ishizaki K, Leaver CJ (2005) Comparative transcriptome analysis reveals significant differences in gene expression and signalling pathways between developmental and dark/starvation-induced senescence in Arabidopsis. Plant J. **42:** 567-585

Camara B, Hugueney P, Bouvier F, Kuntz M, Moneger R (1995) Biochemistry and molecular biology of chromoplast development. Int. Rev. Cytol. **163:** 175-247

Cha KW, Lee YJ, Koh HJ, Lee BM, Nam YW, Paek NC (2002) Isolation, characterization, and mapping of the stay green mutant in rice. Theor. Appl. Genet. **104:** 526-532

Chen Y, Mills JD, Periasamy A (2003) Protein localization in living cells and tissues using FRET and FLIM. Differentiation **71:** 528-541

Clough SJ, Bent AF (1998) Floral dip: a simplified method for Agrobacterium-mediated transformation of Arabidopsis thaliana. Plant J. **16:** 735-743

Costa ML, Civello PM, Chaves AR, Martinez GA (2002) Characterization of Mg-dechelatase activity obtained from *Fragaria* x *ananassa* fruit. Plant Physiol. Biochem. **40:** 111-118

Curty C, Engel N, Gossauer A (1995) Evidence for a monooxygenase-catalyzed primary process in the catabolism of chlorophyll. FEBS Lett. **364:** 41-44

Efrati A, Eyal Y, Paran I (2005) Molecular mapping of the *chlorophyll retainer* (*cl*) mutation in pepper (*Capsicum* spp.) and screening for candidate genes using tomato ESTs homologous to structural genes of the chlorophyll catabolism pathway. Genome **48:** 347-351

Emanuelsson O, Nielsen H, Von Heijne G (1999) ChloroP, a neural network-based method for predicting chloroplast transit peptides and their cleavage sites. Protein Sci. **8:** 978-984

Endler A, Meyer S, Schelbert S, Schneider T, Weschke W, Peters SW, Keller F, Baginsky S, Martinoia E, Schmidt UG (2006) Identification of a vacuolar sucrose transporter in barley and arabidopsis mesophyll cells by a tonoplast proteomic approach. Plant Physiol. **141:** 196-207

Engel N, Curty C, Gossauer A (1996) Chlorophyll catabolism in *Chlorella prototheco*ides. 8. Facts and artefacts. Plant Physiol. Biochem. **34:** 77-83

Exposito-Rodriguez M, Borges AA, Borges-Perez A, Perez JA (2008) Selection of internal control genes for quantitative real-time RT-PCR studies during tomato development process. Bmc Plant Biol. **8:**

Fields S, Song OK (1989) A Novel Genetic System to Detect Protein Protein Interactions. Nature **340:** 245-246

Fitzpatrick LM, Keegstra K (2001) A method for isolating a high yield of Arabidopsis chloroplasts capable of efficient import of precursor proteins. Plant J. **27:** 59-65

Frankenberg N, Mukougawa K, Kohchi T, Lagarias JC (2001) Functional genomic analysis of the HY2 family of ferredoxin-dependent bilin reductases from oxygenic photosynthetic organisms. Plant Cell **13:** 965-978

Frelet-Barrand A, Kolukisaoglu HU, Plaza S, Ruffer M, Azevedo L, Hörtensteiner S, Marinova K, Weder B, Schulz B, Klein M (2008) Comparative mutant analysis of arabidopsis ABCC-type ABC transporters: AtMRP2 contributes to detoxification, vacuolar organic anion transport and chlorophyll degradation. Plant Cell Physiol. **49:** 557-569

Gan S, Amasino RM (1997) Making sense of senescence. Molecular genetic regulation and manipulation of leaf senescence. Plant Physiol. **113:** 313-319

Garcia AL, Galindo L (1991) Chlorophyllase in Citrus Leaves - Localization and Partial-Purification of the Enzyme. Photosynthetica **25:** 105-111

Gaude N, Brehelin C, Tischendorf G, Kessler F, Dörmann P (2007) Nitrogen deficiency in Arabidopsis affects galactolipid composition and gene expression and results in accumulation of fatty acid phytyl esters. Plant J. **49:** 729-739

Goff SA, Klee HJ (2006) Plant volatile compounds: Sensory cues for health and nutritional value? Science **311:** 815-819

Goldschmidt EE (2001) Chlorophyll decomposition in senescing leaves and ripening fruits: functional and evolutionary perspectives. *In* R Ben-Arie, S Philosoph-Hadas, eds, Proceedings of the 4th International Conference on Postharvest Science, pp 331-335

Goldschmidt EE, Huberman M, Goren R (1993) Probing the Role of Endogenous Ethylene in the Degreening of Citrus-Fruit with Ethylene Antagonists. Plant Growth Regul. **12:** 325-329

Gray J, Janick-Bruckner D, Bruckner B, Close PS, Johal GS (2002) Light-dependent death of maize *lls1* cells is mediated by mature chloroplasts. Plant Physiol. **130:** 1894-1907

Greenberg JT, Guo A, Klessig DF, Ausubel FM (1994) Programmed cell death in plants: a pathogen-triggered response activated coordinately with multiple defense functions. Cell **77:** 551-563

Greenberg JT, Ausubel FM (1993) *Arabidopsis* mutants compromised for the control of cellular damage during pathogenesis and aging. Plant J. **4:** 327-341

Grimm B (1998) Novel insights in the control of tetrapyrrole metabolism of higher plants. Curr. Opin. Plant Biol. **1:** 245-250

Guo YF, Gan SS (2006) AtNAP, a NAC family transcription factor, has an important role in leaf senescence. Plant J. **46:** 601-612

Hardwick LJA, Velamakanni S, van Veen HW (2007) The emerging pharmacotherapeutic significance of the breast cancer resistance protein (ABCG2). Brit. J. Pharmacol. **151:** 163-174

Harpaz-Saad S, Azoulay T, Arazi T, Ben-Yaakov E, Mett A, Shiboleth YM, Hörtensteiner S, Gidoni D, Gal-On A, Goldschmidt EE, Eyal Y (2007) Chlorophyllase is a rate-limiting enzyme in chlorophyll catabolism and is posttranslationally regulated. Plant Cell **19:** 1007-1022

Harrison MA, Nemson JA, Melis A (1993) Assembly and composition of the chlorophyll *a*-*b* light-harvesting complex of barley (*Hordeum vulgare* L.): immunochemical analysis of chlorophyll *b*-less and chlorophyll *b*-deficient mutants. Photosynth. Res. **38:** 141-151

He YH, Tang WN, Swain JD, Green AL, Jack TP, Gan SS (2001) Networking senescence-regulating pathways by using Arabidopsis enhancer trap lines. Plant Physiol. **126:** 707-716

Hellens R, Edwards EA, Leyland NR, Bean S, Mullineaux PM (2000) pGreen: a versatile and flexible binary Ti vector for *Agrobacterium*-mediated plant transformation. Plant Mol. Biol. **42:** 819-832**Himelblau E, Amasino RM** (2001) Nutrients mobilized from leaves of Arabidopsis thaliana during leaf senescence. J. Plant Physiol. **158:** 1317-1323

Himelblau E, Amasino RM (2001) Nutrients mobilized from leaves of Arabidopsis thaliana during leaf senescence. J. Plant Physiol. **158:** 1317-1323

Hinder B, Schellenberg M, Rodoni S, Ginsburg S, Vogt E, Martinoia E, Matile P, Hörtensteiner S (1996) How plants dispose of chlorophyll catabolites. Directly energized uptake of tetrapyrrolic breakdown products into isolated vacuoles. J. Biol. Chem. **271:** 27233-27236

Hinderhofer K, Zentgraf U (2001) Identification of a transcription factor specifically expressed at the onset of leaf senescence. Planta **213:** 469-473

Horie Y, Ito H, Kusaba M, Tanaka R, Tanaka A (2009) Participation of chlorophyll b reductase in the initial step of the degradation of light-harvesting chlorophyll a/b-protein complexes in Arabidopsis. J Biol Chem. **284**: 17449-17456

Horn R, Paulsen H (2004) Early steps in the assembly of light-harvesting chlorophyll *a*/*b* complex - Time-resolved fluorescence measurements. J. Biol. Chem. **279:** 44400-44406

Hörtensteiner S (2009) Stay-green regulates chlorophyll and chlorophyll-binding protein degradation during senescence. Trends Plant Sci. **14:** 155-162

Hörtensteiner S (2006) Chlorophyll degradation during senescence. Annu. Rev. Plant Biol. **57:** 55-77

Hörtensteiner S (1999) Chlorophyll breakdown in higher plants and algae. Cell. Mol. Life Sci. **56:** 330-347

Hörtensteiner S (1998) NCC malonyltransferase catalyses the final step of chlorophyll breakdown in rape (*Brassica napus*). Phytochemistry **49:** 953-956

Hörtensteiner S, Feller U (2002) Nitrogen metabolism and remobilization during senescence. J. Exp. Bot. **53:** 927-937

Hörtensteiner S, Rodoni S, Schellenberg M, Vicentini F, Nandi OI, Qiu Y-L, Matile P (2000) Evolution of chlorophyll degradation: the significance of RCC reductase. Plant Biol. **2:** 63-67

Hörtensteiner S, Wüthrich KL, Matile P, Ongania K-H, Kräutler B (1998) The key step in chlorophyll breakdown in higher plants. Cleavage of pheophorbide *a* macrocycle by a monooxygenase. J. Biol. Chem. **273:** 15335-15339

Hörtensteiner S, Vicentini F, Matile P (1995) Chlorophyll breakdown in senescent cotyledons of rape, *Brassica napus* L.: enzymatic cleavage of phaeophorbide *a in vitro*. New Phytol. **129:** 237-246

Hu CD, Chinenov Y, Kerppola TK (2002) Visualization of interactions among bZip and Rel family proteins in living cells using bimolecular fluorescence complementation. Mol. Cell **9:** 789-798

Hu G, Yalpani N, Briggs SP, Johal GS (1998) A porphyrin pathway impairment is responsible for the phenotype of a dominant disease lesion mimic mutant of maize. Plant Cell **10:** 1095-1105

Ischebeck T, Zbierzak AM, Kanwischer M, Dormann P (2006) A salvage pathway for phytol metabolism in *Arabidopsis*. J. Biol. Chem. **281:** 2470-2477

Ito H, Ohysuka T, Tanaka A (1996) Conversion of chlorophyll *b* to chlorophyll *a via* 7-hydroxymethyl chlorophyll. J. Biol. Chem. **271:** 1475-1479

Iturraspe J, Moyano N, Frydman B (1995) A new 5-formylbilinone as the major chlorophyll *a* catabolite in tree senescent leaves. J. Org. Chem. **60:** 6664-6665

Jakob-Wilk D, Holland D, Goldschmidt EE, Riov J, Eyal Y (1999) Chlorophyll breakdown by chlorophyllase: isolation and functional expression of the *Chlase1* gene from ethylene-treated *Citrus* fruit and its regulation during development. Plant J. **20:** 653-661

Jiang H, Li M, Liang N, Yan H, Wei Y, Xu X, Liu J, Xu Z, Chen F, Wu G (2007) Molecular cloning and function analysis of the *stay green* gene in rice. Plant J. **52:** 197-209

Jonker JW, Buitelaar M, Wagenaar E, van der Valk MA, Scheffer GL, Scheper RJ, Plösch T, Kuipers F, Oude Elferink RPJ, Rosing H, Beijnen JH, Schinkel AH (2002) The breast cancer resistance protein protects against a major chlorophyll-derived dietary phototoxin and protoporphyria. Proc. Natl. Acad. Sci. USA **99:** 15649-15654

Kariola T, Brader G, Li J, Palva ET (2005) Chlorophyllase 1, a damage control enzyme, affects the balance between defense pathways in plants. Plant Cell **17:** 282-294

Kato M, Ikoma Y, Matsumoto H, Sugiura M, Hyodo H, Yano M (2004) Accumulation of carotenoids and expression of carotenoid biosynthetic genes during maturation in citrus fruit. Plant Physiol. **134:** 824-837

Klee HJ, Hayford MB, Kretzmer KA, Barry GF, Kishore GM (1991) Control of Ethylene Synthesis by Expression of a Bacterial Enzyme in Transgenic Tomato Plants. Plant Cell **3:** 1187-1193

Koch M, Breithaupt C, Kiefersauer R, Freigang J, Huber R, Messerschmidt A (2004) Crystal structure of protoporphyrinogen IX oxidase: a key enzyme in haem and chlorophyll biosynthesis. Embo J. **23:** 1720-1728

Kräutler B (2003) Chlorophyll breakdown and chlorophyll catabolites. *In* KM Kadish, KM Smith, R Guilard, eds, The Porphyrin Handbook, Vol 13. Elsevier Science, pp 183-209

Kräutler B, Banala S, Moser S, Vergeiner C, Müller T, Lütz C, Holzinger A (2010) A novel blue fluorescent chlorophyll catabolite accumulates in senescent leaves of the peace lily and indicates a split path of chlorophyll breakdown. FEBS Lett. **584**:4215-4221

Kräutler B, Mühlecker W, Anderl M, Gerlach B (1997) Breakdown of chlorophyll: partial synthesis of a putative intermediary catabolite. Helv. Chim. Acta **80:** 1355-1362

Kräutler B, Jaun B, Bortlik K-H, Schellenberg M, Matile P (1991) On the enigma of chlorophyll degradation: the constitution of a secoporphinoid catabolite. Angew. Chem. Int. Ed. Engl. **30:** 1315-1318

Kreuz K, Tommasini R, Martinoia E (1996) Old enzymes for a new job. Herbicide detoxification in plants. Plant Physiol. **111:** 349-353

Kusaba M, Ito H, Morita R, Iida S, Sato Y, Fujimoto M, Kawasaki S, Tanaka R, Hirochika H, Nishimura M, Tanaka A (2007) Rice NON-YELLOW COLORING1 is involved in light-harvesting complex II and grana degradation during leaf senescence. Plant Cell **19:** 1362-1375

Lim PO, Woo HR, Nam HG (2003) Molecular genetics of leaf senescence in *Arabidopsis*. Trends Plant Sci. **8:** 272-278

Lin JF, Wu SH (2004) Molecular events in senescing *Arabidopsis* leaves. Plant J. **39:** 612-628

Lineweaver H, Burk D (1934) The determination of enzyme dissociation constants. J. Am. Chem. Soc. **56:** 658-666

Lorrain S, Vailleau F, Balaqué C, Roby D (2003) Lesion mimic mutants: keys for deciphering cell death and defense pathways in plants? Trends Plant Sci. **8:** 263-271

Lu Y-P, Li Z-S, Drozdowicz Y-M, Hörtensteiner S, Martinoia E, Rea PA (1998) AtMRP2, an Arabidopsis ATP binding cassette transporter able to transport glutathione *S*-conjugates and chlorophyll catabolites: functional comparisons with AtMRP1. Plant Cell **10:** 267-282

Mach JM, Castillo AR, Hoogstraten R, Greenberg JT (2001) The *Arabidopsis*-accelerated cell death gene *ACD2* encodes red chlorophyll catabolite reductase and suppresses the spread of disease symptoms. Proc. Natl. Acad. Sci. USA **98:** 771-776

Matile P, Hörtensteiner S, Thomas H (1999) Chlorophyll degradation. Annu. Rev. Plant Physiol. Plant Mol. Biol. **50:** 67-95

Matile P, Schellenberg M, Vicentini F (1997) Localization of chlorophyllase in the chloroplast envelope. Planta **201:** 96-99

Matile P, Schellenberg M (1996) The cleavage of pheophorbide *a* is located in the envelope of barley gerontoplasts. Plant Physiol. Biochem. **34:** 55-59

Matile P, Schellenberg M, Peisker C (1992) Production and release of a chlorophyll catabolite in isolated senescent chloroplasts. Planta **187:** 230-235

Matile P, Ginsburg S, Schellenberg M, Thomas H (1988) Catabolites of chlorophyll in senescing barley leaves are localized in the vacuoles of mesophyll cells. Proc. Natl. Acad. Sci. USA **85:** 9529-9532

Meyer A, Eskandari S, Grallath S, Rentsch D (2006) AtGAT1, a high affinity transporter for g-aminobutyric acid in *Arabidopsis thaliana*. J. Biol. Chem. **281:** 7197-7204

Moore BJ, Donnison IS, Harper JA, Armstead IP, King J, Thomas H, Jones RN, Jones TH, Thomas HM, Morgan WG, Thomas A, Ougham HJ, Huang L, Fentem T, Roberts LA, King IP (2005) Molecular tagging of a senescence gene by introgression mapping of a stay-green mutation from *Festuca pratensis*. New Phytol. **165:** 801-806

Morita R, Sato Y, Masuda Y, Nishimura M, Kusaba M (2009) Defect in non-yellow coloring 3, an alpha/beta hydrolase-fold family protein, causes a stay-green phenotype during leaf senescence in rice (vol 59, pg 940, 2009). Plant J. **60:** 1110-1110

Moser S, Müller T, Ebert MO, Jockusch S, Turro NJ, Kräutler B (2008) Blue Luminescence of Ripening Bananas. Angew. Chem. Int. Edit. **47:** 8954-8957

Mühlecker W, Kräutler B, Moser D, Matile P, Hörtensteiner S (2000) Breakdown of chlorophyll: a fluorescent chlorophyll catabolite from sweet pepper (*Capsicum annuum*). Helv. Chim. Acta **83:** 278-286

Mühlecker W, Ongania K-H, Kräutler B, Matile P, Hörtensteiner S (1997) Tracking down chlorophyll breakdown in plants: elucidation of the constitution of a 'fluorescent' chlorophyll catabolite. Angew. Chem. Int. Ed. Engl. **36:** 401-404

Mühlecker W, Kräutler B (1996) Breakdown of chlorophyll: constitution of nonfluorescing chlorophyll-catabolites from senescent cotyledons of the dicot rape. Plant Physiol. Biochem. **34:** 61-75

Müller T, Ulrich M, Ongania KH, Kräutler B (2007) Colorless tetrapyrrolic chlorophyll catabolites found in ripening fruit are effective antioxidants. Angew. Chem. Int. Edit. **46:** 8699-8702

Müller T, Moser S, Ongania K-H, Pružinská A, Hörtensteiner S, Kräutler B (2006) A divergent path of chlorophyll breakdown in the model plant *Arabidopsis thaliana*. Chem. Bio. Chem. **7:** 40-42

Nogaj LA, Srivastava A, van Lis R, Beale SI (2005) Cellular levels of glutamyl-tRNA reductase and glutamate-1-semialdehyde aminotransferase do not control chlorophyll synthesis in Chlamydomonas reinhardtii. Plant Physiol. **139:** 389-396

Oberhuber M, Berghold J, Breuker K, Hörtensteiner S, Kräutler B (2003) Breakdown of chlorophyll: a nonenzymatic reaction accounts for the formation of the colorless "nonfluorescent" chlorophyll catabolites. Proc. Natl. Acad. Sci. USA **100:** 6910-6915

Oh SA, Park J-H, Lee GI, Paek KH, Park SK, Nam HG (1997) Identification of three genetic loci controlling leaf senescence in *Arabidopsis thaliana*. Plant J. **12:** 527-535

Okazawa A, Tang L, Itoh Y, Fukusaki E, Kobayashi A (2006) Characterization and subcellular localization of chlorophyllase from *Ginkgo biloba*. Z. Naturforsch. C **61:** 111-117

Ori N, Juarez MT, Jackson D, Yamaguchi J, Banowetz GM, Hake S (1999) Leaf senescence is delayed in tobacco plants expressing the maize homeobox gene knotted1 under the control of a senescence-activated promoter. Plant Cell **11:** 1073-1080

Ougham H, Hörtensteiner S, Armstead I, Donnison I, King I, Thomas H, Mur L (2008) The control of chlorophyll catabolism and the status of yellowing as a biomarker of leaf senescence. Plant Biol. **10:** 4-14

Ougham HJ, Morris P, Thomas H (2005) The colors of autumn leaves as symptoms of cellular recycling and defenses against environmental stresses. Curr. Top. Dev. Biol. **66**: 135-160

Paran I, van der Knaap E (2007) Genetic and molecular regulation of fruit and plant domestication traits in tomato and pepper. J. Exp. Bot. **58:** 3841-3852

Park S-Y, Yu J-W, Park J-S, Li J, Yoo S-C, Lee N-Y, Lee S-K, Jeong S-W, Seo HS, Koh H-J, Jeon J-S, Park Y-I, Paek N-C (2007) The senescence-induced staygreen protein regulates chlorophyll degradation. Plant Cell **19:** 1649-1664

Patterson GW, Hugly S, Harrison D (1993) Sterols and phytyl esters of *Arabidopsis thaliana* under normal and chilling temperatures. Phytochemistry **33:** 1381-1383

Pear JR, Ridge N, Rasmussen R, Rose RE and Houck CM (1989) Isolation and characterization of a fruit-specific cDNA and the corresponding genomic clone from tomato. Plant Mol. Biol. **13**: 639-651

Peisker C, Düggelin T, Rentsch D, Matile P (1989) Phytol and the breakdown of chlorophyll in senescent leaves. J. Plant Physiol. **135:** 428-432

Pružinská A, Anders I, Aubry S, Schenk N, Tapernoux-Lüthi E, Müller T, Kräutler B, Hörtensteiner S (2007) In vivo participation of red chlorophyll catabolite reductase in chlorophyll breakdown. Plant Cell **19:** 369-387

Pružinská A, Tanner G, Aubry S, Anders I, Moser S, Müller T, Ongania K-H, Kräutler B, Youn J-Y, Liljegren SJ, Hörtensteiner S (2005) Chlorophyll breakdown in senescent Arabidopsis leaves: characterization of chlorophyll catabolites and of chlorophyll catabolic enzymes involved in the degreening reaction. Plant Physiol. **139:** 52-63

Pružinská A, Anders I, Tanner G, Roca M, Hörtensteiner S (2003) Chlorophyll breakdown: pheophorbide *a* oxygenase is a Rieske-type iron-sulfur protein, encoded by the *accelerated cell death 1* gene. Proc. Natl. Acad. Sci. USA **100:** 15259-15264

Rea PA (2007) Plant ATP-Binding cassette transporters. Ann. Rev. Plant Biol. **58:** 347-375

Ren G, An K, Liao Y, Zhou X, Cao Y, Zhao H, Ge X, Kuai B (2007) Identification of a novel chloroplast protein AtNYE1 regulating chlorophyll degradation during leaf senescence in Arabidopsis. Plant Physiol. **144:** 1429-1441

Rise M, Cojocaru M, Gottlieb HE, Goldschmidt EE (1989) Accumulation of -tocopherol in senescing organs as related to chlorophyll degradation. Plant Physiol. **89:** 1028-1030

Robatzek S, Somssich IE (2001) A new member of the *Arabidopsis* WRKY transcription factor family, *At*WRKY6, is associated with both senescence- and defence-related processes. Plant J. **28:** 123-133

Roca M, Minguez-Mosquera MI (2006) Chlorophyll catabolism pathway in fruits of *Capsicum annuum* (L.): Stay-green versus red fruits. J. Agric. Food Chem. **54:** 4035-4040

Roca M, Hornero-Mendez D, Gandul-Rojas B, Minguez-Mosquera MI (2006) Stay-green phenotype slows the carotenogenic process in *Capsicum annuum* (L.) fruits. J. Agric. Food Chem. **54:** 8782-8787

Roca M, James J, Pružinská A, Hörtensteiner S, Thomas H, Ougham H (2004) Analysis of the chlorophyll catabolism pathway in leaves of an introgression senescence mutant of *Lolium temulentum*. Phytochemistry **65:** 1231-1238

Rodoni S, Mühlecker W, Anderl M, Kräutler B, Moser D, Thomas H, Matile P, Hörtensteiner S (1997) Chlorophyll breakdown in senescent chloroplasts. Cleavage of pheophorbide *a* in two enzymic steps. Plant Physiol. **115:** 669-676

Rodoni S, Vicentini F, Schellenberg M, Matile P, Hörtensteiner S (1997) Partial purification and characterization of red chlorophyll catabolite reductase, a stroma protein involved in chlorophyll breakdown. Plant Physiol. **115:** 677-682

Rontani J-F, Cuny P, Grossi V (1996) Photodegradation of chlorophyll phytol chain in senescent leaves of higher plants. Phytochemistry **42:** 347-351

Rüdiger W (2002) Biosynthesis of chlorophyll *b* and the chlorophyll cycle. Photosynth. Res. **74:** 187-193

Sanchez-Fernandez R, Davies TGE, Coleman JOD, Rea PA (2001) The *Arabidopsis thaliana* ABC protein superfamily, a complete inventory. J. Biol. Chem. **276:** 30231-30244

Sato Y, Morita R, Katsuma S, Nishimura M, Tanaka A, Kusaba M (2009) Two short-chain dehydrogenase/reductases, NON-YELLOW COLORING 1 and NYC1-LIKE, are required for chlorophyll b and light-harvesting complex II degradation during senescence in rice. Plant J. **57:** 120-131

Sato Y, Morita R, Nishimura M, Yamaguchi H, Kusaba M (2007) Mendel's green cotyledon gene encodes a positive regulator of the chlorophyll-degrading pathway. Proc. Natl. Acad. Sci. USA **104:** 14169-14174

Schelbert S, Aubry S, Burla B, Agne B, Kessler F, Krupinska K, Hörtensteiner S (2009) Pheophytin Pheophorbide Hydrolase (Pheophytinase) Is Involved in Chlorophyll Breakdown during Leaf Senescence in Arabidopsis. Plant Cell **21:** 767-785

Schenk N, Schelbert S, Kanwischer M, Goldschmidt EE, Dörmann P, Hörtensteiner S (2007) The chlorophyllases AtCLH1 and AtCLH2 are not essential for senescence-related chlorophyll breakdown in *Arabidopsis thaliana*. FEBS Lett. **581:** 5517-5525

Schwacke R, Flügge UI, Kunze R (2004) Plant membrane proteome databases. Plant Physiol. Biochem. **42:** 1023-1034

Seki M, Narusaka M, Kamiya A, Ishida J, Satou M, Sakurai T, Nakajima M, Enju A, Akiyama K, Oono Y, Muramatusu M, Hayashizaki Y, Kawai J, Carninci P, Itoh M, Ishii Y, Arakawa T, Shibata K, Shinagawa A, Shinozaki K (2002) Functional annotation of a full-length Arabidopsis cDNA collection. Science **296:** 141-145

Shioi Y, Tomita N, Tsuchiya T, Takamiya K (1996) Conversion of chlorophyllide to pheophorbide by Mg-dechelating substance in extracts of *Chenopodium album*. Plant Physiol. Biochem. **34:** 41-47

Shioi Y, Watanabe K, Takamiya K (1996) Enzymatic conversion of pheophorbide *a* to a precursor of pyropheophorbide *a* in leaves of *Chenopodium album*. Plant Cell Physiol. **37:** 1143-1149

Sim S, Chang T, Curley J, Warnke SE, Barker RE, Jung G (2005) Chromosomal rearrangements differentiating the ryegrass genome from the Triticeae, oat, and rice genomes using common heterologous RFLP probes. Theor. Appl. Genet. **110:** 1011-1019

Spassieva S, Hille J (2002) A lesion mimic phenotype in tomato obtained by isolating and silencing an *Lls1* homologue. Plant Sci. **162:** 543-549

Stephens DJ, Banting G (2000) The use of yeast two-hybrid screens in studies of protein: protein interactions involved in trafficking. Traffic **1:** 763-768

Strain HH, Cope BT, Svec WA (1971) Analytical procedures for the isolation, identification, estimation and investigation of the chlorophylls. Method Enzymol. **23:** 452-476

Sugishima M, Okamoto Y, Noguchi M, Kohchi T, Tamiaki H, Fukuyama K (2010) Crystal structures of the substrate-bound forms of red chlorophyll catabolite reductase: implications for site-specific and stereospecific reaction. J. Mol. Biol. **402**: 879-891

Sugishima M, Kitamori Y, Noguchi M, Kohchi T, Fukuyama K (2009) Crystal Structure of Red Chlorophyll Catabolite Reductase: Enlargement of the Ferredoxin-Dependent Bilin Reductase Family. J. Mol. Biol. **389:** 376-387

Suzuki T, Kunieda T, Murai F, Morioka S, Shioi Y (2005) Mg-dechelation activity in radish cotyledons with artificial and native substrates, Mg-chlorophyllin *a* and chlorophyllide *a*. Plant Physiol. Biochem. **43:** 459-464

Suzuki T, Shioi Y (2002) Re-examination of Mg-dechelation reaction in the degradation of chlorophylls using chlorophyllin *a* as substrate. Photosynth. Res. **74:** 217-223

Suzuki Y, Doi M, Shioi Y (2002) Two enzymatic reaction pathways in the formation of pyropheophorbide *a*. Photosynth. Res. **74:** 225-233

Suzuki Y, Shioi Y (1999) Detection of chlorophyll breakdown products in the senescent leaves of higher plants. Plant Cell Physiol. **40:** 909-915

Suzuki Y, Tanabe K, Shioi Y (1999) Determination of chemical oxidation products of chlorophyll and porphyrin by high-performance liquid chromatography. J. Chromatogr. A. **839:** 85-91

Takamiya K, Tsuchiya T, Ohta H (2000) Degradation pathway(s) of chlorophyll: what has gene cloning revealed? Trends Plant Sci. **5:** 426-431

Tanaka A, Ito H, Tanaka R, Tanaka NK, Yoshida K, Okada K (1998) Chlorophyll *a* oxygenase (*CAO*) is involved in chlorophyll *b* formation from chlorophyll *a*. Proc. Natl. Acad. Sci. USA **95:** 12719-12723

Tanaka R, Tanaka A (2005) Effects of chlorophyllide a oxygenase overexpression on light acclimation in Arabidopsis thaliana. Photosynth. Res. **85:** 327-340

Tanaka R, Hirashima M, Satoh S, Tanaka A (2003) The *Arabidopsis-accelerated cell death* gene *ACD1* is involved in oxygenation of pheophorbide *a*: inhibition of pheophorbide *a* oxygenase activity does not lead to the "stay-green" phenotype in *Arabidopsis*. Plant Cell Physiol. **44:** 1266-1274

Tanaka R, Koshino Y, Sawa S, Ishiguro S, Okada K, Tanaka A (2001) Overexpression of chlorophyllide a oxygenase (CAO) enlarges the antenna size of photosystem II in *Arabidopsis thaliana*. Plant J. **26:** 365-373

Thomas H, Huang L, Young M, Ougham H (2009) Evolution of plant senescence. Bmc Evolutionary Biology **9:**

Thomas H, Ougham HJ, Wagstaff C, Stead AD (2003) Defining senescence and death. J. Exp. Bot. **54:** 1127-1132

Thomas H, Howarth CJ (2000) Five ways to stay green. J. Exp. Bot. **51:** 329-337

Thomas H, Evans C, Thomas HM, Humphreys MW, Morgan G, Hauck B, Donnison I (1997) Introgression, tagging and expression of a leaf senescence gene in *Festulolium*. New Phytol. **137:** 29-34

Thomas H, Ougham HJ, Davies TGE (1992) Leaf senescence in a non-yellowing mutant of *Festuca pratensis*. Transcripts and translation products. J. Plant Physiol. **139:** 403-412

Thomas H (1987) *Sid*: a Mendelian locus controlling thylakoid membrane disassembly in senescing leaves of *Festuca pratensis*. Theor. Appl. Genet. **73:** 551-555

Tommasini R, Vogt E, Fromenteau M, Hörtensteiner S, Matile P, Amrhein N, Martinoia E (1998) An ABC transporter of *Arabidopsis thaliana* has both glutathione-conjugate and chlorophyll catabolite transport activity. Plant J. **13:** 773-780

Thomson WW, Whatley JM (1980) Development of Non-Green Plastids. Ann. Rev. Plant Physiol. Plant Mol. Biol. **31:** 375-394

Trebitsh T, Goldschmidt EE, Riov J (1993) Ethylene induces *de novo* synthesis of chlorophyllase, a chlorophyll degrading enzyme, in *Citrus* fruit peel. Proc. Natl. Acad. Sci. USA **90:** 9441-9445

Tsuchiya T, Ohta H, Okawa K, Iwamatsu A, Shimada H, Masuda T, Takamiya K (1999) Cloning of chlorophyllase, the key enzyme in chlorophyll degradation: finding of a lipase motif and the induction by methyl jasmonate. Proc. Natl. Acad. Sci. USA **96:** 15362-15367

Valentin HE, Lincoln K, Moshiri F, Jensen PK, Qi Q, Venkatesh TV, Karunanandaa B, Baszis SR, Norris SR, Savidge B, Gruys KJ, Last RL (2006) The arabidopsis *vitamin E pathway gene5-1* mutant reveals a critical role for phytol kinase in seed tocopherol biosynthesis. Plant Cell **18:** 212-224

Vavilin D, Vermaas W (2007) Continuous chlorophyll degradation accompanied by chlorophyllide and phytol reutilization for chlorophyll synthesis in Synechocystis sp PCC 6803. BBA Bioenergetics **1767:** 920-929

Vavilin D, Brune DC, Vermaas W (2005) N-15-labeling to detennine chlorophyll synthesis and degradation in Synechocystis sp PCC 6803 strains lacking one or both photosystems. BBA Bioenergetics **1708:** 91-101

Vicentini F, Iten F, Matile P (1995) Development of an assay for Mg-dechelatase of oilseed rape cotyledons, using chlorophyllin as the substrate. Physiol. Plant. **94:** 57-63

Wagner D, Przybyla D, op den Camp R, Kim C, Landgraf F, Lee KP, Würsch M, Laloi C, Nater M, Hideg E, Apel K (2004) The genetic basis of singlet oxygen-induced stress responses of *Arabidopsis thaliana*. Science **306:** 1183-1185

Walter M, Chaban C, Schutze K, Batistic O, Weckermann K, Nake C, Blazevic D, Grefen C, Schumacher K, Oecking C, Harter K, Kudla J (2004) Visualization of protein interactions in living plant cells using bi-molecular fluorescence complementation. Plant J. **40:** 428-438

Wedel N, Soll J, Paap BK (1997) CP12 provides a new mode of light regulation of Calvin cycle activity in higher plants. P. Natl. Acad. Sci. USA **94:** 10479-10484

Wesley SV, Helliwell CA, Smith NA, Wang M, Rouse DT, Liu Q, Gooding PS, Singh SP, Abbot D, Stoutjesdijk PA, Robinson SP, Gleave AP, Green AG, Waterhouse PM (2001) Construct design for efficient, effective and high-throuput gene silencing in plants. Plant J. **27:** 581-590

Willstätter R, Stoll A (1913) Die Wirkungen der Chlorophyllase. *In* R Willstätter, A Stoll, eds, Untersuchungen über Chlorophyll. Verlag Julius Springer, Berlin, pp 172-187

Wüthrich KL, Bovet L, Hunziker PE, Donnison IS, Hörtensteiner S (2000) Molecular cloning, functional expression and characterisation of RCC reductase involved in chlorophyll catabolism. Plant J. **21:** 189-198

Yang M, Wardzala E, Johal GS, Gray J (2004) The wound-inducible *Lls1* gene from maize is an orthologue of the *Arabidopsis Acd1* gene, and the LLS1 protein is present in non-photosynthetic tissues. Plant Mol. Biol. **54:** 175-191

Yao N, Greenberg JT (2006) *Arabidopsis* ACCELERATED CELL DEATH2 modulates programmed cell death. Plant Cell **18:** 397-411

Yao N, Eisfelder BJ, Marvin J, Greenberg JT (2004) The mitochondrion - an organelle commonly involved in programmed cell death in *Arabidopsis thaliana*. Plant J. **40:** 596-610

You SC, Cho SH, Zhang H, Paik HC, Lee CH, Li J, Yoo JH, Lee BW, Koh HJ, Seo HS, Paek NC (2007) Quantitative trait loci associated with functional stay-green SNU-SG1 in rice. Molecules and Cells **24:** 83-94

Zimmermann P, Hirsch-Hoffmann M, Hennig L, Gruissem W (2004) GENEVESTIGATOR. Arabidopsis microarray database and analysis toolbox. Plant Physiol. **136:** 2621-2632

VII Acknowledgements

First of all, I would like to thanks Stefan Hörtensteiner for providing an excellent working environment. His supervision with great interests, delivery of new ideas and advices, pushed and greatly supported my work.

I would like to thank Enrico Martinoia, Beat Keller and Felix Kessler who agreed to join my thesis committee.

My “lab” thanks to Sylvain Aubry and Bastien Christ and Aurélie Egert which were perfect lab mate.

Thanks to Kathrin Salinger for her persistent work on the crossings and for her open ear which contributed to a relaxed and enjoyable working atmosphere.

My thanks go to all members of the Enrico Martinoia laboratory. Especially, I would like to thank Barbara Weder who greatly contributed to this enjoyable period with her cheerful nature.

Thanks to my husband Daniel Hofstetter who accompanied and supported me though all the steps since I am interested at plant biology.

Many thanks go to my family who in any time supported my wish of a second education.

This work was supported by the Swiss National Science Foundation (grants 3100A0-105389 and 3100A0-117940).

VIII Curriculum vitae

SCHELBERT HOFSTETTER
Silvia Monika
24/05/1975
Muotathal SZ

Education

2007-2010 **PhD Thesis**. Institute of Plant Physiology, University of Zürich (UZH).
Dissertation under supervision of Prof. Dr. S. Hörtensteiner
Title: *Biochemical and molecular identification of pheophytinase, an important esterase of chlorophyll breakdown during leaf senescence and fruit ripening*.

2004-2006 **Master of Science.** Microbiology and Plant Biology at UZH.
Master Thesis. Institute of Plant Physiology, UZH.
Under supervision of Prof. Dr. E. Martinoia
Title: *Identification of novel vacuolar membrane proteins in barley by a proteomic approach*

2001-2004 **Bachelor** in Biology at UZH.

1998-2001 **Maturität** mit Schwerpunkt Biologie und Chemie; Kantonale Maturitätsschule für Erwachsene, Zürich.
Maturitäts Thesis in Geography
Title: *Das Korallenriff in Gefahr*

1991-1994 **Appreniceship** for Pharma-Assistent in the Rathausapotheke, Baar.

Work and Research Experiences

2006-2007 **Science Assistant** 6 month placement at Institute of Plant Physiology, UZH and Institute of Plant Science, UniBern.

2005-2006 **Master Thesis** 12 month placement at Institute of Plant Physiology, UZH.

2004 **Botanical Teacher** part-time in the Botanical Garden of UZH.

1994-2006 **Pharma-Assistent** in full and part-time at Herti Apotheke, Zug and Bahnhof-Apotheke, Zürich.

8.1 Publications

Schelbert S, Aubry S, Burla B, Agne B, Kessler F, Krupinska K, Hörtensteiner S (2009) Pheophytin Pheophorbide Hydrolase (Pheophytinase) Is Involved in Chlorophyll Breakdown during Leaf Senescence in Arabidopsis. Plant Cell **21:** 767-785

Schenk N*, Schelbert S*, Kanwischer M, Goldschmidt EE, Dörmann P, Hörtensteiner S (2007) The chlorophyllases AtCLH1 and AtCLH2 are not essential for senescence-related chlorophyll breakdown in *Arabidopsis thaliana*. FEBS Lett. **581:** 5517-5525
*Joint first co-authors

Schmidt UG, Endler A, Schelbert S, Brunner A, Schnell M, Neuhaus HE, Marty-Mazars D, Marty F, Baginsky S, Martinoia E (2007) Novel tonoplast transporters identified using a proteomic approach with vacuoles isolated from cauliflower buds. Plant Physiol. **145:** 216-229

Endler A, Meyer S, Schelbert S, Schneider T, Weschke W, Peters SW, Keller F, Baginsky S, Martinoia E, Schmidt UG (2006) Identification of a vacuolar sucrose transporter in barley and arabidopsis mesophyll cells by a tonoplast proteomic approach. Plant Physiol. **141:** 196-207